

Supplementary Information

**Late-Stage Modification of π -Electron Systems Based on
Asymmetric Oxidation of Medium-Sized Sulfur-Containing Ring**

Masashiro Hayakawa, Satoshi Horike, Yuh Hijikata, Kosuke Yasui, Shigehiro Yamaguchi,
and Aiko Fukazawa

Table of Contents

1. Summary of the Previous Relevant Reports on the Asymmetric Oxidation of Sulfur.....	S2
2. Experimental Details for the Synthesis	S3
3. VT-NMR Spectra	S11
4. Photophysical Properties	S15
5. Quantum Chemical Calculations.....	S17
6. Single-Crystal X-ray Diffraction Analysis	S27
7. TGA of 8 and 13	S33
8. Phase-transition Behaviors of 8 and 13	S33
9. MD Simulations	S35
10. NMR Spectra of New Compounds	S37
11. Results of HPLC Analyses for Optically Active Compounds.....	S52
12. Author Contributions.....	S55
13. References	S55

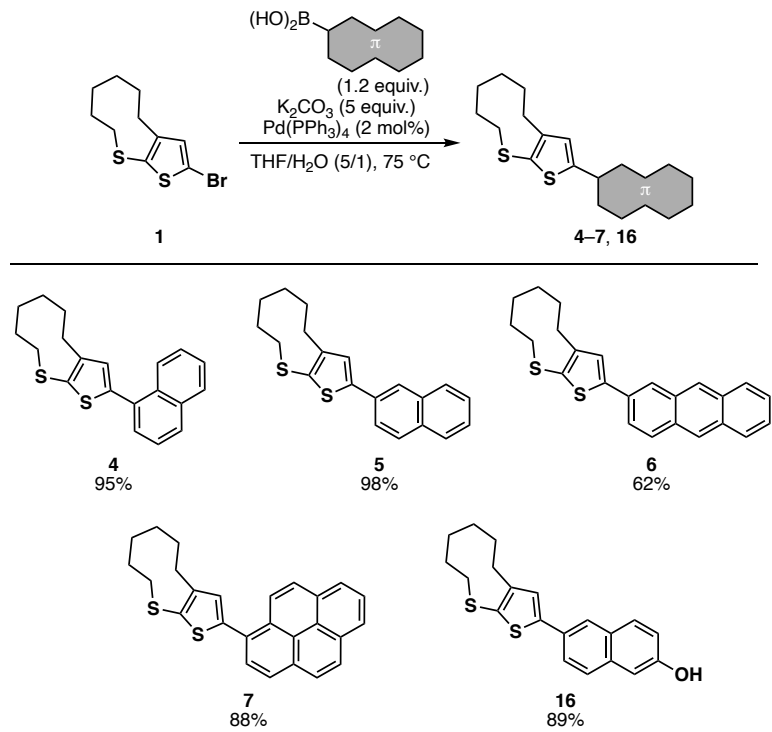
1. Summary of the Previous Relevant Reports on the Asymmetric Oxidation of Sulfur

In this study, we focused on the reaction systems using metal catalysts together with a chiral Schiff base as a ligand among various studies on the asymmetric oxidation of alkyl aryl sulfides. The prototype of this method is the combination of VO(acac)₂/chiral Schiff base first reported by Bolm and coworkers in 1995,^{S1} which has several advantages over the other conditions such as modified Sharpless reagent^{S2} and transition metal-chiral salen complexes:^{S3} (1) the reaction proceeds under mild conditions without the exclusion of oxygen or moisture, (2) H₂O₂ aq., one of the cheapest and the most easy-to-handle oxidants, can be used, (3) high catalyst activity and excellent enantioselectivity can be obtained by simply mixing the readily available chiral Schiff base with a catalytic amount of the metal complex, and (4) the formation of the over-oxidation product, sulfone, can be reasonably suppressed. While the Al-salen complexes,^{S4} chiral Brønsted acids,^{S5} and Mn-tetradeinate chiral oxazoline complexes^{S6} also have the similar advantages yet show much better performances, the availability of the chiral Schiff base is still attractive. In addition, considering the poor solubility of many π -electron systems in polar solvents, the other advantage of this reaction system is the possible use of CH₂Cl₂ as a solvent. Spectroscopic^{S7} and computational studies^{S8} have suggested that vanadium(V)oxoperoxo species bearing the chiral Schiff base as a tridentate ligand is likely a key intermediate.

Based on the Bolm's report, several other metal precatalysts have been investigated with the chiral Schiff base above mentioned, and excellent results have been reported with Cu(acac)₂^{S9} and Fe(acac)₃^{S10} for the asymmetric oxidation of a variety of alkyl aryl sulfides. In light of these precedent reports, we investigated Cu(acac)₂, Fe(acac)₃, and VO(acac)₂ complexes as candidate catalyst precursors under the condition that the ligand is fixed to the chiral Schiff base **3** reported by Jackson and co-workers.^{S11} The results thus obtained were shown in Table 1 in the manuscript.

2. Experimental Details for the Synthesis

General. Melting points (mp) were determined with a Yanaco MP-S3 instrument (MP-S3) or a Hitachi X-DSC7000 (DSC). ^1H , $^{13}\text{C}\{\text{H}\}$, and ^{19}F NMR spectra were recorded with a JEOL ECA 400 II spectrometer (400 MHz for ^1H and 100 MHz for ^{13}C) or Bruker AVANCE III spectrometer (500 MHz for ^1H , 125 MHz for ^{13}C , and 470 MHz for ^{19}F) in chloroform-*d* (CDCl_3) or dichloromethane-*d*₂ (CD_2Cl_2). The chemical shifts in ^1H NMR spectra are reported in δ ppm using the residual proton of the solvents, *i.e.*, CHCl_3 (7.26 ppm) and CH_2Cl_2 (5.32 ppm) as an internal standard, and those in ^{13}C NMR spectra are reported in δ ppm using the solvent signals of CDCl_3 (77.16 ppm) and CH_2Cl_2 (53.84 ppm) as an internal standard. The chemical shifts in ^{19}F NMR spectra are reported using CF_3COOH (−78.50 ppm) as an external standard. Mass spectra were measured with a Bruker solarix (FT-ICR) system with the ionization method of APCI and a Thermo Fisher Scientific Exactive with the ionization method of ESI. Thermal gravimetric analyses (TGA) for the determination of the 5% weight loss temperature (T_{d5}) were conducted using a SII TGA6200 instrument. Differential scanning calorimetry (DSC) was conducted with a Hitachi X-DSC7000. Thin layer chromatography (TLC) was performed on plates coated with 0.25 mm thickness of silica gel 60F₂₅₄ (Merck). Column chromatography was performed using silica gel PSQ100B, silica gel PSQ60B (Fuji Silysia Chemicals), or Wakosil® HC-N (FUJIFILM Wako Chemicals). Enantiomeric excess (*ee*) was determined by HPLC analysis with JASCO EXTREMA HPLC system equipped with a DAICEL Chiralpak IG column, a JASCO PU-4189 binary pump, a JASCO RI-4035 refractive index detector, and a JASCO MD-4010 photodiode array (PDA) detector. Optical rotations were measured with a JASCO P-1020 polarimeter. Anhydrous THF and CH_2Cl_2 were purchased from Kanto Chemicals and further purified by Glass Contour solvent purifier systems. 2-Bromo-4,5,6,7,8,9-hexahydrothieno[2,3-*b*]thionine (1)^s¹² 4,4,5,5-tetramethyl-2-{3,4,5-tris(dodecyloxy)phenyl}-1,3,2-dioxaborolane^{S13} were prepared according to the literature method.



Scheme S1. Synthesis of **4–7** and **16**.

Typical Procedure for the Synthesis of a π -Electron System Bearing TN-fused Thienyl Group.

Synthesis of 2-(naphthalen-1-yl)-4,5,6,7,8,9-hexahydrothieno[2,3-*b*]thionine (4). A solution of **1** (59 mg, 0.21 mmol), 1-naphthylboronic acid (45 mg, 0.26 mmol), K_2CO_3 (148 mg, 1.07 mmol), and $\text{Pd}(\text{PPh}_3)_4$ (5 mg, 4 μmol) in THF (2 mL) and H_2O (0.4 mL) was stirred at 75 °C for 12 h. The resulting mixture was diluted CH_2Cl_2 , separated into two layers, and the aqueous layer was extracted with CH_2Cl_2 (3 \times 10 mL). The combined organic layer was washed with brine, dried over anhydrous Na_2SO_4 , and concentrated in vacuo. The resulting crude product was purified by silica gel column chromatography (hexane/ CH_2Cl_2 4/1 as an eluent, $R_f = 0.75$) to afford 65 mg of **4** as colorless viscous liquid (0.20 mmol, 95% yield). ^1H NMR (500 MHz, CDCl_3): δ 1.24–1.29 (m, 2H), 1.61–1.66 (m, 2H), 1.69–1.74 (m, 2H), 1.87–1.92 (m, 2H), 3.02 (td, $J = 6.3$ Hz, 1.6 Hz, 4H), 6.98 (s, 1H), 7.46–7.52 (m, 3H), 7.54 (dd, $J = 7.0$ Hz, 1.2 Hz, 1H), 7.84 (d, $J = 8.2$ Hz, 1H), 7.88–7.90 (m, 1H), 8.24–8.26 (m, 1H). $^{13}\text{C}\{\text{H}\}$ NMR (125 MHz, CDCl_3): δ 20.6, 21.5, 26.3, 27.2, 27.5, 40.0, 125.3, 125.8, 126.1, 126.6, 128.0, 128.5, 128.6, 129.5, 131.1, 131.6, 132.5, 134.0, 144.7, 148.4. HRMS (ESI): m/z Calcd. for $\text{C}_{20}\text{H}_{21}\text{S}_2$: 325.1079 ($[M+\text{H}]^+$). Obsd. 325.1079.

2-(Naphthalen-2-yl)-4,5,6,7,8,9-hexahydrothieno[2,3-*b*]thionine (5). This compound was prepared in a similar manner as described for **4** using naphthalen-2-ylboronic acid (106 mg, 0.62 mmol), **1** (139 mg, 0.50 mmol), K_2CO_3 (351 mg, 1.07 mmol), and $\text{Pd}(\text{PPh}_3)_4$ (5 mg, 11 μmol) in THF (5 mL) and H_2O (1 mL). Purification by silica gel column chromatography (hexane/ CH_2Cl_2 = 1/1 as eluent, $R_f = 0.83$) afforded 159 mg of **5** as white solids (0.49 mmol, 98% yield). Mp (MP-S3): 102.9–103.7 °C. ^1H NMR (500 MHz, CDCl_3): δ 1.22 (td, $J = 13.3$ Hz, 6.0 Hz, 2H), 1.60–1.65 (m, 2H), 1.68 (quint., $J = 6.3$ Hz,

2H), 1.83–1.89 (m, 2H), 2.99 (q, J = 6.1 Hz, 4H), 7.19 (s, 1H), 7.44–7.50 (m, 2H), 7.69 (dd, J = 8.5 Hz, 1.8 Hz, 1H), 7.80–7.85 (m, 3H), 8.00 (d, J = 1.2 Hz). $^{13}\text{C}\{\text{H}\}$ NMR (125 MHz, CDCl_3): δ 20.6, 21.4, 26.3, 27.1, 27.4, 40.0, 124.0, 124.1, 125.4, 126.2, 126.7, 127.8, 128.2, 128.6, 130.8, 131.6, 132.9, 133.7, 146.6, 149.4. HRMS (APCI): m/z Calcd. for $\text{C}_{20}\text{H}_{21}\text{S}_2$: 325.1079 ($[M+\text{H}]^+$). Obsd. 325.1077.

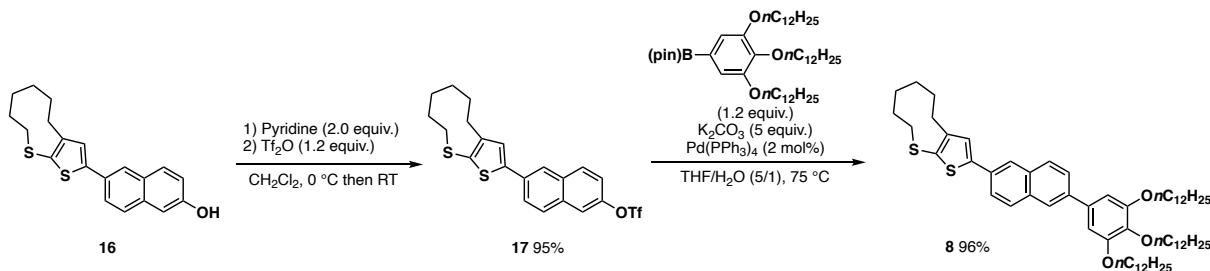
2-(Anthracen-2-yl)-4,5,6,7,8,9-hexahydrothieno[2,3-*b*]thionine (6). This compound was prepared in a similar manner as described for **4** using anthracen-2-ylboronic acid (226 mg, 1.02 mmol), **1** (332 mg, 1.20 mmol), K_2CO_3 (696 mg, 5.03 mmol), and $\text{Pd}(\text{PPh}_3)_4$ (30 mg, 26 μmol) in THF (8 mL) and H_2O (1.6 mL). Purification by silica gel column chromatography (hexane to hexane/ CH_2Cl_2 1/1 as eluent, R_f = 0.70 in hexane/ CH_2Cl_2 1/1) afforded 236 mg of **6** as yellow solids (0.63 mmol, 62% yield). Mp (MP-S3): 146.8–147.2 °C. ^1H NMR (500 MHz, CD_2Cl_2): δ 1.22 (td, J = 9.5 Hz, 5.2 Hz, 2H), 1.62–1.72 (m, 4H), 1.84–1.89 (m, 2H), 3.00 (td, J = 6.3 Hz, 4.9 Hz), 7.28 (s, 1H), 7.47–7.49 (m, 2H), 7.71 (dd, J = 8.8 Hz, 1.8 Hz, 1H), 8.00–8.03 (m, 3H), 8.18 (d, J = 0.9 Hz, 1H), 8.40 (s, 1H), 8.43 (s, 1H). $^{13}\text{C}\{\text{H}\}$ NMR (125 MHz, CD_2Cl_2): δ 20.8, 21.8, 26.6, 27.4, 27.7, 40.4, 124.0, 124.1, 126.00, 126.03, 126.1, 126.8, 128.5, 128.6, 129.3, 146.7, 149.9, one signal assignable to the carbon atom of the aromatic region was not observed due to overlap to the other signals. HRMS (APCI): m/z Calcd. for $\text{C}_{24}\text{H}_{23}\text{S}_2$: 375.1236 ($[M+\text{H}]^+$). Obsd. 375.1235.

2-(Pyren-1-yl)-4,5,6,7,8,9-hexahydrothieno[2,3-*b*]thionine (7). This compound was prepared in a similar manner as described for **4** using pyren-1-ylboronic acid (253 mg, 1.03 mmol), **1** (331 mg, 1.19 mmol), K_2CO_3 (704 mg, 5.10 mmol), and $\text{Pd}(\text{PPh}_3)_4$ (27 mg, 23 μmol) in THF (8 mL) and H_2O (1.6 mL). Purification by silica gel column chromatography (hexane to hexane/ CH_2Cl_2 1/1 as eluent, R_f = 0.93 in hexane/ CH_2Cl_2 1/1) afforded 360 mg of **7** as pale yellow solids (0.90 mmol, 88% yield). Mp (MP-S3): 119.0–119.8 °C. ^1H NMR (500 MHz, CDCl_3): δ 1.29–1.34 (m, 2H), 1.66–1.71 (m, 2H), 1.75 (quint, J = 6.3 Hz, 2H), 1.93 (quint., J = 6.6 Hz, 2H), 3.08 (q, J = 6.0 Hz, 4H), 7.12 (s, 1H), 8.02 (t, J = 7.6 Hz, 1H), 8.06–8.11 (m, 4H), 8.17 (d, J = 7.9 Hz, 1H), 8.20 (t, J = 6.6 Hz, 2H). $^{13}\text{C}\{\text{H}\}$ NMR (125 MHz, CDCl_3): δ 20.7, 21.5, 26.3, 27.2, 27.5, 40.0, 124.7, 124.9, 125.0, 125.1, 125.2, 125.5, 126.2, 127.4, 127.9, 128.1, 128.2, 128.8, 129.7, 130.0, 131.0, 131.1, 131.5, 131.7, 145.3, 148.7. HRMS (APCI): m/z Calcd. for $\text{C}_{26}\text{H}_{23}\text{S}_2$: 399.1236 ($[M+\text{H}]^+$). Obsd. 399.1234.

6-(4,5,6,7,8,9-Hexahydrothieno[2,3-*b*]thionin-2-yl)naphthalen-2-ol (16). This compound was prepared in a similar manner as described for **4** using 6-(4,4,5,5-tetramethyl-1,3,2-dioxaborolan-2-yl)naphthalen-2-ol (1.46 g, 5.41 mmol), **1** (1.36 g, 4.89 mmol), K_2CO_3 (3.40 g, 24.6 mmol), and $\text{Pd}(\text{PPh}_3)_4$ (116 mg, 0.10 mmol) in THF (50 mL) and H_2O (10 mL). Purification by silica gel column chromatography (CH_2Cl_2 /ethyl acetate 4/1 to 1/1 as eluent, R_f = 0.38 in CH_2Cl_2 /ethyl acetate 1/1) afforded 1.71 g of **16** as pale yellow solids (4.37 mmol, 89% yield). Mp (MP-S3): 124.8–125.8 °C. ^1H NMR (500 MHz, CDCl_3): δ 1.18–1.24 (m, 2H), 1.59–1.64 (m, 2H), 1.68 (quint., J = 6.3 Hz, 2H), 1.86 (quint., J = 6.6 Hz, 2H), 2.98 (q, J = 6.8 Hz, 4H), 7.10–7.13 (m, 3H), 7.62–7.67 (m, 2H), 7.75 (d, J = 8.5 Hz, 1H), 7.92 (d, J = 0.9 Hz, 1H). $^{13}\text{C}\{\text{H}\}$ NMR (125 MHz, CDCl_3): δ 20.6, 21.4, 26.3, 27.1, 27.4,

40.0, 109.7, 118.6, 124.1, 124.7, 124.9, 127.1, 129.1, 129.5, 130.0, 130.2, 134.1, 146.8, 149.3, 153.8.

HRMS (APCI): m/z Calcd. for $C_{20}H_{21}OS_2$: 341.1028 ($[M+H]^+$). Obsd. 341.1026.



Scheme S2. Synthesis of **8**.

6-(4,5,6,7,8,9-Hexahydrothieno[2,3-*b*]thionin-2-yl)naphthalen-2-yl trifluoromethanesulfonate (17). To solution of **16** (1.71 g, 4.37 mmol) and pyridine (0.71 mL, 8.74 mmol) in CH_2Cl_2 was added Tf_2O (0.88 mL, 5.24 mmol) dropwise at 0 °C over 2 min. After stirring for 15 min, the resulting solution was allowed to warm to ambient temperature and stirred for 8 h. The reaction mixture was quenched with water, and the aqueous phase was extracted with CH_2Cl_2 (15 mL × 3). The combined organic layer was washed with brine, dried over anhydrous Na_2SO_4 , and concentrated in vacuo. The resulting crude product was purified by silica gel column chromatography (CH_2Cl_2 as eluent, $R_f = 0.73$ in hexane/ CH_2Cl_2 1/1) to afford 2.18 mg of **17** as off-white solids (4.16 mmol, 95% yield). Mp (MP-S3): 91.1–92.0 °C. 1H NMR (500 MHz, $CDCl_3$): δ 1.19–1.25 (m, 2H), 1.61–1.71 (m, 4H), 1.86 (quint., $J = 6.3$ Hz, 2H), 2.99 (q, $J = 6.2$ Hz, 4H), 7.21 (s, 1H), 7.38 (dd, $J = 9.2$ Hz, 2.4 Hz, 1H), 7.72 (d, $J = 2.4$ Hz, 1H), 7.79 (dd, $J = 8.7$ Hz, 1.7 Hz, 1H), 7.86 (d, $J = 8.5$ Hz, 1H), 7.91 (d, $J = 9.2$ Hz, 1H). $^{13}C\{^1H\}$ NMR (125 MHz, $CDCl_3$): δ 20.6, 21.4, 26.3, 27.1, 27.4, 40.0, 118.9 (q, $J = 319$ Hz), 119.3, 120.4, 123.9, 125.8, 126.1, 128.8, 130.8, 131.8, 132.72, 132.74, 133.1, 145.5, 147.2, 149.6. ^{19}F NMR (470 MHz, $CDCl_3$): δ –75.7. HRMS (APCI): m/z Calcd. for $C_{21}H_{20}F_3O_3S_3$: 473.0521 ($[M+H]^+$). Obsd. 473.0520.

2-[6-{3,4,5-Tris(dodecyloxy)phenyl}naphthalen-2-yl]-4,5,6,7,8,9-hexahydrothieno[2,3-*b*]thionine (8). A solution of **17** (189 mg, 0.36 mmol), 4,4,5,5-tetramethyl-2-(3,4,5-tris(dodecyloxy)phenyl)-1,3,2-dioxaborolane (330 mg, 0.44 mmol), K_2CO_3 (251 mg, 1.82 mmol), and $Pd(PPh_3)_4$ (10 mg, 2 mol%) in THF (3.6 mL) and H_2O (0.75 mL) was stirred at 75 °C for 12 h. The mixture was diluted CH_2Cl_2 , and the resulting aqueous layer was extracted with CH_2Cl_2 (15 mL × 3). The combined organic layer was washed with brine, dried over anhydrous Na_2SO_4 , and concentrated in vacuo. The resulting crude product was purified by silica gel column chromatography (hexane to hexane/ CH_2Cl_2 4/1 as eluent, $R_f = 0.10$ in hexane/ CH_2Cl_2 4/1) to afford 331 mg of **8** as white solids (0.35 mmol, 96% yield). Mp (DSC): 51.3 °C. 1H NMR (500 MHz, $CDCl_3$): δ 0.88–0.91 (m, 9H), 1.20–1.39 (m, 50H), 1.51 (q, $J = 7.6$ Hz, 6H), 1.63–1.72 (m, 4H), 1.78–1.89 (m, 8H), 3.00 (q, $J = 6.0$ Hz, 4H), 4.04 (t, $J = 6.6$ Hz, 2H), 4.09 (t, $J = 6.4$ Hz, 4H), 6.89 (s, 2H), 7.20 (s, 1H), 7.71 (dd, $J = 8.7$, 1.7 Hz, 2H), 7.88 (dd, $J = 8.5$, 3.4 Hz, 2H), 7.95 (s, 1H), 8.01 (s, 1H). $^{13}C\{^1H\}$ NMR (125 MHz, $CDCl_3$): δ 14.3, 20.6, 21.5, 22.8, 26.3, 27.1, 27.4, 29.52, 29.56, 29.61, 29.7, 29.82, 29.87, 29.90, 29.93, 30.6, 32.1, 40.0, 69.5, 73.7, 106.4, 123.9, 124.5,

125.38, 125.41, 126.4, 128.6, 128.8, 130.8, 131.5, 132.8, 133.2, 136.3, 138.4, 139.2, 146.6, 149.4, 153.6, several signals assignable to the carbon atoms of the alkyl chains were not observed due to overlap to the other signals. HRMS (APCI): m/z Calcd. for $C_{62}H_{97}O_3S_2$: 953.6874 ($[M+H]^+$). Obsd. 953.6873.

Typical Procedure for the Oxidation of TN-Capped π -Electron Systems. Synthesis of *rac*-2-bromo-4,5,6,7,8,9-hexahydrothieno[2,3-*b*]thionine S-oxide (2). To a solution of **1** (1.39 g, 5.00 mmol) in CH_2Cl_2 (7.5 mL) and 2,2,2-trifluoroethanol (TFE, 7.5 mL) was added 30% H_2O_2 aq. (0.92 mL, 9.00 mmol) dropwise at an ambient temperature. After stirring for 18 h, the resulting mixture was quenched by Na_2SO_3 aq., and the aqueous layer was extracted with CH_2Cl_2 . The combined organic layer was washed with brine, dried over anhydrous Na_2SO_4 , and concentrated under reduced pressure. The resulting crude product was purified by silica gel column chromatography (CH_2Cl_2 then $CHCl_3$ as eluent, $R_f = 0.15$ ($CHCl_3$)) to afford 1.35 g of *rac*-**2** as white solids (4.62 mmol, 93% yield). Mp (MP-S3): 112.6–113.2 °C. 1H NMR (400 MHz, $CDCl_3$): δ 1.10–1.25 (m, 2H), 1.32–1.41 (m, 2H), 1.50–1.57 (m, 1H), 1.69–1.75 (m, 1H), 1.86–1.99 (m, 2H), 2.52 (ddd, $J = 14.2$ Hz, 11.4 Hz, 2.8 Hz 1H), 2.88 (ddd, $J = 14.0$ Hz, 6.6 Hz, 2.6 Hz, 1H), 3.04 (ddd, $J = 12.8$ Hz, 7.0 Hz, 3.0 Hz, 1H), 3.27 (ddd, $J = 13.2$ Hz, 10 Hz, 3.2 Hz, 1H), 6.84 (s, 1H). $^{13}C\{^1H\}$ NMR (100 MHz, $CDCl_3$): δ 23.0, 25.4, 27.1, 27.5, 30.3, 62.0, 118.1, 132.7, 142.9, 145.6. HRMS (ESI): m/z Calcd. for $C_{10}H_{13}OS_2BrNa$: 314.9489 ($[M+Na]^+$). Obsd. 314.9482.

The *rac*-**2** thus obtained was resolved by HPLC equipped with a DAICEL Chiraldak IG using acetonitrile as an eluent to give analytically pure (*S*)- and (*R*)-**2**. The absolute configurations of these enantiomers were identified by the single-crystal X-ray analyses, and the results were shown in Figure S7.

(*R*)-**2**. Mp (MP-S3): 143.5–144.4 °C. $[\alpha]_D^{20} = +96.1$ ($c = 1.03$ g/L in $CHCl_3$ using the sample with >99% *ee*).

(*S*)-**2**. Mp (MP-S3): 145.5–146.0 °C. $[\alpha]_D^{20} = -97.5$ ($c = 1.03$ g/L in $CHCl_3$ using the sample with >99% *ee*).

Typical Procedure for the Asymmetric Oxidation of TN-Capped π -Electron Systems. Synthesis of (*S*)-2. A solution of (*S*)-**3** (1.9 mg, 4.1 μ mol, 2 mol% based on **1**) and metal source (1 mol% based on **1**) in CH_2Cl_2 (0.3 M) was stirred for 30 min at an ambient temperature. To the resulting mixture was added **1** (57 mg, 0.20 mmol), and the mixture was stirred at 0 °C or an ambient temperature for 30 min. Subsequently, 30% H_2O_2 aq. (31 μ L, 0.30 mmol) was added to the mixture, which was stirred at the same temperature for 16 h. The reaction was quenched with sat. Na_2SO_3 aq. After standard aqueous workup, the resulting crude product was purified by silica gel column chromatography (CH_2Cl_2 to CH_2Cl_2 /ethyl acetate 9/1 as eluent, $R_f = 0.35$ (CH_2Cl_2 /ethyl acetate 9/1)) to afford analytically pure **2**, which was further subjected to the HPLC analysis for the determination of *ee*. 1H and ^{13}C NMR spectra were identical to those of *rac*-**2**. The result of the HPLC analysis is shown in the middle panel of Figure

Asymmetric oxidation of TN-Capped Bromothiophene **1 using the Chiral Schiff Base **3** with the Opposite Configuration.** Compound **1** was subjected to asymmetric oxidation in a similar manner as described for (*S*)-**2** using **1** (57 mg, 0.21 mmol), (*R*)-**3** (1.9 mg, 4.0 μ mol), VO(acac)₂ (0.56 mg, 2.1 μ mol), 30% H₂O₂ aq. (32 μ L, 0.31 mmol) in CH₂Cl₂ (0.7 mL). The conversion and the NMR yield were determined to be 99% and 81%, respectively, by ¹H NMR analysis using 1,3,5-trimethoxybenzene as an internal standard. Purification by silica gel column chromatography (CH₂Cl₂ to CH₂Cl₂/ethyl acetate 9/1 as eluent, R_f = 0.35 (CH₂Cl₂/ethyl acetate 9/1)) afforded 46 mg of (*R*)-**2** as white solids (0.16 mmol, 75% isolated yield, 86 % ee). ¹H NMR spectrum was identical with those of *rac*-**2**. The result of HPLC analysis is shown in the bottom panel of Figure S40.

2-(Naphthalen-1-yl)-4,5,6,7,8,9-hexahydrothieno[2,3-*b*]thionine *S*-oxide (*rac*-9**).** This compound was prepared in a similar manner as described for *rac*-**2** using **4** (53 mg, 0.16 mmol) and 30% H₂O₂ aq (30 μ L, 0.29 mmol) in CH₂Cl₂ (1.6 mL) and TFE (1.6 mL). Purification by silica gel column chromatography (CH₂Cl₂/ethyl acetate 9/1 as eluent, R_f = 0.38) afforded 50 mg of *rac*-**9** as white solids (0.15 mmol, 90% yield). Mp (MP-S3): 137.2–138.1 °C. ¹H NMR (500 MHz, CDCl₃): δ 1.22–1.35 (m, 2H), 1.42–1.49 (m, 2H), 1.57–1.62 (m, 1H), 1.82–1.88 (m, 1H), 1.96 (ddd, J = 15.5 Hz, 8.2 Hz, 3.9 Hz, 1H), 2.04 (dddd, J = 18.8 Hz, 9.3 Hz, 4.7 Hz, 2.3 Hz, 1H), 2.67 (ddd, J = 14.1 Hz, 11.5 Hz, 3.1 Hz, 1H) 3.03 (ddd, J = 14.2 Hz, 6.9 Hz, 2.4 Hz, 1H), 3.15 (ddd, J = 12.8 Hz, 7.3 Hz, 3.1 Hz, 1H), 3.35 (ddd, J = 13.0 Hz, 10.1 Hz, 3.1 Hz, 1H), 7.01 (s, 1H), 7.49–7.55 (m, 3H), 7.58 (dd, J = 7.0 Hz, 1.2 Hz, 1H), 7.88–7.92 (m, 2H), 8.16–8.19 (m, 1H). ¹³C{¹H} NMR (125 MHz, CDCl₃): δ 23.1, 25.8, 27.3, 27.9, 30.5, 62.0, 125.3, 125.4, 126.4, 127.0, 128.3, 129.4, 130.0, 131.5, 134.0, 141.2, 145.4, 147.1. HRMS (ESI): *m/z* Calcd. for C₂₀H₂₁OS₂: 341.1028 ([M+H]⁺). Obsd. 341.1028.

(*S*)-9**.** This compound was prepared in a similar manner as described for (*S*)-**2** using **4** (40 mg, 0.12 mmol), (*S*)-**3** (1.21 mg, 2.5 μ mol), VO(acac)₂ (0.33 mg, 1.2 μ mol), 30% H₂O₂ aq. (19 μ L, 0.19 mmol) in CH₂Cl₂ (1.2 mL). Purification by silica gel column chromatography (CH₂Cl₂ to CH₂Cl₂/ethyl acetate 9/1 as eluent, R_f = 0.38 (CH₂Cl₂/ethyl acetate 9/1)) afforded 34 mg of (*S*)-**9** as white solids (0.10 mmol, 81% yield, 64 % ee). Mp (MP-S3): 159.6–160.6 °C (for the sample with 64 % ee). ¹H and ¹³C NMR spectra were identical with those of *rac*-**9**. The result of HPLC analysis is shown in Figure S41. $[\alpha]_D^{20}$ = +109.2 (*c* = 0.28 g/L in CHCl₃ using the sample with >99% ee after purification by chiral HPLC).

2-(Naphthalen-2-yl)-4,5,6,7,8,9-hexahydrothieno[2,3-*b*]thionine *S*-oxide (*rac*-10**).** This compound was prepared in a similar manner as described for *rac*-**2** using **5** (35 mg, 0.11 mmol) and 30% H₂O₂ aq. (20 μ L, 0.20 mmol) in CH₂Cl₂ (1.0 mL) and TFE (1.0 mL). Purification by silica gel column chromatography (CH₂Cl₂/ethyl acetate 9/1 as eluent, R_f = 0.35) afforded 35 mg of *rac*-**10** as white solids (0.10 mmol, 95% yield). Mp (MP-S3): 138.2–138.7 °C. ¹H NMR (500 MHz, CDCl₃): δ 1.20–1.33 (m, 2H), 1.38–1.46 (m, 2H), 1.54–1.64 (m, 1H), 1.78–1.84 (m, 1H), 1.91 (dquint., J = 19.1 Hz, 15.4 Hz,

1H), 2.00–2.06 (m, 1H), 2.62 (dd, J = 13.4 Hz, 11.9 Hz, 1H), 3.00 (dd, J = 13.6 Hz, 6.3 Hz, 1H), 3.12 (ddd, J = 12.7 Hz, 7.2 Hz, 3.0 Hz, 1H), 3.34 (ddd, J = 12.7 Hz, 10.1 Hz, 2.8 Hz, 1H), 7.21 (d, J = 0.9 Hz, 1H), 7.48–7.53 (m, 2H), 7.72 (d, J = 8.5 Hz, 1H), 7.83–7.88 (m, 3H), 8.07 (s, 1H). $^{13}\text{C}\{\text{H}\}$ NMR (125 MHz, CDCl_3): δ 23.1, 25.8, 27.3, 27.8, 30.6, 62.0, 123.9, 124.9, 125.9, 126.7, 127.0, 127.9, 128.4, 129.0, 130.9, 133.3, 133.6, 140.5, 146.3, 149.2. HRMS (APCI): m/z Calcd. for $\text{C}_{20}\text{H}_{21}\text{OS}_2$: 341.1028 ($[M+\text{H}]^+$). Obsd. 341.1026.

(S)-10. This compound was prepared in a similar manner as described for (S)-**2** using **5** (57 mg, 0.18 mmol), (S)-**3** (1.71 mg, 3.6 μmol), $\text{VO}(\text{acac})_2$ (0.48 mg, 1.8 μmol), 30% H_2O_2 aq. (27 μL , 0.26 mmol) in CH_2Cl_2 (1.8 mL). Purification by silica gel column chromatography (CH_2Cl_2 /ethyl acetate 9/1 as eluent, R_f = 0.35) afforded 53 mg of (S)-**10** as white solids (0.15 mmol, 88% yield, 93 % ee). Mp (MP-S3): 64.8–65.3 °C (for the sample with 93% ee). ^1H and ^{13}C NMR spectra were identical to those of *rac*-**10**. The result of the HPLC analysis is shown in Figure S42. $[\alpha]_{\text{D}}^{20} = +174.2$ (c = 0.25 g/L in CHCl_3 using the sample with >99% ee after purification by chiral HPLC).

2-(Anthracen-2-yl)-4,5,6,7,8,9-hexahydrothieno[2,3-*b*]thionine *S*-oxide (*rac*-11**).** This compound was prepared in a similar manner as described for *rac*-**2** using **6** (55 mg, 0.15 mmol) and 30% H_2O_2 aq. (27 μL , 0.26 mmol) in CH_2Cl_2 (2.1 mL) and TFE (0.7 mL). Purification by silica gel column chromatography (CH_2Cl_2 to CH_2Cl_2 /ethyl acetate 9/1 as eluent, R_f = 0.35 (CH_2Cl_2 /ethyl acetate 9/1)) afforded 52 mg of *rac*-**11** as pale yellow solids (0.13 mmol, 91% yield). Mp (MP-S3): 186.9–187.9 °C. ^1H NMR (500 MHz, CD_2Cl_2): δ 1.18–1.26 (m, 1H), 1.28–1.36 (m, 1H), 1.37–1.45 (m, 2H), 1.54–1.57 (m, 1H), 1.74–1.83 (m, 1H), 1.88–1.95 (m, 1H), 2.03 (dddd, J = 19.6 Hz, 10.1 Hz, 4.9 Hz, 2.5 Hz, 1H), 2.63 (ddd, 1H, J = 14.1 Hz, 11.5 Hz, 2.7 Hz, 1H), 3.02 (ddd, J = 14.0 Hz, 6.7 Hz, 2.4 Hz, 1H), 3.08 (ddd, J = 12.7 Hz, 7.1 Hz, 3.0 Hz, 1H), 3.31 (ddd, J = 13.0 Hz, 10.2 Hz, 2.9 Hz, 1H), 7.31 (s, 1H), 7.48–7.52 (m, 2H), 7.75 (dd, J = 8.8 Hz, 1.8 Hz, 1H), 8.01–8.04 (m, 2H), 8.07 (d, J = 9.2 Hz, 1H), 8.28 (d, J = 0.9 Hz, 1H), 8.44 (s, 1H), 8.47 (s, 1H). $^{13}\text{C}\{\text{H}\}$ NMR (125 MHz, CD_2Cl_2): δ 23.3, 26.0, 27.5, 28.0, 30.8, 62.4, 123.9, 124.9, 126.2, 126.3, 126.5, 126.6, 127.1, 128.49, 128.55, 129.5, 130.6, 131.4, 131.8, 132.5, 132.7, 141.2, 146.7, 149.0. HRMS (APCI): m/z Calcd. for $\text{C}_{24}\text{H}_{23}\text{OS}_2$: 391.1185 ($[M+\text{H}]^+$). Obsd. 391.1184.

(S)-11. This compound was prepared in a similar manner as described for (S)-**2** using **6** (105 mg, 0.28 mmol), (S)-**3** (2.8 mg, 5.9 μmol), $\text{VO}(\text{acac})_2$ (0.90 mg, 3.4 μmol), 30% H_2O_2 aq. (43 μL , 0.42 mmol) in CH_2Cl_2 (3.0 mL). Purification by silica gel column chromatography (hexane/ CH_2Cl_2 /ethyl acetate 1/1/0 to 1/3/0, 0/1/1 as eluent, R_f = 0.30 (CH_2Cl_2 /ethyl acetate 9/1)) afforded 78 mg of (S)-**11** as yellow solids (0.20 mmol, 71% yield, 86 % ee). Mp (MP-S3): 105.1–106.0 °C (for the sample with 86% ee). ^1H and ^{13}C NMR spectra were identical with those of *rac*-**11**. The result of HPLC analysis is shown in Figure S43. $[\alpha]_{\text{D}}^{20} = +207.2$ (c = 1.04 g/L in CHCl_3 using the sample with >99% ee after purification by chiral HPLC).

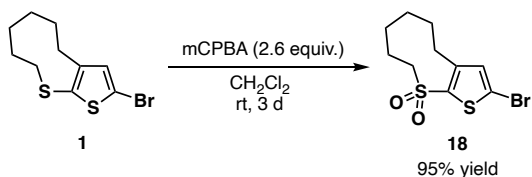
2-(Pyren-1-yl)-4,5,6,7,8,9-hexahydrothieno[2,3-*b*]thionine *S*-oxide (*rac*-12). This compound was prepared in a similar manner as described for *rac*-2 using 7 (51 mg, 0.13 mmol) and 30% H₂O₂ aq. (20 μL, 0.20 mmol) in CH₂Cl₂ (1.5 mL) and TFE (1.5 mL). Purification by silica gel column chromatography (hexane/CH₂Cl₂ 1/1 to 1/2 as eluent, *R*_f = 0.20 (CH₂Cl₂/ethyl acetate 9/1)) afforded 54 mg of *rac*-12 as pale yellow solids (0.13 mmol, quant.). Mp (MP-S3): 178.8–179.5 °C. ¹H NMR (500 MHz, CDCl₃): δ 1.31–1.41 (m, 2H), 1.48–1.52 (m, 2H), 1.64–1.66 (m, 1H), 1.86–1.91 (m, 1H), 1.98–2.10 (m, 2H), 2.72 (ddd, *J* = 14.1 Hz, 11.5 Hz, 2.5 Hz, 1H), 3.09 (ddd, *J* = 14.2 Hz, 6.9 Hz, 2.4 Hz, 1H), 3.21 (ddd, *J* = 12.7 Hz, 7.2 Hz, 3.0 Hz, 1H), 3.39 (ddd, *J* = 13.0 Hz, 10.2 Hz, 2.9 Hz, 1H), 7.14 (s, 1H), 8.05 (t, *J* = 7.6 Hz, 1H), 8.08–8.14 (m, 4H), 8.19–8.24 (m, 3H), 8.45 (d, *J* = 9.5 Hz, 1H). ¹³C{¹H} NMR (125 MHz, CDCl₃): δ 23.1, 25.8, 27.3, 27.9, 30.5, 62.0, 124.5, 124.72, 124.73, 125.1, 125.4, 125.8, 126.4, 127.4, 128.2, 128.3, 128.5, 128.7, 129.0, 130.5, 130.9, 131.5, 131.6, 141.7, 145.6, 147.8. HRMS (APCI): *m/z* Calcd. for C₂₆H₂₂OS₂: 415.1185 ([M+H]⁺). Obsd. 415.1183.

(S)-12. This compound was prepared in a similar manner as described for (S)-2 using 7 (121 mg, 0.30 mmol), (S)-3 (3.0 mg, 6.3 μmol), VO(acac)₂ (0.90 mg, 3.4 μmol), 30% H₂O₂ aq. (47 μL, 0.46 mmol) in CH₂Cl₂ (3.5 mL). Purification by silica gel column chromatography (hexane/CH₂Cl₂/ethyl acetate 1/1/0 to 0/1/0, 0/93/7 as eluent, *R*_f = 0.20 (CH₂Cl₂/ethyl acetate 9/1)) afforded 98 mg of (S)-12 as yellow solids (0.24 mmol, 78% yield, 86 % ee). Mp (MP-S3): 114.8–115.3 °C (for the sample with >99% ee). ¹H and ¹³C NMR spectra were identical with those of *rac*-12. The result of HPLC analysis is shown in Figure S44. [α]_D²⁰ = +85.7 (*c* = 0.55 g/L in CHCl₃ using the sample with >99% ee after purification by chiral HPLC).

2-[6-{3,4,5-Tris(dodecyloxy)phenyl}naphthalen-2-yl]-4,5,6,7,8,9-hexahydrothieno[2,3-*b*]thionine *S*-oxide (*rac*-13). This compound was prepared in a similar manner as described for *rac*-2 using 8 (139 mg, 0.15 mmol) and 30% H₂O₂ aq. (27 μL, 0.26 mmol) in CH₂Cl₂ (1.4 mL) and TFE (0.7 mL). Purification by silica gel column chromatography (CH₂Cl₂ to CH₂Cl₂/ethyl acetate 9/1 as eluent, *R*_f = 0.45) afforded 99 mg of *rac*-13 as highly viscous colorless liquids (0.10 mmol, 70% yield). Mp (DSC): 67.6 °C. ¹H NMR (500 MHz, CDCl₃): δ 0.88 (td, *J* = 6.9 Hz, 2.9 Hz, 9H), 1.27–1.41 (m, 53H), 1.48–1.60 (m, 6H), 1.76–1.88 (m, 7H), 1.89–1.94 (m, 1H), 2.00–2.07 (m, 1H), 2.62 (ddd, *J* = 14.0 Hz, 11.6 Hz, 2.4 Hz, 1H), 3.00 (ddd, *J* = 14.2 Hz, 6.7 Hz, 2.3 Hz, 1H), 3.13 (ddd, *J* = 12.7 Hz, 7.2 Hz, 2.9 Hz, 1H), 3.34 (ddd, *J* = 12.8 Hz, 10.2 Hz, 2.8 Hz, 1H), 4.02 (t, *J* = 6.6 Hz, 2H), 4.08 (dd, *J* = 12.7 Hz, 6.0 Hz, 4H), 6.89 (s, 2H), 7.22 (s, 1H), 7.74 (dq, *J* = 8.6 Hz, 1.7 Hz, 2H), 7.90 (q, *J* = 4.4 Hz, 2H), 7.96 (s, 1H), 8.08 (s, 1H). ¹³C{¹H} NMR (125 MHz, CDCl₃): δ 14.3, 22.8, 23.1, 25.8, 26.30, 26.32, 27.3, 27.8, 29.51, 29.55, 29.59, 29.7, 29.8, 29.86, 29.90, 29.92, 30.5, 32.08, 32.10, 106.4, 124.4, 124.6, 125.4, 125.9, 126.7, 128.8, 129.1, 130.8, 132.7, 133.5, 136.2, 138.5, 139.7, 140.5, 146.3, 149.1, 153.7, several signals assignable to the carbon atoms of the alkyl chains were not observed due to overlap to the other signals. HRMS (APCI): *m/z* Calcd. for C₆₂H₉₇O₄S₂: 969.6823 ([M+H]⁺). Obsd. 969.6827.

(S)-13. This compound was prepared in a similar manner as described for (S)-2 using 8 (95 mg, 0.10

mmol), (*S*)-**3** (1.2 mg, 2.5 μ mol), VO(acac)₂ (0.50 mg, 1.9 μ mol), 30% H₂O₂ aq. (15 μ L, 0.15 mmol) in CH₂Cl₂ (2.0 mL). Purification by silica gel column chromatography (CH₂Cl₂ to CH₂Cl₂/ethyl acetate 95/5 as eluent, R_f = 0.45 (CH₂Cl₂/ethyl acetate 9/1)) afforded 65 mg of (*S*)-**13** as white solids (0.068 mmol, 67% yield, 97 % *ee*). Mp (DSC): 67.6 °C (for the sample with >99% *ee*). ¹H and ¹³C NMR spectra were identical with those of *rac*-**13**. The result of HPLC analysis is shown in Figure S45. $[\alpha]_D^{20} = -1.9$ ($c = 0.28$ g/L in CHCl₃ using the sample with >99% *ee* after purification by chiral HPLC).



Scheme S3. Synthesis of the sulfone derivatives of TN-capped 2-bromothiophene **18**

Preparation of the Sulfone Derivative of TN-Capped Bromothiophene as a Reference Compound.
Synthesis of 2-bromo-4,5,6,7,8,9-hexahydrothieno[2,3-*b*]thionine *S,S*-dioxide (18). To a solution of **1** (52 mg, 0.19 mmol) in anhydrous CH₂Cl₂ (0.6 mL) was added wet mCPBA (containing 28 wt% water, 107 mg, 0.48 mmol). After stirring for 3 days at an ambient temperature, the resulting mixture was quenched by sat. Na₂SO₃ aq., and the aqueous layer was extracted with CH₂Cl₂ three times. The combined organic layer was washed with brine, dried over anhydrous Na₂SO₄, filtered, and concentrated under reduced pressure to afford 55 mg of analytically pure **18** as white solids (0.18 mmol, 95% yield). Mp (MP-S3): 121.3–122.1 °C. ¹H NMR (400 MHz, CDCl₃): δ 1.18–1.22 (m, 2H), 1.56–1.62 (m, 2H), 1.73–1.80 (m, 2H), 2.24–2.30 (m, 2H), 3.07 (t, J = 6.9 Hz, 2H), 3.30–3.33 (m, 2H), 6.92 (s, 1H). ¹³C{¹H} NMR (100 MHz, CDCl₃): δ 20.9, 21.7, 27.5, 28.2, 29.2, 57.1, 120.5, 133.3, 138.9, 148.5. HRMS (ESI): *m/z* Calcd. for C₁₀H₁₃O₂S₂BrNa: 330.9438 ([M+Na]⁺). Obsd. 330.9431.

3. VT-NMR Spectra

Method. Variable-temperature (VT) ¹H NMR spectra of **1** were measured between 20 °C and –80 °C in CD₂Cl₂ with a JEOL ECA 400 II spectrometer (400 MHz) (Figure S1).

The ¹H NMR signals of **1** thus obtained were assigned based on the comparison with the simulated NMR chemical shifts by GIAO method at B3LYP/6-31+G(d) level of theory implemented in the Gaussian16 Revision B.01^{S14} using the optimized geometry of **1** at the same level of theory was used. The stationary points were optimized without any symmetry assumptions and characterized by frequency analysis at the same level of theory (the number of imaginary frequencies was 0). For GIAO calculations, the CH₂Cl₂ solvent effect was taken into account by using the polarizable continuum model (PCM). The default thresholds and algorithms were used for all the computations. The cartesian coordinates for the optimized geometry and the calculated NMR chemical shifts are given in Tables S1 and S2.

Results and Discussion. The methylene protons in the 9-membered ring were initially observed as five multiplet signals at 20 °C, of which three signals showed line broadening upon cooling. The most pronounced change was observed for the signal at around $\delta = 2.90$ ppm, assignable to the protons H^a, H^b, H^c, and H^d in Figure S1. This signal began to split into two broad signals at –30 °C, coalesced at –60 °C (213 K), and further split into three distinct signals with $\delta = 3.14$ ppm (H^b and H^d), 2.63 ppm (H^c), and 2.51 ppm (H^a) at –85 °C. These results indicate that the flipping process of the 9-membered ring is suppressed below –60 °C. Based on these results, the activation free energy for racemization, ΔG^\ddagger , was estimated based on the coalescence method by using the following equations:

$$k_{T_c} = \frac{\pi}{\sqrt{2}} \Delta\nu = \frac{RT}{N_A \cdot h} e^{-\frac{\Delta G^\ddagger}{RT}} \quad (1)$$

$$\Delta G^\ddagger = RT_c \cdot \ln \frac{\sqrt{2}RT_c}{\pi \cdot N_A \cdot h \cdot \Delta\nu} \quad (2)$$

where $\Delta\nu$, R , T_c , N_A , and h represent the difference in the chemical shifts (in Hz) of the two signals without exchange, the gas constant, the coalescence temperature, the Avogadro number, and the Planck constant, and k_{T_c} represents the rate constant at $T = T_c$. As a result, ΔG^\ddagger was calculated to be 9.7 kcal mol⁻¹. This small ΔG^\ddagger value, which is comparable with that of cyclohexane ($\Delta G^\ddagger = 10.3$ kcal mol⁻¹),^{S15} demonstrates the high conformational flexibility of a sulfide-based TN moiety. The rate constant for the ring inversion at 293 K (k_{inv}) was estimated to be as large as 3.9×10^5 M s⁻¹, which indicates that the k_{inv} value is substantially larger than the rate constant of the oxidation of **1**. These results strongly support that the dynamic kinetic resolution is likely possible in the asymmetric oxidation of **1** (Scheme S4).

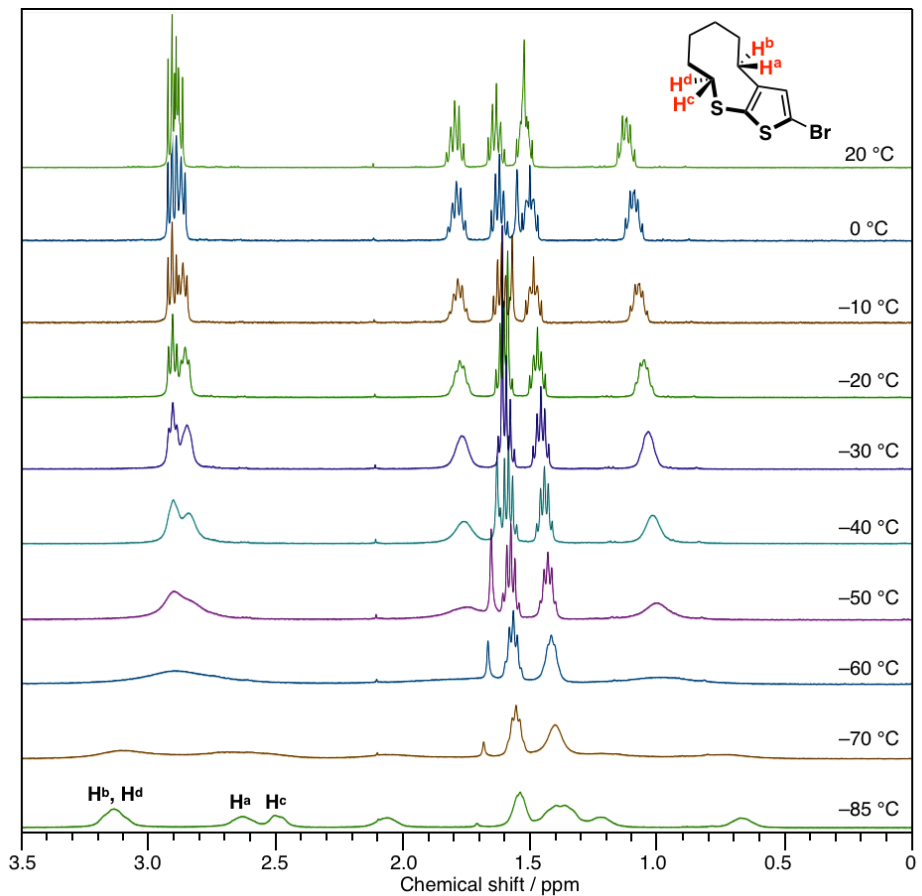
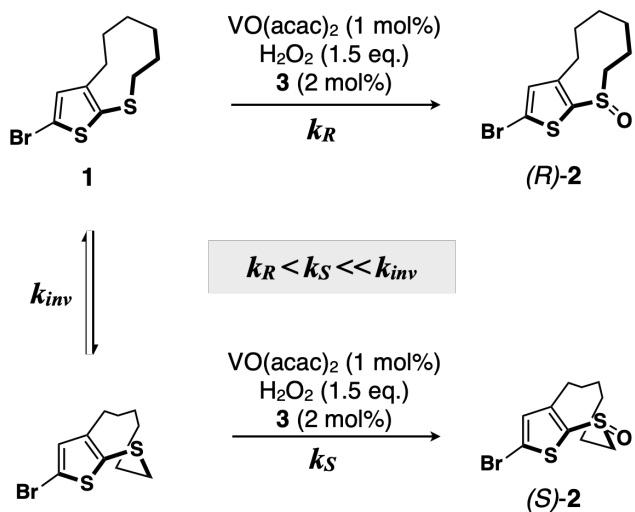


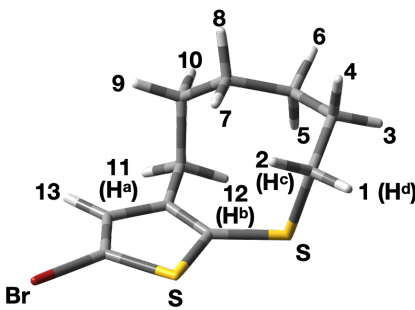
Figure S1. VT- ^1H NMR spectra of **1** in CD_2Cl_2 (400 MHz).



Scheme S4. Schematic representation of the dynamic kinetic resolution in the asymmetric oxidation of **1**.

Table S1. Cartesian coordinates (Å) of the optimized geometry for **1**

Br	3.72910445	0.14719677	-0.35535795
S	1.04248463	-1.44558538	0.09957529
S	-1.88896105	-1.60971630	0.88067321
C	-0.23551499	0.72163932	0.78218423
C	1.89942552	0.06182883	0.09613350
C	-0.43457307	-0.63673570	0.61790614
C	1.11046832	1.11201738	0.47375505
H	1.46906275	2.13338782	0.54552270
C	-2.70413489	-1.59592777	-0.79957124
H	-1.92419350	-1.31108730	-1.50953237
H	-2.96708376	-2.63794084	-1.00696812
C	-2.66140128	1.55525599	-0.98913143
H	-1.90571199	0.89285707	-1.42805456
H	-3.02889282	2.17272408	-1.81918686
C	-1.96485438	2.46739365	0.03535518
H	-2.69347145	3.17020931	0.46375705
H	-1.21140997	3.07710574	-0.48155427
C	-1.28442608	1.71870712	1.21014637
H	-0.81599274	2.46292893	1.86644459
H	-2.03925681	1.20493639	1.81279020
C	-3.82740537	0.72857346	-0.39857181
H	-3.72989106	0.67352661	0.69101055
H	-4.77685408	1.24790799	-0.58370120
C	-3.95444250	-0.70903015	-0.92698276
H	-4.21940736	-0.69943150	-1.99544719
H	-4.79077782	-1.19651700	-0.40886772

Table S2. Chemical shifts of **1** simulated by GIAO-NMR method ^a

Proton	Chemical Shift ^a	Proton	Chemical shift ^a
1	3.2244	8	1.4081
2	2.7482	9	1.6077
3	1.67945	10	1.6077
4	1.67945	11	2.5501
5	2.2519	12	3.2244
6	1.5216	13	6.8344
7	1.0719		

^a Calculated at B3LYP/6-31+G* level of theory with PCM model (CH₂Cl₂). ^b Referenced with the value of tetramethylsilane (Me₄Si) calculated at the same level of theory.

4. Photophysical Properties

UV/Vis absorption spectra were measured with a Shimadzu UV-3600 spectrophotometer with a resolution of 0.2 nm using dilute sample solutions in spectral grade solvents in a 1 cm square quartz cuvette. Photoluminescence spectra were measured with a JASCO FP-6600 fluorescence spectrophotometer with a resolution of 0.6 nm. The electronic circular dichroism (ECD) spectra were recorded with a JASCO J-720WI spectrophotometer. The resulting spectra are shown in Figures 2a, S2, and S3, and the sample concentrations and photophysical data were summarized in Table S3.

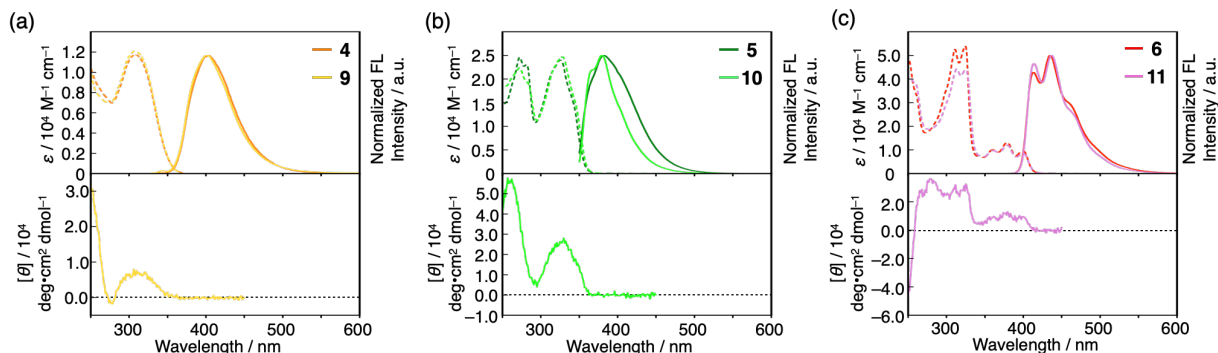


Figure S2. UV/vis absorption (broken line, top) and photoluminescence spectra (solid line, top) of (a) **4** and (*S*)-**9**, (b) **5** and (*S*)-**10**, (c) **6** and (*S*)-**11** in THF at ambient temperature. The corresponding electronic circular dichroism (ECD) spectra of enantiomerically pure sulfoxides (*S*)-**9**, **10**, and **11**, which were purified by chiral HPLC prior to the measurements, are given in the bottom panels.

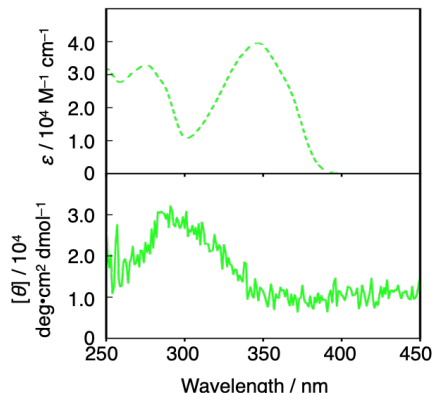


Figure S3. UV/vis absorption (top) and electronic circular dichroism (ECD) spectra (bottom) of (*S*)-**13** in THF ($c = 1.19 \times 10^{-5}$ M). The enantiomerically pure (*S*)-**13**, purified by chiral HPLC, was used for the measurements.

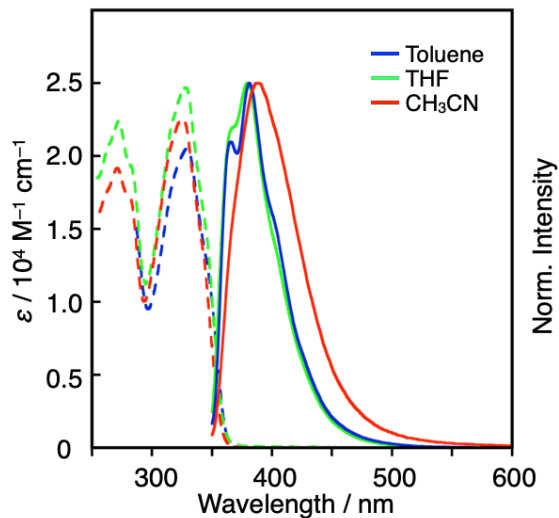


Figure S4. UV/vis absorption (broken lines) and fluorescence spectra (solid lines) of **10** in toluene (blue), THF (green), and CH₃CN (red).

Table S3. Summary of Photophysical Data of **4–13**.

Cmpd	Solvent	Concentration / 10 ⁵ M	UV/Vis Absorption		Fluorescence
			λ _{abs} / nm ^a	ε / 10 ⁴ M ⁻¹ cm ⁻¹ ^b	λ _{em} / nm ^c
4	THF	1.18	308	1.18	404
5	THF	1.48	325	2.40	382
6	THF	1.57	399	0.97	413
7	THF	2.12	348	3.00	434
8	toluene	4.05	344	3.41	409
	CH ₂ Cl ₂	2.94	344	3.77	420
	acetone	2.90	342	3.97	429
	CH ₃ CN	n.d. ^d	341	n.d.	448
9	THF	3.79	308	1.21	401
10	toluene	3.11	329	2.05	381
	THF	1.41	328	2.47	380
	CH ₃ CN	4.60	325	2.26	387
11	THF	1.11	399	0.86	414
12	THF	2.53	347	2.91	421
13	toluene	2.56	346	3.74	415
	CH ₂ Cl ₂	1.35	346	3.49	464
	acetone	1.85	345	3.67	466
	CH ₃ CN	n.d. ^d	345	n.d.	481

^aAbsorption maximum wavelength of the longest-wavelength absorption band. ^bMolar extinction coefficient.

^cFluorescence maximum wavelength. ^dNot determined because of the lack of accuracy due to poor solubility.

5. Quantum Chemical Calculations

Computational Methods. The geometry optimizations for the π -electron system bearing TN-fused thienyl group **4–7** and **8'** and corresponding sulfoxide **9–12** and **13'** were carried out at B3LYP/6-31+G(d) level of theory implemented in the Gaussian16 Revision B.01^{S14} with default thresholds and algorithms. The stationary points were optimized without any symmetry assumptions and characterized by frequency analysis at the same level of theory (the number of imaginary frequencies was 0). The cartesian coordinates for the optimized geometries are given in Tables S4–13. Time-dependent (TD)-DFT vertical excitation energy calculations for the optimized geometries of **4–7**, **8'**, **9–12**, and **13'** were performed at the TD-B3LYP/6-31+G(d) level of theory as well. The results are summarized in Figure S5.

Discussion. The TD-DFT calculations demonstrated that the lowest-energy ($S_0 \rightarrow S_1$) transitions for a series of TN-capped π -electron systems **4–7** and **8'**, and the corresponding sulfoxides **9–12** and **13'** are attributable to HOMO–LUMO transitions. The spatial distribution of the HOMOs and LUMOs of these compounds could be characterized to be π and π^* orbitals delocalized over the π -conjugated skeletons (Figure S5). Notably, the $S_0 \rightarrow S_1$ transitions of the TN-capped π -electron systems **4–7** without 1,3,5-trialkoxyphenyl group exhibited almost comparable oscillator strengths (f) with those of the corresponding sulfoxides **9–12**, consistent with their spatial distribution of HOMOs and LUMOs remains virtually unchanged even upon sulfur oxidation. This negligible effect of the sulfur oxidation should be ascribed to the suppression of the electron-donating character of the endocyclic sulfur atom in sulfide-based TN by the stereoelectronic effect of nine-membered ring, as has already demonstrated in our previous report.^{S12} The decrease of the HOMO and LUMO energy levels upon sulfur oxidation can be best explained by the enhanced –I effect.

On the other hand, the f value of TN-capped thiénylnaphthalene bearing a 1,3,5-trialkoxyphenyl group, **8'** and **(S)-13'**, decreased upon oxidation of a sulfide to a sulfoxide to a greater extent than the other derivatives. In addition, the LUMOs of these compounds **8'** and **(S)-13'** are localized on the thiénylnaphthalene moiety, while their HOMOs are delocalized over the entire π -conjugated framework. These results indicate the weak intramolecular charge-transfer (ICT) character in the lowest-energy transitions of **8'** and **(S)-13'**, which are consistent with their solvatofluorochromic behaviours observed experimentally. Moreover, the larger solvatofluorochromism **(S)-13'** than **8'** supported that the enhancement of ICT character upon sulfur oxidation.

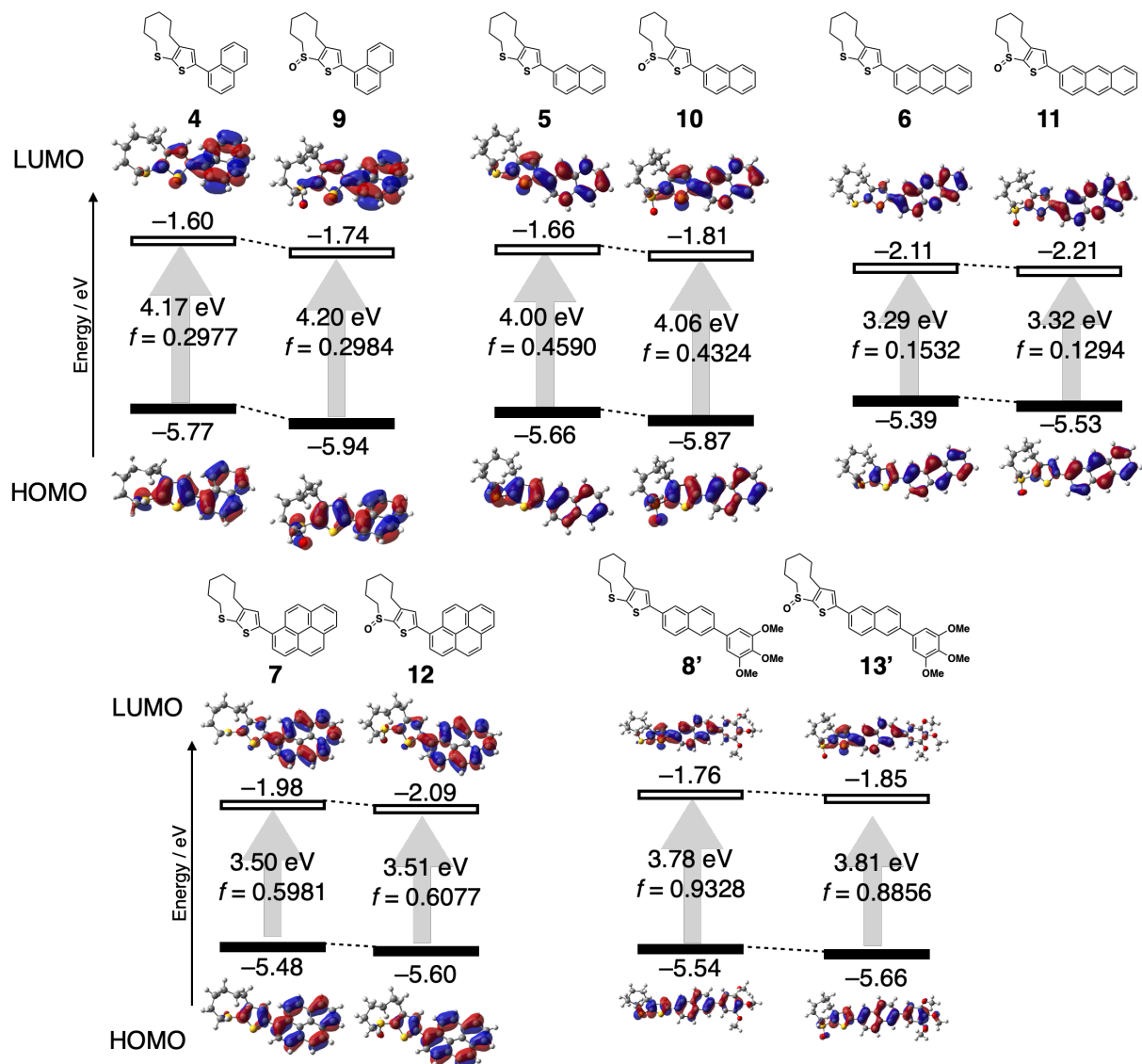


Figure S5. Orbital energy diagrams, the pictorial representations of the Kohn–Sham frontier molecular orbitals, and TD-DFT vertical excitation energies and the oscillator strengths (f) for the lowest energy transitions of **4–7**, **8'**, **9–12**, and **13'** calculated at the TD-B3LYP/6-31+G* level of theory.

Table S4. Cartesian coordinates (Å) of the optimized geometry for **4**

H	3.90580254	3.19297488	-1.60823283
C	4.10045866	2.27735467	-1.05547864
H	2.05090878	1.67838472	-1.06727363
C	3.05676929	1.42962191	-0.74759774
C	5.67717038	0.78430268	0.00419948
C	3.27601118	0.21750609	-0.03393073
C	5.42452401	1.96034864	-0.66657465
C	4.62593243	-0.11831809	0.32748173
C	2.21790956	-0.69734295	0.31133601
H	6.23838825	2.63867627	-0.90943867
H	5.91967469	-1.59043641	1.25087205
H	6.69293981	0.52174050	0.29207816
C	2.53798529	-1.89542784	0.93608826
H	1.73882961	-2.58232978	1.20109504

C	3.87056409	-2.22655686	1.26923838
H	4.07758774	-3.17045079	1.76663639
C	4.89298993	-1.35001235	0.98389721
C	0.06937262	0.72860933	0.35784451
H	0.49730389	1.56291885	0.90600337
C	0.80198972	-0.39018309	0.02339695
C	-1.29751403	0.69452932	-0.05448762
C	-1.60773336	-0.48433927	-0.71095315
S	-0.21226798	-1.53832862	-0.81425669
S	-3.14285192	-0.97754176	-1.43554936
C	-2.29707471	1.78440364	0.24514515
H	-2.93283233	1.91969267	-0.63604632
H	-1.76333473	2.73145311	0.38742152
C	-3.18309601	1.48838915	1.49492602
H	-3.00578368	0.46165046	1.82944399
H	-2.85393792	2.12295962	2.32823493
C	-4.18164375	-1.40061113	0.05654312
H	-4.44561851	-2.45941675	-0.03823461
H	-3.52749996	-1.30697870	0.92412057
C	-5.47128746	-0.57177072	0.19927199
H	-5.93970579	-0.87386637	1.14936436
H	-6.16581064	-0.89205288	-0.58968675
C	-5.38331264	0.96500940	0.13263746
H	-6.41660059	1.33601781	0.08366964
H	-4.92644741	1.24816971	-0.82268553
C	-4.69469157	1.71427622	1.29132845
H	-5.20799042	1.46686667	2.23271504
H	-4.86589709	2.78922002	1.13096686

Table S5. Cartesian coordinates (Å) of the optimized geometry for **5**

C	-0.29218270	0.69356208	-0.72044762
H	0.13066996	1.63599056	-1.05613034
C	0.48996517	-0.36462364	-0.30395162
C	-1.69405263	0.43143217	-0.73945227
C	-1.98276525	-0.85466827	-0.31470113
S	-0.52339499	-1.72629778	0.10935012
S	-3.55091730	-1.66008328	-0.19975673
C	-2.73756589	1.44445737	-1.14087803
H	-3.50207980	0.93469507	-1.73633227
H	-2.27805376	2.18784406	-1.80283821
C	-3.40533586	2.16332813	0.07252720
H	-3.08461078	1.68128461	1.00125851
H	-3.02466757	3.19124051	0.13617060
C	-4.31575271	-0.85074147	1.29834396
H	-4.48614015	-1.64854586	2.02921328
H	-3.55418779	-0.18966716	1.71327618
C	-5.64509186	-0.12258378	1.02909085
H	-5.93882863	0.36210994	1.97358011
H	-6.41262594	-0.88446119	0.83465903
C	-5.71636489	0.90033637	-0.12065483
H	-6.77693167	1.16089535	-0.24310092
H	-5.43000168	0.39937500	-1.05263078
C	-4.94526499	2.22775254	0.02556918
H	-5.29419543	2.74636706	0.93120902
H	-5.23931903	2.86935517	-0.81846621
C	1.95391245	-0.42378765	-0.19611887
H	2.17781398	1.66568794	0.24296562

C	2.69036199	0.72221988	0.07168599
C	4.02576752	-1.71244944	-0.28324701
C	4.10613552	0.69802352	0.15755001
C	2.65467633	-1.65647671	-0.36952723
C	4.79597749	-0.54588232	-0.02172213
C	4.86733510	1.87013728	0.42834454
H	2.09303543	-2.55921497	-0.59420616
H	6.73290608	-1.51459879	-0.06879493
H	4.54001537	-2.66052029	-0.42542171
C	6.24224574	1.81607234	0.51142127
H	4.34462094	2.81402045	0.56803944
H	6.81092051	2.71932031	0.71728963
C	6.92321690	0.58516921	0.32968340
H	8.00760866	0.55499253	0.39743552
C	6.21362392	-0.56862316	0.06970608

Table S6. Cartesian coordinates (Å) of the optimized geometry for **6**

C	-1.36690649	0.50207158	-0.80410566
H	-0.86643077	1.37458091	-1.21381215
C	-0.67643178	-0.59768497	-0.33498995
C	-2.78676509	0.37695789	-0.77122477
C	-3.18410692	-0.84484738	-0.25355194
S	-1.80270049	-1.82538113	0.19231704
S	-4.81760318	-1.48564953	-0.04986541
C	-3.74092556	1.45795588	-1.21543632
H	-4.56727287	0.98702909	-1.75788216
H	-3.23263236	2.10962420	-1.93578263
C	-4.30183195	2.31386657	-0.03746769
H	-4.00214712	1.86270663	0.91347719
H	-3.82291590	3.30180995	-0.05026247
C	-5.45962841	-0.51136885	1.40712557
H	-5.68388944	-1.24020513	2.19337586
H	-4.62760065	0.09893649	1.75989442
C	-6.72132805	0.32219138	1.11866799
H	-6.94181256	0.89215080	2.03507080
H	-7.56237147	-0.37342258	0.99164109
C	-6.72762214	1.27182974	-0.09445886
H	-7.76152330	1.62595809	-0.20986428
H	-6.51747564	0.68718502	-0.99757308
C	-5.82922533	2.52461312	-0.05359192
H	-6.10055356	3.13090403	0.82371612
H	-6.08505951	3.13704625	-0.93106711
C	0.77659798	-0.79031804	-0.25504114
H	1.21535839	1.28863503	0.01834267
C	1.62548348	0.28792354	-0.09285569
C	2.70256091	-2.29776365	-0.29147537
C	3.04263345	0.13132070	-0.03744636
C	1.34896673	-2.10646594	-0.34921063
C	3.60336274	-1.19653709	-0.13727377
C	3.90803959	1.22411469	0.12224751
H	0.69055874	-2.95930756	-0.49014167
H	5.41178904	-2.36220446	-0.15674661
H	3.11483911	-3.30113690	-0.37254032
C	5.29926675	1.06162720	0.18108526
H	3.48815232	2.22548727	0.20110950
C	6.19195268	2.16905122	0.34122147
C	5.85841760	-0.26773181	0.07644955

H	7.69812131	-1.42191074	0.05790639
C	4.99233812	-1.36050601	-0.07942602
C	7.54983891	1.97962869	0.39459344
H	5.77067240	3.16897038	0.42013048
H	8.21500905	2.83065501	0.51640760
C	8.10132807	0.66726844	0.29095923
H	9.17931991	0.53529879	0.33507885
C	7.27943860	-0.42091357	0.13692200

Table S7. Cartesian coordinates (Å) of the optimized geometry for **7**

C	1.20680149	-0.59428530	0.40384553
H	0.72085571	-1.30563370	1.06526777
C	0.54659714	0.49662911	-0.12144209
C	2.58084531	-0.70070727	0.03040406
C	2.97313508	0.34233004	-0.79114230
S	1.64505132	1.44325864	-1.09673410
S	4.55009281	0.63267500	-1.53510586
C	3.50859925	-1.78268957	0.52589624
H	4.15524425	-2.08794948	-0.30331090
H	2.91770546	-2.66577900	0.79607846
C	4.38172256	-1.34318869	1.74216617
H	4.25579136	-0.26900689	1.90918466
H	3.99816292	-1.82226219	2.65254129
C	5.57593099	1.22897803	-0.09398379
H	5.90140648	2.24476664	-0.34289034
H	4.89706820	1.30611466	0.75603256
C	6.81281640	0.36644690	0.21672666
H	7.27463594	0.78829886	1.12341942
H	7.54304819	0.52295244	-0.58927950
C	6.63929336	-1.15511419	0.38545145
H	7.65068507	-1.58291988	0.42756324
H	6.18982533	-1.55927004	-0.52896180
C	5.88223931	-1.67746478	1.62330789
H	6.38696318	-1.31397589	2.53105863
H	5.99564194	-2.77176729	1.63605287
H	-0.26578052	2.91578311	0.63312974
C	-1.10646483	2.24371819	0.48434064
C	-0.85204841	0.92182042	0.07678630
C	-3.49923989	1.84124475	0.59689017
C	-1.94922349	0.03710122	-0.11822167
C	-2.39499855	2.69712465	0.73747251
C	-3.27763848	0.49904737	0.15910452
C	-1.79434665	-1.30458682	-0.61700994
H	-2.55310948	3.72195267	1.065557597
C	-2.86274469	-2.13571298	-0.78240367
H	-0.80126732	-1.64845180	-0.88298568
H	-2.71418444	-3.14125277	-1.17013586
C	-4.19897702	-1.71448552	-0.47029693
C	-5.31050547	-2.56170551	-0.62298298
C	-4.39589703	-0.37769567	-0.00766857
C	-6.59685038	-2.10969830	-0.32878574
H	-5.15662820	-3.57857459	-0.97709038
H	-7.44562454	-2.77756460	-0.45151130
C	-6.80135198	-0.80389333	0.11834630
H	-7.80722342	-0.45574038	0.34225855
C	-5.71995600	0.07902331	0.28340602
C	-4.84005188	2.27438863	0.87857320

H	-4.99104916	3.29796504	1.21426536
C	-5.90166345	1.43219908	0.73304589
H	-6.91060915	1.77443406	0.95222156

Table S8. Cartesian coordinates (Å) of the optimized geometry for **8'**

C	-4.02389989	0.22234863	-0.97974373
H	-3.58408773	0.85645766	-1.74401799
C	-3.26074924	-0.52144723	-0.10228924
C	-5.43270546	0.04294425	-0.84959483
C	-5.74647741	-0.85073622	0.16084110
S	-4.30128385	-1.45630038	0.94453677
S	-7.33304510	-1.43190241	0.67641771
C	-6.45710361	0.76476920	-1.68977684
H	-7.25198557	0.05728658	-1.94773193
H	-5.99445341	1.06520030	-2.63721988
C	-7.07044597	2.01473793	-0.98541857
H	-6.73879646	2.04290053	0.05706798
H	-6.65851662	2.92405794	-1.44257263
C	-8.03397106	0.04180341	1.58252467
H	-8.20767016	-0.28205989	2.61433952
H	-7.24303343	0.79213657	1.60827305
C	-9.34876512	0.59025220	0.99905524
H	-9.60431672	1.48945968	1.58162803
H	-10.14216289	-0.13883228	1.21430996
C	-9.42104734	0.91172933	-0.50593539
H	-10.47658154	1.11768837	-0.73202821
H	-9.17397290	0.00466835	-1.06966123
C	-8.60848208	2.10698697	-1.04358656
H	-8.91744761	3.01861945	-0.51035074
H	-8.90687841	2.25794115	-2.09176084
C	-1.79701530	-0.58065932	0.00118128
H	-1.49364970	1.43517572	-0.67530887
C	-1.01682800	0.51190953	-0.35534540
C	0.23192698	-1.82603509	0.54664832
C	0.39806957	0.47111134	-0.28814064
C	-1.13904855	-1.76117602	0.46400958
C	1.04578854	-0.72156468	0.16946193
C	1.21152138	1.58151517	-0.64909386
H	-1.73451855	-2.62895482	0.73476718
H	2.93499302	-1.66376199	0.61654758
H	0.71169981	-2.73773863	0.89618601
C	2.58325546	1.51319012	-0.56825301
H	0.73191288	2.49123745	-1.00419501
H	3.18289344	2.36621139	-0.87354095
C	3.24225527	0.32864492	-0.12075833
C	2.46167715	-0.75953535	0.24035713
C	4.72546841	0.27842049	-0.04552108
C	7.54693315	0.17950233	0.09207962
C	5.45724320	1.38931805	0.39076143
C	5.41752517	-0.89310687	-0.40686619
C	6.81202930	-0.94804425	-0.33631404
C	6.85287554	1.33983281	0.46389504
H	4.96194027	2.30306128	0.70326586
H	4.85626410	-1.74459418	-0.77271494
O	7.55982369	-2.03762430	-0.68289543
O	8.91561211	0.13366981	0.19740277
O	7.52700920	2.47330709	0.85379993

C	8.20331016	2.39585885	2.11669480
H	7.48230409	2.20551946	2.92288207
H	8.66749132	3.37332335	2.26643768
H	8.96932169	1.61482603	2.10693736
C	9.62712981	0.25703618	-1.04191219
H	9.38506731	-0.57252677	-1.71497025
H	10.68819931	0.22345272	-0.78412344
H	9.39418948	1.21485177	-1.52368869
C	6.88728719	-3.21854044	-1.10085163
H	6.22522020	-3.59950054	-0.31253291
H	7.67285013	-3.94962435	-1.29986688
H	6.30688522	-3.04645599	-2.01673850

Table S9. Cartesian coordinates (Å) of the optimized geometry for **9**

H	4.23175255	2.60991146	-2.20895945
C	4.33121416	1.82384798	-1.46472247
H	2.23275211	1.43633349	-1.40290140
C	3.20656419	1.16860737	-1.00813745
C	5.74583536	0.45474238	-0.06394210
C	3.30046164	0.12696814	-0.04250315
C	5.61501517	1.47402403	-0.98083632
C	4.60821427	-0.24966215	0.41942598
C	2.15617860	-0.58517883	0.46568522
H	6.49358175	2.00096047	-1.34388035
H	5.74429910	-1.60154865	1.67409187
H	6.72885962	0.16484553	0.30086896
C	2.35139583	-1.64348768	1.34280484
H	1.48682926	-2.17763125	1.72736534
C	3.64267072	-2.01965032	1.77574104
H	3.75263700	-2.84817840	2.47029272
C	4.74789173	-1.32792066	1.33441670
C	0.16014951	1.01462078	0.14993019
H	0.66489771	1.90655940	0.50981209
C	0.77775012	-0.21345084	0.08409958
C	-1.20434332	1.01771961	-0.28106615
C	-1.60379508	-0.24648200	-0.66424896
S	-0.32104026	-1.42546942	-0.53568125
S	-3.20550220	-0.78096695	-1.30047719
O	-2.94513058	-2.05829633	-2.08737161
C	-2.06672234	2.25850617	-0.25737622
H	-2.86250521	2.16683678	-1.00481969
H	-1.45754612	3.11647847	-0.56981558
C	-3.99312547	-1.34003238	0.31364846
H	-3.19157208	-1.47711008	1.04335015
H	-4.38629469	-2.32648357	0.04689428
C	-2.67825545	2.57970838	1.13097067
H	-1.86511693	2.82341024	1.82773943
H	-3.28648914	3.49015222	1.03164550
C	-5.11164890	-0.41749583	0.82219129
H	-5.40123233	-0.78368446	1.81802340
H	-5.99489136	-0.54213522	0.18213281
C	-3.52743161	1.44760546	1.73464662
H	-3.83841501	1.73840183	2.74639323
H	-2.88310853	0.57008751	1.86586914
C	-4.77211928	1.08331050	0.89200798
H	-5.64900153	1.61639059	1.28172937
H	-4.64911113	1.44795561	-0.13473843

Table S10. Cartesian coordinates (Å) of the optimized geometry for **10**

C	-0.20882565	0.80069852	-0.96174735
H	0.28303904	1.67784572	-1.37223804
C	0.48566742	-0.25464508	-0.41161271
C	-1.62509720	0.61574510	-1.01680442
C	-1.98478561	-0.60317680	-0.47838385
S	-0.61017466	-1.53171549	0.06851807
S	-3.62682443	-1.33647904	-0.33245073
O	-3.41250589	-2.84006941	-0.22480879
C	-2.56648193	1.65471842	-1.58043208
H	-3.47492597	1.16600017	-1.94938400
H	-2.09549016	2.11648724	-2.45772777
C	-4.05331960	-0.76433907	1.40820344
H	-3.12240642	-0.46855771	1.89760157
H	-4.40624795	-1.69030023	1.87384653
C	-2.93888359	2.78073420	-0.58128281
H	-2.03501887	3.35947113	-0.34809689
H	-3.62799252	3.47088218	-1.08874195
C	-5.13137211	0.32920012	1.46428422
H	-5.20100457	0.65712437	2.51175146
H	-6.10407581	-0.11654780	1.21836728
C	-3.56697592	2.28901281	0.73444876
H	-3.71103048	3.14854577	1.40179875
H	-2.83942899	1.64293463	1.23995499
C	-4.91023170	1.54587075	0.54586653
H	-5.74210662	2.24603030	0.69649103
H	-5.00742203	1.20568180	-0.49192299
C	1.93882471	-0.38903521	-0.23274822
H	2.26163497	1.71022991	0.07907273
C	2.72652649	0.73101969	-0.00630223
C	3.93298871	-1.79189394	-0.14097297
C	4.13370077	0.63534835	0.14646531
C	2.57220914	-1.66761040	-0.29403199
C	4.75688642	-0.65400682	0.08007215
C	4.94874466	1.77968571	0.37529498
H	1.96984345	-2.55132865	-0.48615774
H	6.63497596	-1.72838988	0.18525458
H	4.39742225	-2.77387285	-0.19799174
C	6.31343468	1.65584135	0.52483959
H	4.47607213	2.75809266	0.42917704
H	6.92435273	2.53815756	0.69748702
C	6.92887666	0.37984580	0.45496380
H	8.00582894	0.29488259	0.57444987
C	6.16578259	-0.74829705	0.23794669

Table S11. Cartesian coordinates (Å) of the optimized geometry for **11**

C	-1.25576596	0.63138753	-1.05288528
H	-0.70362898	1.43842695	-1.52578676
C	-0.63729860	-0.45321159	-0.46888186
C	-2.68355040	0.57327594	-1.05143974
C	-3.12997304	-0.57974024	-0.43764801
S	-1.82450701	-1.60119731	0.11192881
S	-4.82412439	-1.15250141	-0.19990143
O	-4.74138842	-2.66240731	-0.02180529
C	-3.54965389	1.66415496	-1.63699558

H	-4.51166666	1.24236291	-1.94815614
H	-3.07377298	2.03726367	-2.55298728
C	-5.13118222	-0.45989186	1.52197441
H	-4.15949577	-0.22712854	1.96388091
H	-5.54772653	-1.32598409	2.04654517
C	-3.78136106	2.86721241	-0.68632865
H	-2.82125038	3.37225514	-0.51490330
H	-4.42548812	3.59121281	-1.20558285
C	-6.10386086	0.72899102	1.55770391
H	-6.10373539	1.11210481	2.58861798
H	-7.12131742	0.36272469	1.36808734
C	-4.39933781	2.50005266	0.67411283
H	-4.43962144	3.40095797	1.29993353
H	-3.71339942	1.81584881	1.18774980
C	-5.81030280	1.87489708	0.57092811
H	-6.56927516	2.65479192	0.71471517
H	-5.97893053	1.49621474	-0.44421147
C	0.80243926	-0.70772656	-0.32490504
H	1.32533270	1.36321556	-0.16146248
C	1.69291216	0.34059214	-0.19662899
C	2.65467496	-2.29791128	-0.19869943
C	3.09859564	0.12525213	-0.07865396
C	1.31408790	-2.05160306	-0.31880788
C	3.59934019	-1.22994754	-0.07695303
C	4.00739164	1.18664506	0.04687921
H	0.62248396	-2.88169454	-0.43355282
H	5.35111464	-2.47350858	0.04289801
H	3.02256790	-3.32148344	-0.20402892
C	5.38660820	0.96650012	0.16778880
H	3.63210449	2.20860809	0.04904132
C	6.32374089	2.04108389	0.29376145
C	5.88615046	-0.39043527	0.16551713
H	7.66941228	-1.62428007	0.28736048
C	4.97633556	-1.45141089	0.04338310
C	7.66847537	1.79496522	0.41014298
H	5.94721932	3.06172680	0.29549561
H	8.36813130	2.62137133	0.50496588
C	8.16117262	0.45539309	0.40781084
H	9.22956429	0.27867035	0.50088816
C	7.29545981	-0.60273153	0.28924083

Table S12. Cartesian coordinates (Å) of the optimized geometry for **12**

C	1.08558514	-0.89561171	0.40490797
H	0.54617022	-1.61758390	1.01121787
C	0.51048838	0.26987473	-0.04926429
C	2.45452215	-1.07072371	0.02766049
C	2.90332942	0.00305073	-0.71399395
S	1.66156137	1.20213720	-0.98302776
S	4.53174066	0.27030603	-1.44438129
O	4.32761594	1.25261536	-2.58975495
C	3.27240538	-2.26929943	0.45020210
H	4.08080175	-2.43454945	-0.27057622
H	2.63761075	-3.16339721	0.40075122
C	5.31654693	1.27275268	-0.05959558
H	4.51058501	1.64931084	0.57470671
H	5.74727266	2.11873899	-0.60511854
C	3.85358364	-2.16778495	1.88428699

H	3.02307719	-2.16187992	2.60281413
H	4.43015291	-3.08267770	2.08238915
C	6.39545583	0.51728291	0.73161947
H	6.68525409	1.16186762	1.57433539
H	7.29051555	0.41390215	0.10431466
C	4.73453437	-0.93113702	2.13281932
H	5.02136014	-0.90714069	3.19208042
H	4.12013343	-0.03688219	1.97423643
C	6.00245044	-0.87943701	1.24876505
H	6.85471707	-1.29306563	1.80330204
H	5.88028808	-1.53734507	0.38019717
H	-0.13856169	2.68434993	0.86025257
C	-1.02242500	2.08434118	0.66205625
C	-0.85802158	0.77849161	0.16697762
C	-3.43838590	1.84551937	0.73014846
C	-2.01127474	-0.01167312	-0.09659605
C	-2.27878102	2.60970516	0.93697704
C	-3.30687965	0.52374640	0.20269123
C	-1.94525072	-1.32388554	-0.68526476
H	-2.36837882	3.61886315	1.33229662
C	-3.06763072	-2.06356504	-0.91482482
H	-0.97630439	-1.71892567	-0.96865729
H	-2.98574113	-3.04809872	-1.37024629
C	-4.37430926	-1.57046376	-0.58398211
C	-5.54085966	-2.32397139	-0.80281104
C	-4.48194682	-0.25775825	-0.03197708
C	-6.79552320	-1.80257970	-0.48757528
H	-5.45493175	-3.32251087	-1.22537057
H	-7.68777489	-2.39816499	-0.66244533
C	-6.91264669	-0.51903475	0.04695758
H	-7.89406316	-0.11610870	0.28679031
C	-5.77376480	0.27125687	0.28012487
C	-4.74867554	2.35298860	1.03108687
H	-4.83124284	3.35962032	1.43471886
C	-5.86499877	1.60021472	0.82025026
H	-6.84986600	1.99786571	1.05471564

Table S13. Cartesian coordinates (Å) of the optimized geometry for **13'**

C	-3.90944894	0.30816550	-1.25370859
H	-3.45725075	0.92312774	-2.02650211
C	-3.16629102	-0.42953263	-0.35785094
C	-5.32384185	0.14151073	-1.13184870
C	-5.63149603	-0.73167036	-0.10820059
S	-4.21188975	-1.36727216	0.68655451
S	-7.25099802	-1.30443295	0.44290018
O	-7.01360133	-2.62775639	1.15789473
C	-6.31387189	0.86381155	-2.01574996
H	-7.24006405	0.28237860	-2.08195219
H	-5.91014209	0.90447720	-3.03560324
C	-7.56132603	-0.04562031	1.80602760
H	-6.60184877	0.41078573	2.06038830
H	-7.87014620	-0.68287717	2.64109301
C	-6.62922306	2.31252789	-1.56123518
H	-5.71833529	2.91882096	-1.65575556
H	-7.36022846	2.73743782	-2.26394164
C	-8.64517438	0.99047355	1.47024910
H	-8.64535149	1.72955814	2.28469661

H	-9.62754855	0.50126397	1.50140384
C	-7.15823610	2.43204180	-0.12133131
H	-7.26533714	3.49513145	0.13018848
H	-6.38965648	2.04503976	0.55828185
C	-8.50265890	1.70403356	0.11252695
H	-9.33005669	2.41824698	0.01115718
H	-8.66829170	0.96106279	-0.67665132
C	-1.70340577	-0.50073904	-0.23489327
H	-1.38481775	1.52953832	-0.85838737
C	-0.91535480	0.59730905	-0.55362705
C	0.31032089	-1.76741016	0.31008832
C	0.49824719	0.54953395	-0.46505071
C	-1.05912656	-1.69566101	0.20857864
C	1.13357792	-0.65682969	-0.02649540
C	1.32114187	1.66524752	-0.78548956
H	-1.66182784	-2.56755354	0.44811032
H	3.01196153	-1.61684726	0.42859912
H	0.78144305	-2.68939782	0.64377255
C	2.69098277	1.58941419	-0.68377624
H	0.85077562	2.58522144	-1.12624742
H	3.29889262	2.44677353	-0.95868103
C	3.33822658	0.39177882	-0.25402729
C	2.54801623	-0.70199733	0.06695849
C	4.81929564	0.33285787	-0.15575850
C	7.64185458	0.21252225	0.05672489
C	5.54820157	1.42845692	0.31036916
C	5.51206644	-0.83619348	-0.52512849
C	6.90277018	-0.89147872	-0.43404601
C	6.94478437	1.37613197	0.42503406
H	5.05398408	2.33922953	0.63212273
H	4.95764547	-1.67337536	-0.93122889
O	7.65183391	-1.96284405	-0.83801173
O	9.01575308	0.21447243	0.04934918
O	7.54229792	2.53314386	0.84439326
C	8.66003267	2.48985693	1.73573211
H	8.70802608	3.48358813	2.18797913
H	9.58908234	2.27562051	1.20300174
H	8.50124420	1.74197801	2.52303782
C	9.67907046	-0.72382225	0.90705894
H	9.37784944	-0.57020504	1.95215395
H	10.74690073	-0.51847987	0.80100088
H	9.46699490	-1.75316277	0.60784779
C	6.98841408	-3.07861210	-1.41895367
H	6.29973656	-3.55038815	-0.70602079
H	7.77757489	-3.78462721	-1.68368782
H	6.43943861	-2.78785326	-2.32351530

6. Single-Crystal X-ray Diffraction Analysis

X-ray Crystallographic Analysis of (*R*)-2. Colorless block single crystals were grown by slow evaporation into a solution of (*R*)-2 in dichloromethane. Intensity data were collected at 123 K on a Rigaku Single Crystal X-ray diffractometer equipped with a Rigaku Saturn CCD diffractometer with MoK α radiation ($\lambda = 0.71070 \text{ \AA}$). A total of 15102 reflections were measured with the maximum 2θ angle of 55.0°, of which 2561 were independent reflections ($R_{\text{int}} = 0.0282$). The structure was solved by direct methods (SHELXT 2018/2)^{S16} and refined by the full-matrix least-squares on F^2 (SHELXL-

2018/3).^{S17} All hydrogen atoms were placed using AFIX instructions, while all non-hydrogen atoms were refined anisotropically. The crystal data are as follows: C₁₀H₁₃BrOS₂; FW = 293.23, crystal size = 0.17 × 0.16 × 0.10 mm³, orthorhombic, P2₁2₁2₁ (#19), $a = 7.66070(10)$ Å, $b = 9.6197(2)$ Å, $c = 15.2085(3)$ Å, $V = 1120.77(4)$ Å³, $Z = 4$, $D_c = 1.738$ g cm⁻³, $\mu = 4.004$ mm⁻¹, $R_1 = 0.0146$ ($I > 2\sigma(I)$), $wR_2 = 0.0452$ (all data), GOF = 1.214, Flack(x) = -0.003(3). CCDC 2128001 contains the supplementary crystallographic data for this compound. This data can be obtained free of charge from the Cambridge Crystallographic Data Centre (CCDC) at www.ccdc.cam.ac.uk/data_request.cif.

X-ray Crystallographic Analysis of (S)-2. Colorless block single crystals were grown by slow evaporation into a solution of (S)-2 in dichloromethane. Intensity data were collected at 123 K on a Rigaku Single Crystal X-ray diffractometer equipped with a Rigaku Saturn CCD diffractometer with MoK α radiation ($\lambda = 0.71070$ Å). A total of 15314 reflections were measured with the maximum 2 θ angle of 55.0°, of which 2570 were independent reflections ($R_{int} = 0.0362$). The structure was solved by direct methods (SHELXT 2018/2)^{S16} and refined by the full-matrix least-squares on F^2 (SHELXL-2018/3).^{S17} All hydrogen atoms were placed using AFIX instructions, while all non-hydrogen atoms were refined anisotropically. The crystal data are as follows: C₁₀H₁₃BrOS₂; FW = 293.23, crystal size = 0.12 × 0.05 × 0.05 mm³, orthorhombic, P2₁2₁2₁ (#19), $a = 7.6628(2)$ Å, $b = 9.6181(2)$ Å, $c = 15.2176(3)$ Å, $V = 1121.56(4)$ Å³, $Z = 4$, $D_c = 1.737$ g cm⁻³, $\mu = 4.001$ mm⁻¹, $R_1 = 0.0174$ ($I > 2\sigma(I)$), $wR_2 = 0.0384$ (all data), GOF = 1.073, Flack(x) = -0.005(4). CCDC 2128005 contains the supplementary crystallographic data for this compound. This data can be obtained free of charge from the Cambridge Crystallographic Data Centre (CCDC) at www.ccdc.cam.ac.uk/data_request.cif.

X-ray Crystallographic Analysis of 18. Colorless block single crystals were grown by slow evaporation into a solution of 18 in dichloromethane. Intensity data were collected at 123 K on a Rigaku Single Crystal X-ray diffractometer equipped with Rigaku Pilatus 200K diffractometer with MoK α radiation ($\lambda = 0.71073$ Å). A total of 7902 reflections were measured with the maximum 2 θ angle of 55.0°, of which 2656 were independent reflections ($R_{int} = 0.0214$). The structure was solved by direct methods (SHELXT 2018/2)^{S16} and refined by the full-matrix least-squares on F^2 (SHELXL-2018/3).^{S17} All hydrogen atoms were placed using AFIX instructions, while all non-hydrogen atoms were refined anisotropically. The crystal data are as follows: C₁₀H₁₃BrO₂S₂; FW = 309.23, crystal size = 0.20 × 0.05 × 0.01 mm³, monoclinic, P2₁ (#4), $a = 7.7355(3)$ Å, $b = 9.6941(2)$ Å, $c = 8.6079(3)$ Å, $\beta = 114.813(4)$, $V = 585.90(4)$ Å³, $Z = 2$, $D_c = 1.753$ g cm⁻³, $\mu = 3.841$ mm⁻¹, $R_1 = 0.0215$ ($I > 2\sigma(I)$), $wR_2 = 0.0531$ (all data), GOF = 1.097. CCDC 2133269 contains the supplementary crystallographic data for this compound. This data can be obtained free of charge from the Cambridge Crystallographic Data Centre (CCDC) at www.ccdc.cam.ac.uk/data_request.cif.

X-ray Crystallographic Analysis of 5. Colourless block single crystals were grown by *n*-hexane vapour diffusion into a solution of 5 in chloroform. Intensity data were collected at 123 K on a Rigaku Single Crystal X-ray diffractometer equipped with a FR-X generator, a Varimax optics, and a PILATUS 200K

photon counting detector with MoK α radiation ($\lambda = 0.71073 \text{ \AA}$). A total of 24371 reflections were measured with the maximum 2θ angle of 55.0° , of which 3683 were independent reflections ($R_{\text{int}} = 0.0980$). The structure was solved by direct methods (SHELXT 2018/2)^{S16} and refined by the full-matrix least-squares on F^2 (SHELXL-2018/3).^{S17} All hydrogen atoms were placed using AFIX instructions, while all non-hydrogen atoms were refined anisotropically. TN-fused thiophene ring is disordered and therefore solved using appropriate disordered models. Thus, two sets of disordered TN-fused thiophene rings, *i.e.* (S1, S2, C12, C20) and (S3, S4, C21, C22) were placed, and their occupancies were refined to be 0.88 and 0.12, respectively. The two sets of disordered TN-fused thiophene rings were restrained by SADI and SIMU instructions during refinement. The crystal data are as follows: $C_{20}H_{20}S_2$; FW = 324.48, crystal size = $0.10 \times 0.09 \times 0.06 \text{ mm}^3$, orthorhombic, $Pbca$ (#61), $a = 11.3275(4) \text{ \AA}$, $b = 8.1766(3) \text{ \AA}$, $c = 34.8684(13) \text{ \AA}$, $V = 3229.5(2) \text{ \AA}^3$, $Z = 8$, $D_c = 1.335 \text{ g cm}^{-3}$, $\mu = 0.324 \text{ mm}^{-1}$, $R_1 = 0.0586 (I > 2\sigma(I))$, $wR_2 = 0.1108$ (all data), GOF = 1.007. CCDC 2128006 contains the supplementary crystallographic data for this compound. This data can be obtained free of charge from the Cambridge Crystallographic Data Centre (CCDC) at www.ccdc.cam.ac.uk/data_request.cif.

X-ray Crystallographic Analysis of 6. Yellow platelet single crystals were grown by MeOH vapor diffusion into a solution of **6** in chloroform. Intensity data were collected at 143 K on a Rigaku Single Crystal X-ray diffractometer equipped with Rigaku Saturn CCD diffractometer with MoK α radiation ($\lambda = 0.71073 \text{ \AA}$). A total of 24314 reflections were measured with the maximum 2θ angle of 55.0° , of which 4257 were independent reflections ($R_{\text{int}} = 0.0263$). The structure was solved by direct methods (SHELXT 2018/2)^{S16} and refined by the full-matrix least-squares on F^2 (SHELXL-2018/3).^{S17} All hydrogen atoms were placed using AFIX instructions, while all non-hydrogen atoms were refined anisotropically. The crystal data are as follows: $C_{24}H_{22}S_2$; FW = 374.53, crystal size = $0.21 \times 0.19 \times 0.03 \text{ mm}^3$, monoclinic, $P2_1/c$ (#14), $a = 17.5384(3) \text{ \AA}$, $b = 11.5092(2) \text{ \AA}$, $c = 9.5134(2) \text{ \AA}$, $\beta = 102.451(2)^\circ$, $V = 1875.14(6) \text{ \AA}^3$, $Z = 4$, $D_c = 1.327 \text{ g cm}^{-3}$, $\mu = 0.289 \text{ mm}^{-1}$, $R_1 = 0.0309 (I > 2\sigma(I))$, $wR_2 = 0.0994$ (all data), GOF = 1.095. CCDC 2127997 contains the supplementary crystallographic data for this compound. This data can be obtained free of charge from the Cambridge Crystallographic Data Centre (CCDC) at www.ccdc.cam.ac.uk/data_request.cif.

X-ray Crystallographic Analysis of 7. Yellow platelet single crystals were grown by *n*-pentane vapor diffusion into a solution of **7** in Et₂O. Intensity data were collected at 146 K on a Rigaku Single Crystal X-ray diffractometer equipped with Rigaku Saturn CCD diffractometer with MoK α radiation ($\lambda = 0.71073 \text{ \AA}$). A total of 12135 reflections were measured with the maximum 2θ angle of 55.0° , of which 4315 were independent reflections ($R_{\text{int}} = 0.0183$). The structure was solved by direct methods (SHELXT 2018/2)^{S16} and refined by the full-matrix least-squares on F^2 (SHELXL-2018/3).^{S17} All hydrogen atoms were placed using AFIX instructions, while all non-hydrogen atoms were refined anisotropically. The crystal data are as follows: $C_{26}H_{22}S_2$; FW = 398.55, crystal size = $0.28 \times 0.23 \times 0.08 \text{ mm}^3$, triclinic, $P-1$ (#2), $a = 7.59897(14) \text{ \AA}$, $b = 9.8836(2) \text{ \AA}$, $c = 14.0367(3) \text{ \AA}$, $\alpha = 90.1743(18)^\circ$, $\beta = 102.451(2)^\circ$, $\gamma = 110.7438(19)^\circ$, $V = 978.17(4) \text{ \AA}^3$, $Z = 2$, $D_c = 1.353 \text{ g cm}^{-3}$, $\mu = 0.281 \text{ mm}^{-1}$, $R_1 =$

0.0318 ($I > 2\sigma(I)$), $wR_2 = 0.0891$ (all data), GOF = 1.056. CCDC 2128000 contains the supplementary crystallographic data for this compound. This data can be obtained free of charge from the Cambridge Crystallographic Data Centre (CCDC) at www.ccdc.cam.ac.uk/data_request.cif.

X-ray Crystallographic Analysis of (S)-9. Colorless block single crystals were grown by slow evaporation of a solution of **9** (S-form 64% ee) in ethyl acetate. Intensity data were collected at 123 K on a Rigaku Single Crystal X-ray diffractometer equipped with a FR-X generator, a Varimax optics, and a PILATUS 200K photon counting detector with MoK α radiation ($\lambda = 0.71073 \text{ \AA}$). A total of 10819 reflections were measured with the maximum 2θ angle of 55.0°, of which 3763 were independent reflections ($R_{\text{int}} = 0.0111$). The structure was solved by direct methods (SHELXT 2018/2)^{S16} and refined by the full-matrix least-squares on F^2 (SHELXL-2018/3).^{S17} All hydrogen atoms were placed using AFIX instructions, while all non-hydrogen atoms were refined anisotropically. The crystal data are as follows: C₂₀H₂₀OS₂; FW = 340.48, crystal size = 0.29 × 0.12 × 0.06 mm³, monoclinic, P2₁ (#4), $a = 7.23910(10) \text{ \AA}$, $b = 15.9453(2) \text{ \AA}$, $c = 7.41670(10) \text{ \AA}$, $V = 824.34(2) \text{ \AA}^3$, $Z = 2$, $D_c = 1.372 \text{ g cm}^{-3}$, $\mu = 0.325 \text{ mm}^{-1}$, $R_1 = 0.0199$ ($I > 2\sigma(I)$), $wR_2 = 0.0547$ (all data), GOF = 1.057, Flack (x) = 0.016(11). CCDC 2128002 contains the supplementary crystallographic data for this compound. This data can be obtained free of charge from the Cambridge Crystallographic Data Centre (CCDC) at www.ccdc.cam.ac.uk/data_request.cif.

X-ray Crystallographic Analysis of (S)-10. Colorless block single crystals were grown by slow diffusion of *n*-hexane vapor into a solution of **10** (S-form 93% ee) in ethyl acetate. Intensity data were collected at 123 K on a Rigaku Single Crystal X-ray diffractometer equipped with a FR-X generator, a Varimax optics, and a PILATUS 200K photon counting detector with MoK α radiation ($\lambda = 0.71073 \text{ \AA}$). A total of 11347 reflections were measured with the maximum 2θ angle of 55.0°, of which 3880 were independent reflections ($R_{\text{int}} = 0.0115$). The structure was solved by direct methods (SHELXT 2018/2)^{S16} and refined by the full-matrix least-squares on F^2 (SHELXL-2018/3).^{S17} All hydrogen atoms were placed using AFIX instructions, while all non-hydrogen atoms were refined anisotropically. The crystal data are as follows: C₂₀H₂₀OS₂; FW = 340.48, crystal size = 0.68 × 0.07 × 0.06 mm³, monoclinic, P2₁ (#4), $a = 7.44970(10) \text{ \AA}$, $b = 9.42970(10) \text{ \AA}$, $c = 12.1517(2) \text{ \AA}$, $V = 853.38(2) \text{ \AA}^3$, $Z = 2$, $D_c = 1.325 \text{ g cm}^{-3}$, $\mu = 0.314 \text{ mm}^{-1}$, $R_1 = 0.0215$ ($I > 2\sigma(I)$), $wR_2 = 0.0590$ (all data), GOF = 1.034, Flack (x) = 0.009(11). CCDC 2127999 contains the supplementary crystallographic data for this compound. This data can be obtained free of charge from the Cambridge Crystallographic Data Centre (CCDC) at www.ccdc.cam.ac.uk/data_request.cif.

X-ray Crystallographic Analysis of *rac*-12. Yellow platelet single crystals were grown by slow evaporation of a solution of **12** in acetonitrile. Intensity data were collected at 123 K on a Rigaku Single Crystal X-ray diffractometer equipped with a FR-X generator, a Varimax optics, and a PILATUS 200K photon counting detector with MoK α radiation ($\lambda = 0.71073 \text{ \AA}$). A total of 11206 reflections were measured with the maximum 2θ angle of 50.0°, of which 3463 were independent reflections ($R_{\text{int}} =$

0.0193). The structure was solved by direct methods (SHELXT 2018/2)^{S16} and refined by the full-matrix least-squares on F^2 (SHELXL-2018/3).^{S17} All hydrogen atoms were placed using AFIX instructions, while all non-hydrogen atoms were refined anisotropically. The crystal data are as follows: C₂₆H₂₂OS₂; FW = 414.55, crystal size = 0.12 × 0.12 × 0.08 mm³, triclinic, P-1 (#2), a = 9.0966(2) Å, b = 10.4919(2) Å, c = 11.1191(2) Å, α = 91.4630(10)°, β = 91.368(2)°, γ = 111.185(2)°, V = 988.55(4) Å³, Z = 2, D_c = 1.393 g cm⁻³, μ = 0.285 mm⁻¹, R_1 = 0.0514 ($I > 2\sigma(I)$), wR_2 = 0.1243 (all data), GOF = 1.074. CCDC 2128003 contains the supplementary crystallographic data for this compound. This data can be obtained free of charge from the Cambridge Crystallographic Data Centre (CCDC) at www.ccdc.cam.ac.uk/data_request.cif.

X-ray Crystallographic Analysis of (S)-13 at 123 K. Colorless platelet single crystals were grown by a solution of (S)-13 in hexane. Intensity data were collected at 123 K on a Rigaku Single Crystal X-ray diffractometer equipped with a FR-X generator, a Varimax optics, and a PILATUS 200K photon counting detector with MoKα radiation (λ = 0.71073 Å). A total of 37880 reflections were measured with the maximum 2θ angle of 54.2°, of which 12516 were independent reflections (R_{int} = 0.0544). The structure was solved by direct methods (SHELXT 2018/2)^{S16} and refined by the full-matrix least-squares on F^2 (SHELXL-2018/3).^{S17} All hydrogen atoms were placed using AFIX instructions, while all non-hydrogen atoms were refined anisotropically. The crystal data are as follows: C₆₂H₉₆O₄S₂; FW = 969.50, crystal size = 0.20 × 0.18 × 0.02 mm³, monoclinic, P2₁ (#4), a = 8.2061(2) Å, b = 10.2572(2) Å, c = 33.9910(10) Å, β = 93.477(3)° V = 2855.81(12) Å³, Z = 2, D_c = 1.127 g cm⁻³, μ = 0.138 mm⁻¹, R_1 = 0.0444 ($I > 2\sigma(I)$), wR_2 = 0.1137 (all data), GOF = 1.068, Flack(x) = 0.00(3). CCDC 2127998 contains the supplementary crystallographic data for this compound. This data can be obtained free of charge from the Cambridge Crystallographic Data Centre (CCDC) at www.ccdc.cam.ac.uk/data_request.cif.

X-ray Crystallographic Analysis of (S)-13 at 323 K. Colorless platelet single crystals were grown by a solution of (S)-13 in hexane. Intensity data were collected at 323 K on a Rigaku Single Crystal X-ray diffractometer equipped with a FR-X generator, a Varimax optics, and a PILATUS 200K photon counting detector with MoKα radiation (λ = 0.71073 Å). A total of 16539 reflections were measured with the maximum 2θ angle of 54.2°, of which 9923 were independent reflections (R_{int} = 0.0254). The structure was solved by direct methods (SHELXT 2018/2)^{S16} and refined by the full-matrix least-squares on F^2 (SHELXL-2018/3).^{S17} All hydrogen atoms were placed using AFIX instructions, while all non-hydrogen atoms were refined anisotropically. The crystal data are as follows: C₆₂H₉₆O₄S₂; FW = 969.50, crystal size = 0.19 × 0.16 × 0.02 mm³, monoclinic, P2₁ (#4), a = 8.3391(4) Å, b = 10.2673(4) Å, c = 34.7678(15) Å, β = 96.371(4)° V = 2958.4(2) Å³, Z = 2, D_c = 1.088 g cm⁻³, μ = 0.133 mm⁻¹, R_1 = 0.0526 ($I > 2\sigma(I)$), wR_2 = 0.1531 (all data), GOF = 1.010, Flack(x) = 0.06(8). CCDC 2128004 contains the supplementary crystallographic data for this compound. This data can be obtained free of charge from the Cambridge Crystallographic Data Centre (CCDC) at www.ccdc.cam.ac.uk/data_request.cif.

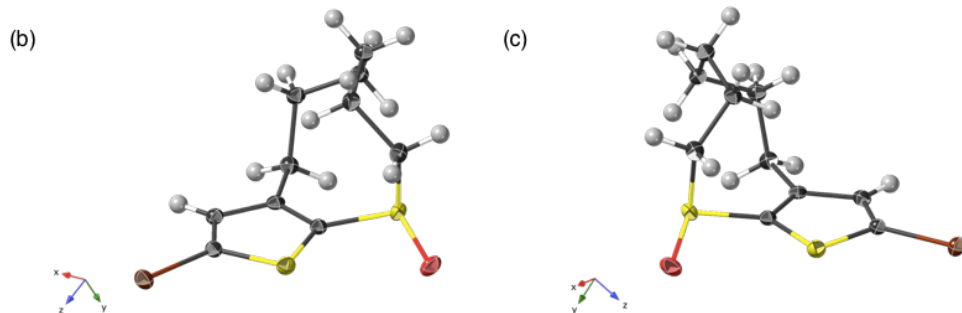
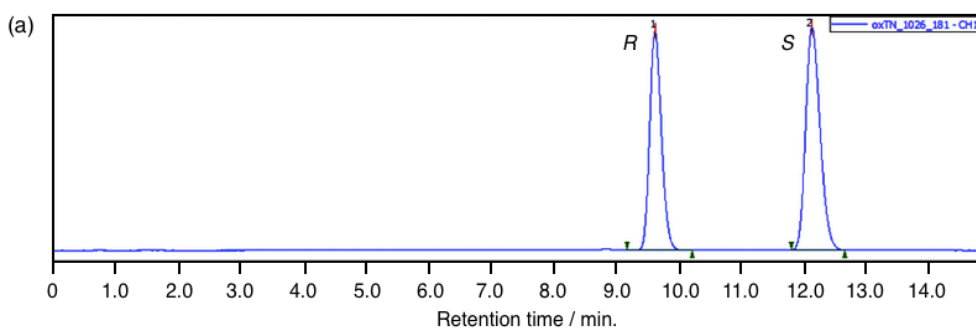


Figure S6. (a) HPLC chart of *rac*-**2** (acetonitrile as an eluent, 1 mL/min, DAICEL Chiraldpak IG) (b) Crystal structure of (*R*)-**2**. Thermal ellipsoid plots (50% probability for thermal ellipsoids) (c) Crystal structure of (*S*)-**2**. Thermal ellipsoid plots (50% probability for thermal ellipsoids).

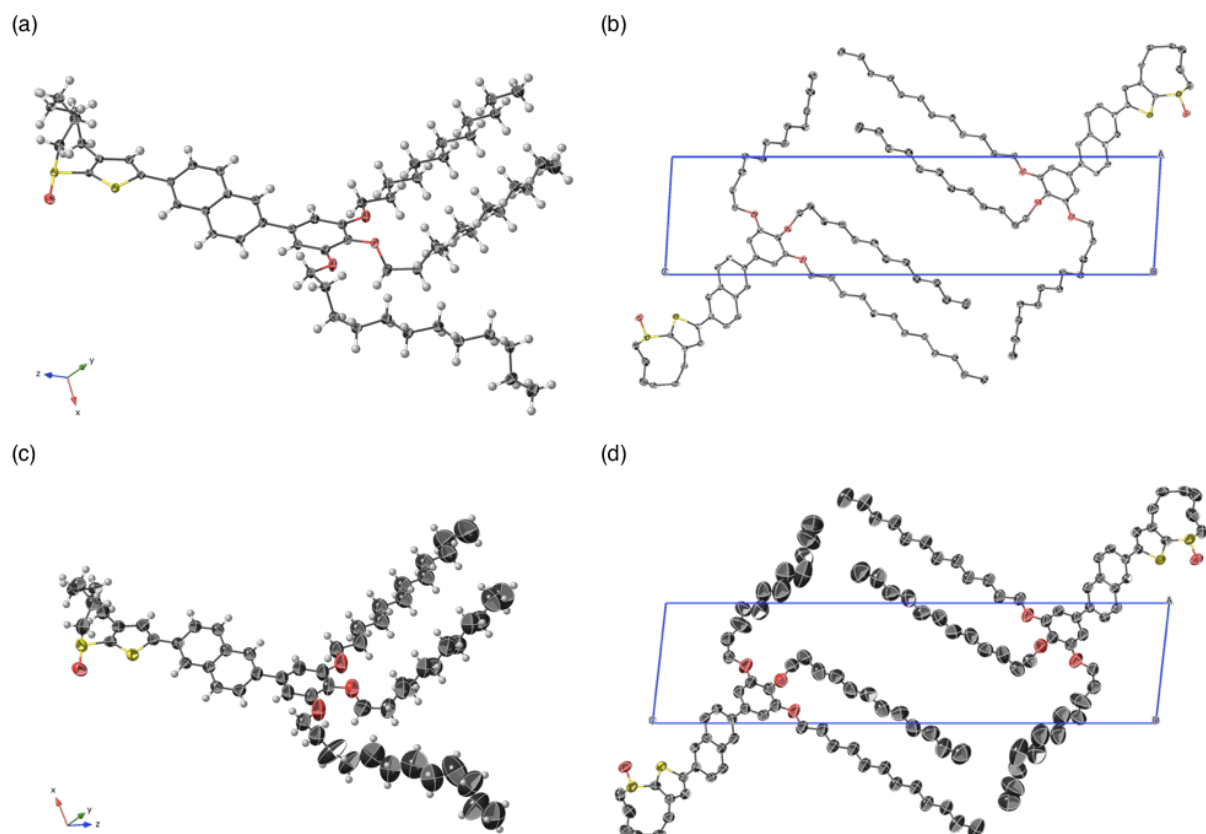


Figure S7. Crystal structures of (*S*)-**13** at 123 K (a, b), 323 K (c, d). (a, c) Thermal ellipsoid plots (50% probability for thermal ellipsoids). (b, d) Unit cell from *b* axis.

7. TGA of **8** and **(S)-13**

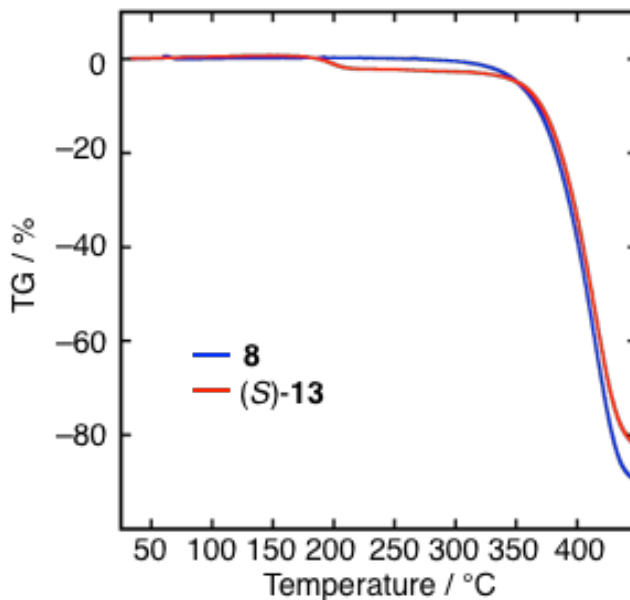


Figure S8. TGA profile of **8** and **(S)-13**.

8. Phase-transition Behaviors of **8** and **13**

Methods. The sample of enantiomerically pure **(S)-13** was purified by preparative chiral HPLC prior to the measurements. Variable-temperature (VT) powder X-ray diffraction (PXRD) patterns were obtained at various temperature on synchrotron radiation (12.398 keV, $\lambda = 1.0002 \text{ \AA}$) at the BL02B2 beamline in SPring-8 (JASRI). The temperature was changed to the target temperature at 20 K/min, and then irradiated for 90 s to obtain the diffraction data.

Phase-transition Behavior of **8.** DSC measurements revealed that **8** underwent reversible phase transitions between the crystalline phase and the isotropic liquid upon heating and cooling in the temperature range of -80 °C to 80 °C, with melting and freezing points observed at 51 °C and -14 °C, respectively (Fig. 4a).

Phase-transition Behavior of **13.** According to the DSC measurements, the enantiomerically pure sulfoxide **(S)-13** showed a two-step endothermic phase transition at 47 °C and 68 °C upon heating the crystals (Fig. 4b, 1st heating). Variable-temperature (VT) PXRD measurements (Fig. 3) and single-crystal XRD analyses (Figure S7 and Table S14) confirmed that the phase transition at 47 °C was a crystal-phase to crystal-phase transition accompanied by a slight elongation of the unit lattice lengths. For clarity, the initial crystalline phase and the latter crystalline mesophase are hereafter denoted as α -phase and β -phase, respectively. Subsequently, when **(S)-13** at the β -phase at 50 °C was subjected to the repeated cooling and heating cycles in the temperature range between 55 °C and -70 °C, the reversible

phase transitions accompanied with pronounced exothermic and endothermic peaks were observed at 41 °C and 47 °C for cooling and heating processes, respectively. According to the VT-PRXD measurements under the similar temperature condition as above mentioned, the diffraction pattern obtained at 27 °C after cooling of sample from 55 °C was identical to the simulated pattern from single-crystal diffraction data for the α -phase (Figure S9(b)). These results support that this reversible phase transition process is attributable to the interconversion between the α - and β -phases.

On the other hand, when (*S*)-**13** at the isotropic liquid phase was cooled from 100 °C to –50 °C, only a gradual baseline shift was observed without accompanying any distinct exothermic peak, even at a slow cooling rate of 2 °C/min (Fig. 3b). When the sample was then heated again from –50 °C to 50 °C, only a broad and weak endothermic peak was observed around 15 °C. Subsequent repetition of the cooling and heating processes yielded virtually identical DSC profiles without distinct peaks. As a result of reproducing the similar temperature conditions by VT-PXRD measurement, the samples after cooling from isotropic liquids showed no clear diffraction pattern at 0 °C, indicating that the (*S*)-**13** underwent a phase transition from the isotropic liquid to the amorphous phase.

Table S14. Comparison of crystal lattice parameters for (*S*)-**13** obtained at –150 °C and 50 °C

Crystal Lattice Parameters		
Measurement Temperature / K	123	323
Crystal system	Monoclinic	Monoclinic
Space group	<i>P</i> 2 ₁	<i>P</i> 2 ₁
<i>a</i> / Å	8.2061(2)	8.3391(4)
<i>b</i> / Å	10.2572(2)	10.2673(4)
<i>c</i> / Å	33.9910(10)	34.7678(15)
β / °	93.477(3)	96.371(4)
<i>V</i> / Å ³	2855.81(12)	2958.4(2)
<i>Z</i>	2	2
<i>D_c</i> / g cm ^{–3}	1.127	1.088

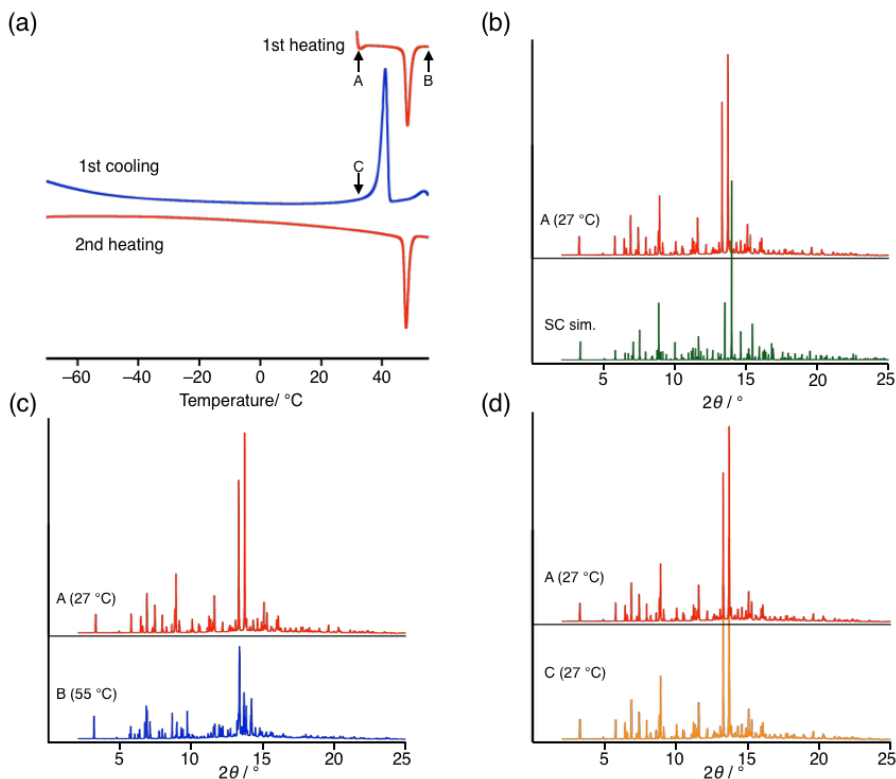


Figure S9. (a) DSC thermograms of (*S*)-**13** between 55 °C and -70 °C. (b-d) Variable-temperature powder X-ray diffraction (VT-PXRD) data of (*S*)-**13**.

9. MD Simulations

Computational Method. Optimization of the TN-fused thiophene **14** and the corresponding sulfoxide **15** was carried out using the self-consistent-charge density functional tight-binding (DFTB) method^{S18} with third-order expansion^{S19} and 3ob parameter set, i.e., Hubbard parameter of -0.1492 for C, -0.1575 for O, -0.110 for S, and -0.1857 for H^{S20,21} as implemented in the DFTB+ package ver. 1.2.2.^{S22} After the geometry optimization, we performed the DFTB with molecular dynamics (MD) simulations for 1 ns with 0.2 fs time-step at 300 K and 500 K under NVT ensemble with the Nose-Hoover thermostat.^{S23,24} The dispersion correction was included in all calculations.^{S25,26,27} In order to analyze the diversity of conformations, MD Frames every 1 ps were collected and optimized by the DFTB because MD frames contain structural fluctuations. Analyzed data are summarized in Figure S10.

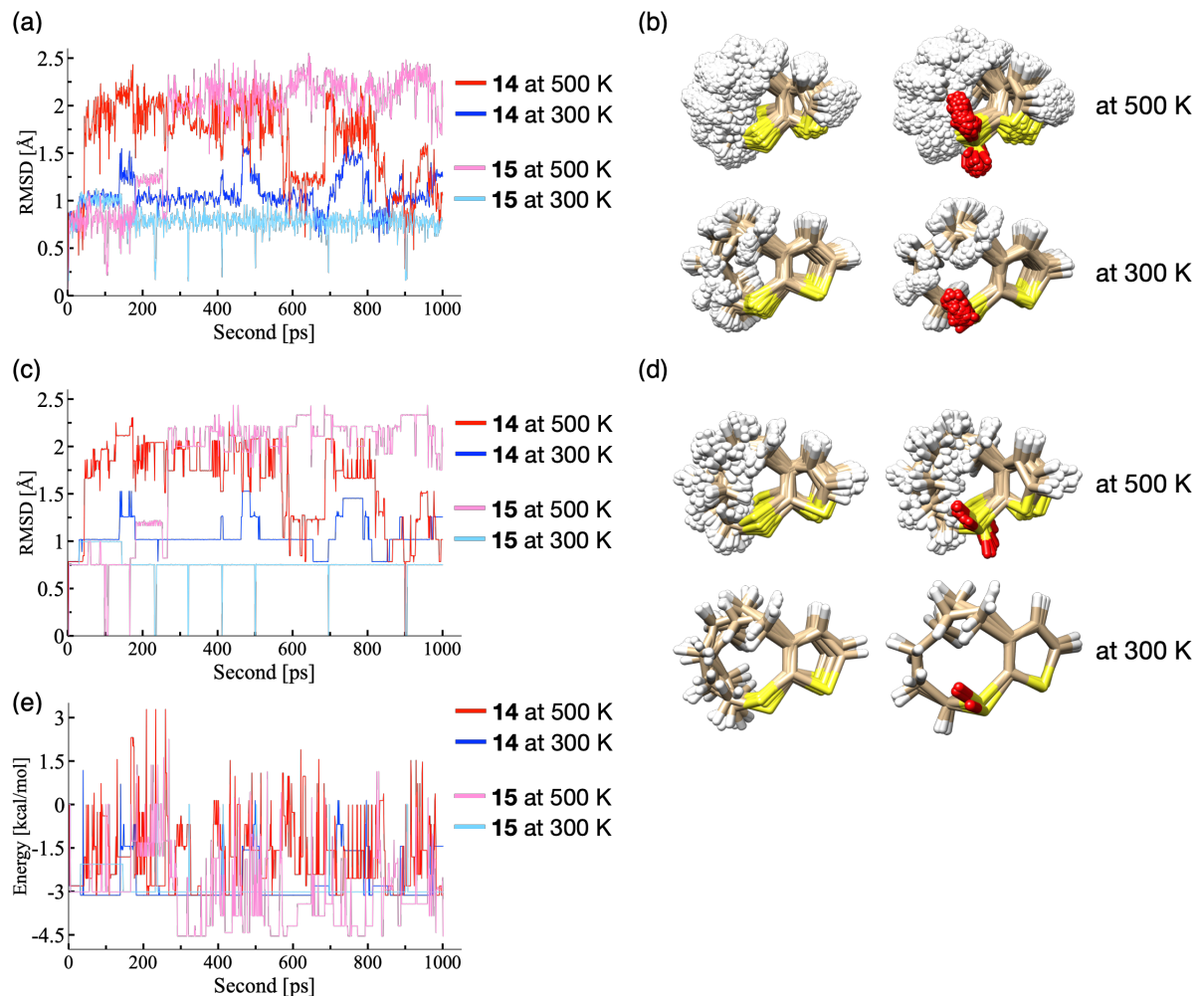


Figure S10. MD simulations for TN-fused thiophene **14** and the corresponding sulfoxide **15** based on the DFTB method. (a) Root mean square deviation (RMSD) of the MD frames per ps at 300 K and 500 K, (b) superimposed structures of the MD frames per ps at 300 K and 500 K, (c) RMSD of the optimized geometries of the MD frames per ps, (d) superimposed structures of the optimized geometries of the MD frames per ps, (e) relative energies of the optimized structures compared to the initial optimized geometry.

10. NMR Spectra of New Compounds

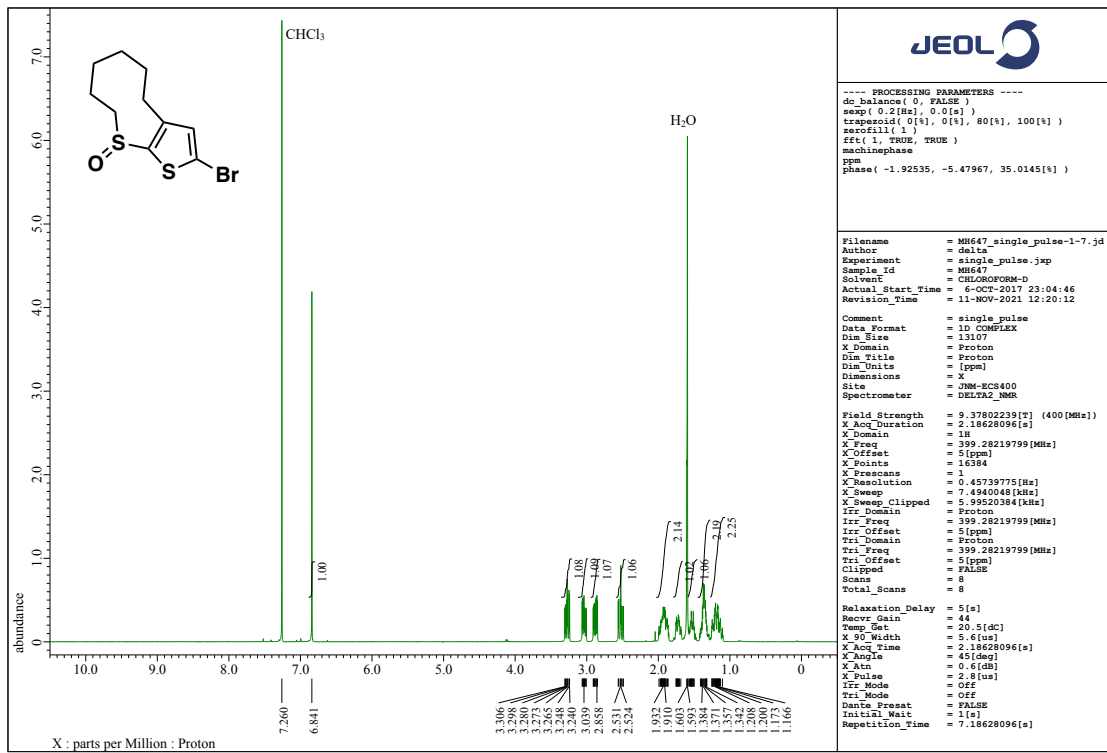


Figure S11. ^1H NMR spectrum of **2** (400 MHz, CDCl_3).

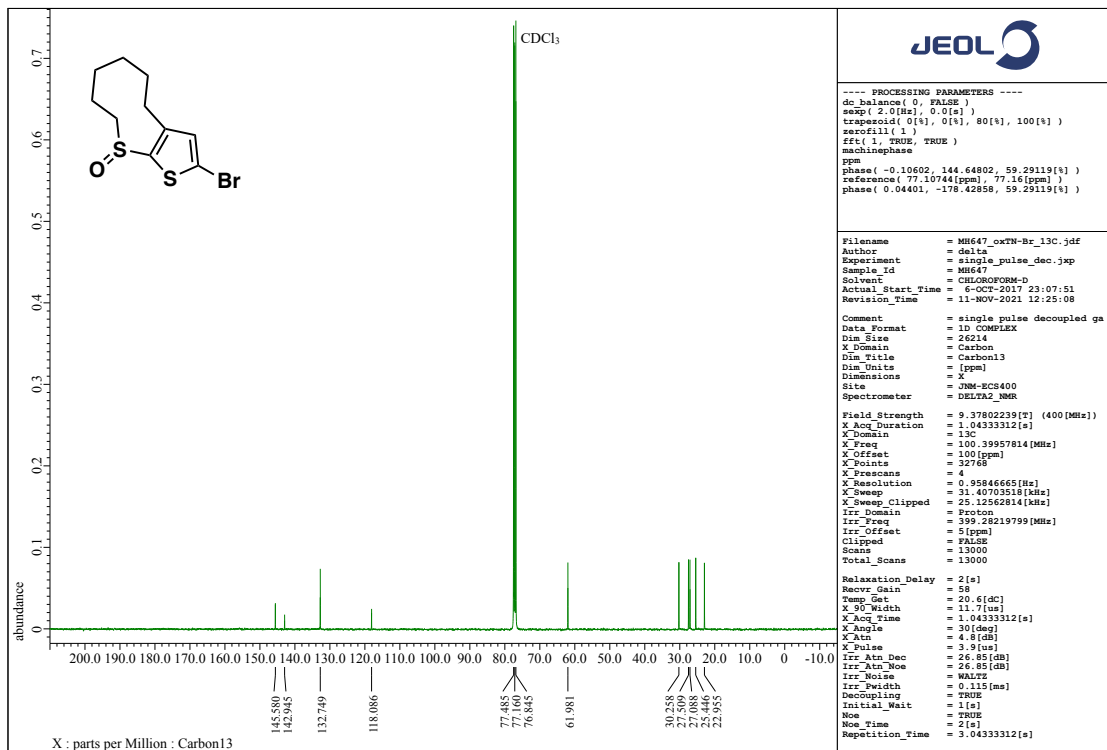


Figure S12. $^{13}\text{C}\{^1\text{H}\}$ NMR spectrum of **2** (100 MHz, CDCl_3).

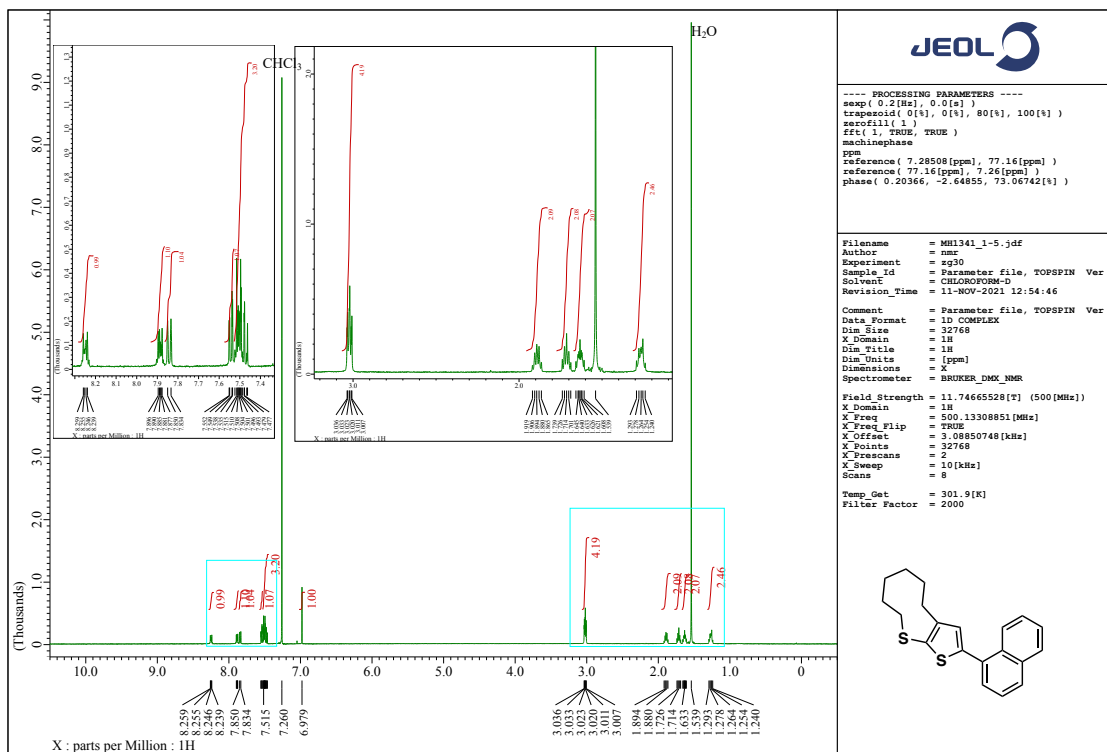


Figure S13. ^1H NMR spectrum of **4** (500 MHz, CDCl_3).

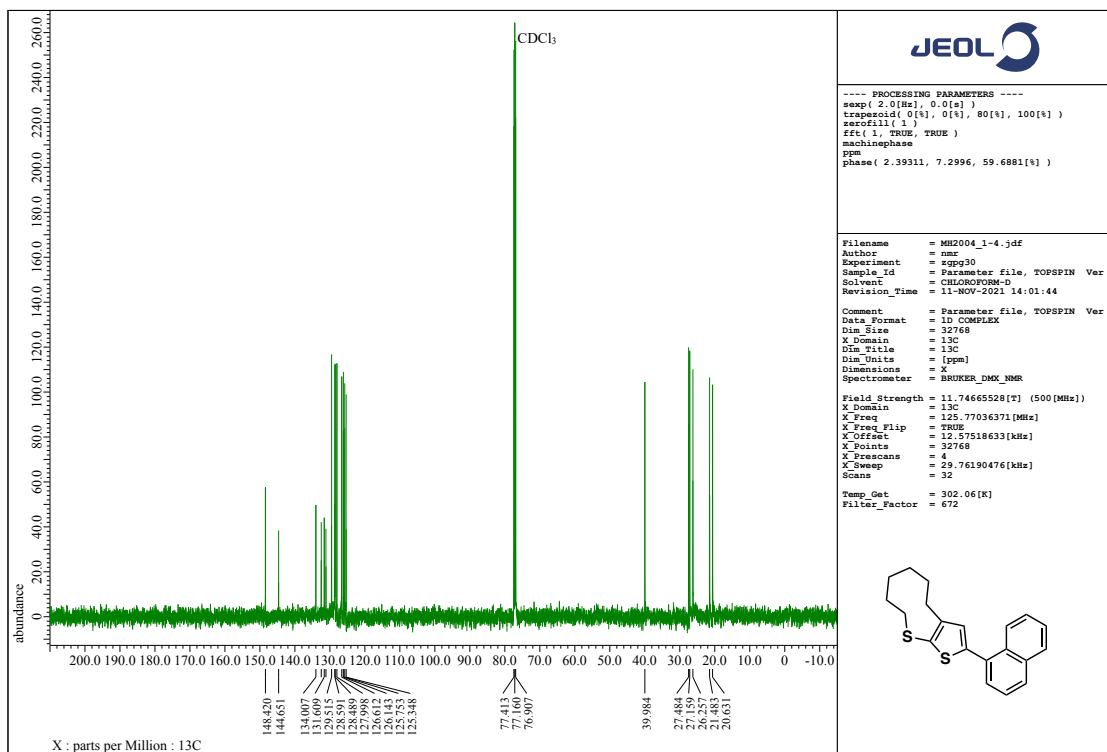


Figure S14. $^{13}\text{C}\{\text{H}\}$ NMR spectrum of **4** (125 MHz, CDCl_3).

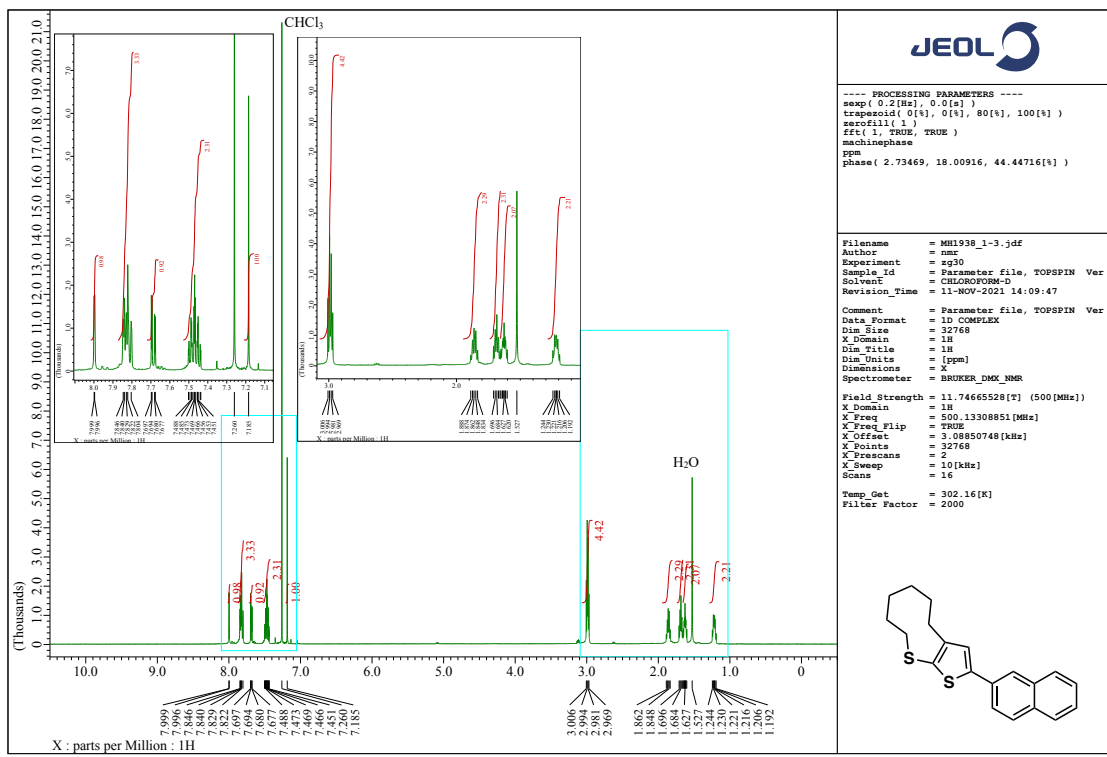


Figure S15. ^1H NMR spectrum of **5** (500 MHz, CDCl_3).

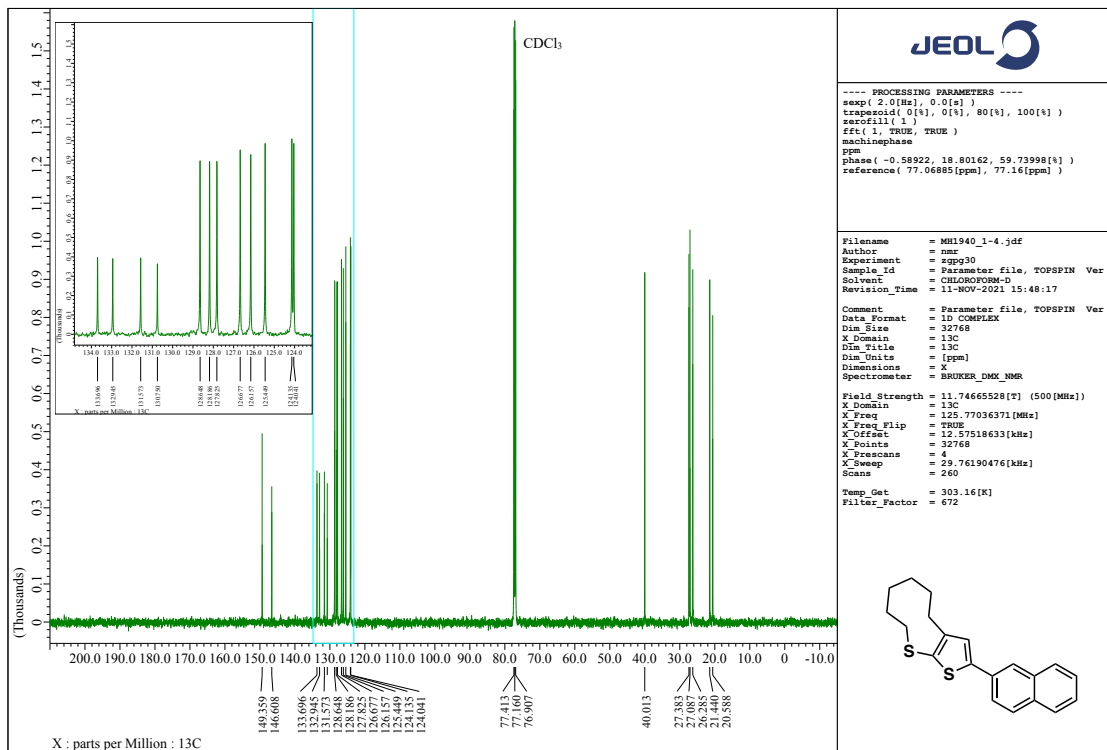


Figure S16. $^{13}\text{C}\{\text{H}\}$ NMR spectrum of **5** (125 MHz, CDCl_3).

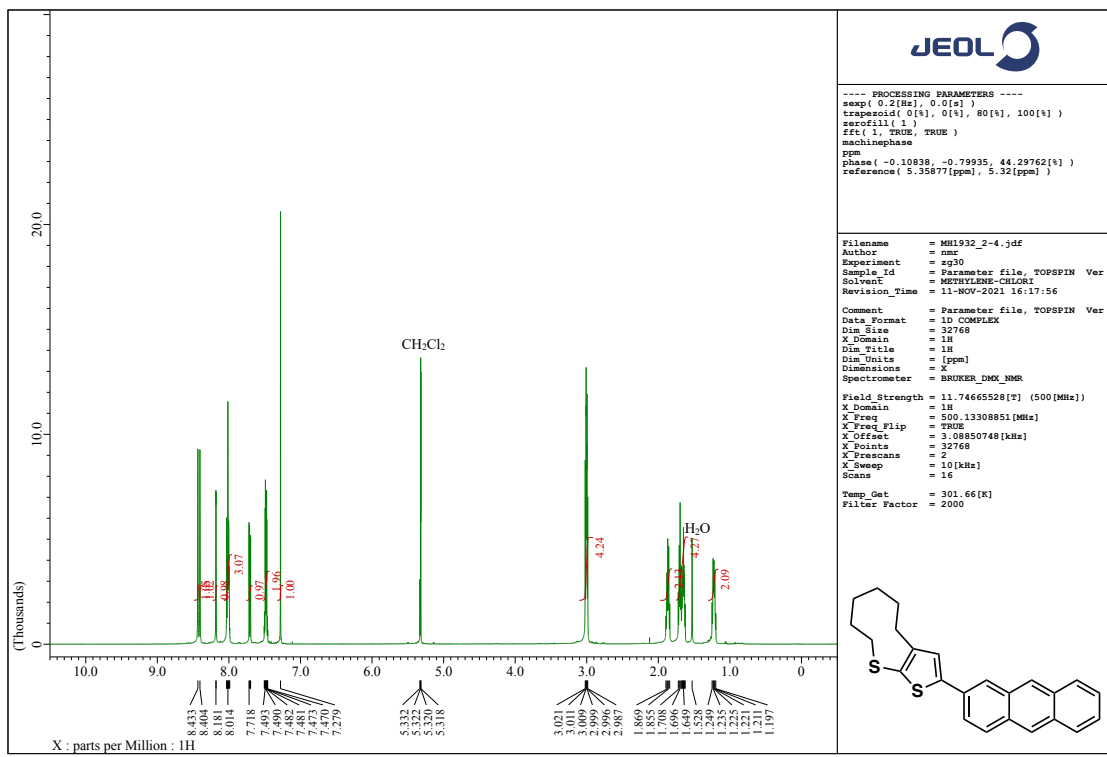


Figure S17. ^1H NMR spectrum of **6** (500 MHz, CD_2Cl_2).

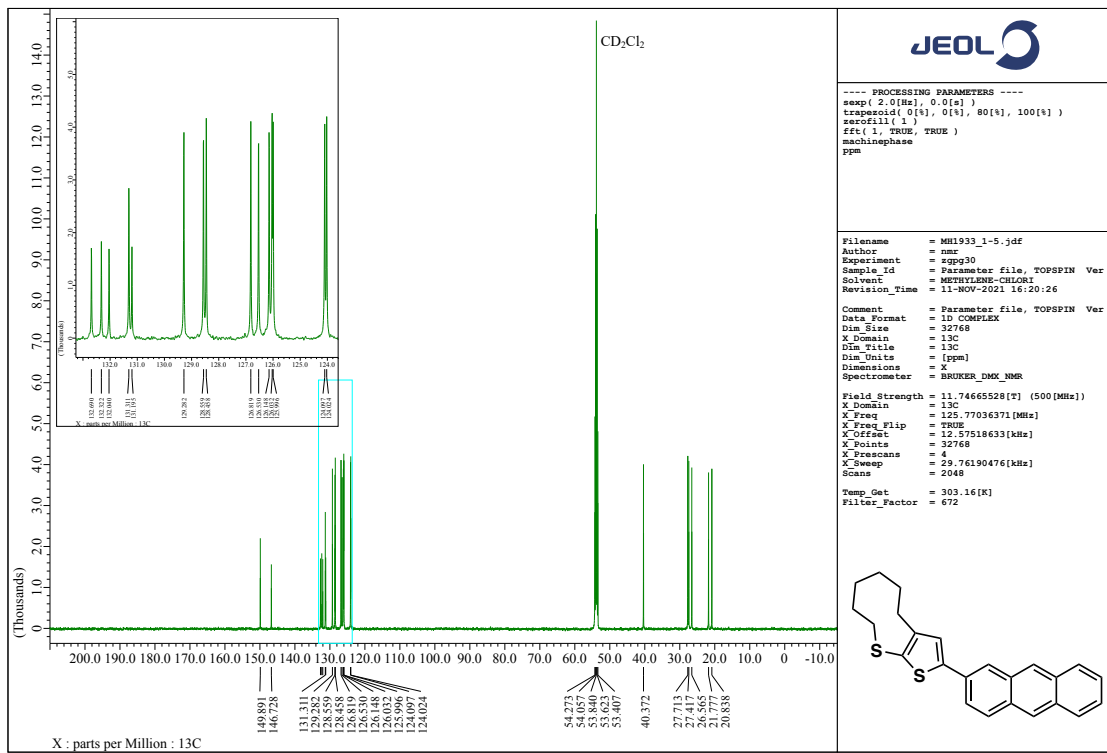


Figure S18. $^{13}\text{C}\{\text{H}\}$ NMR spectrum of **6** (125 MHz, CD_2Cl_2).

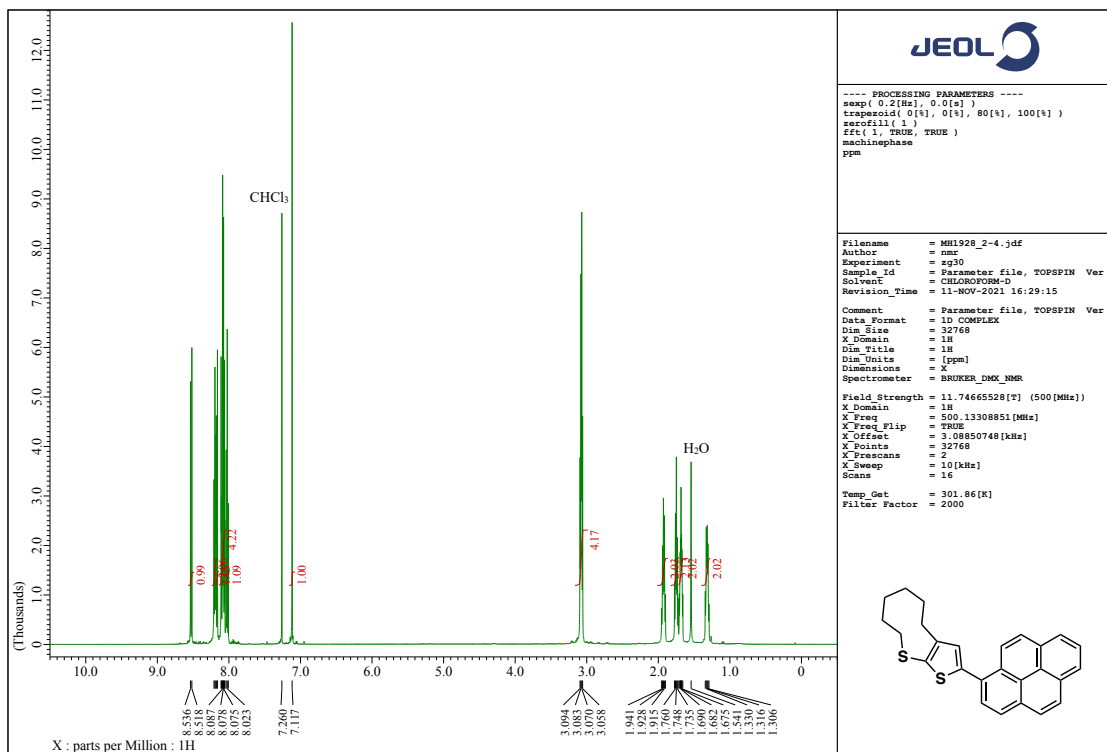


Figure S19. ^1H NMR spectrum of **7** (500 MHz, CDCl_3).

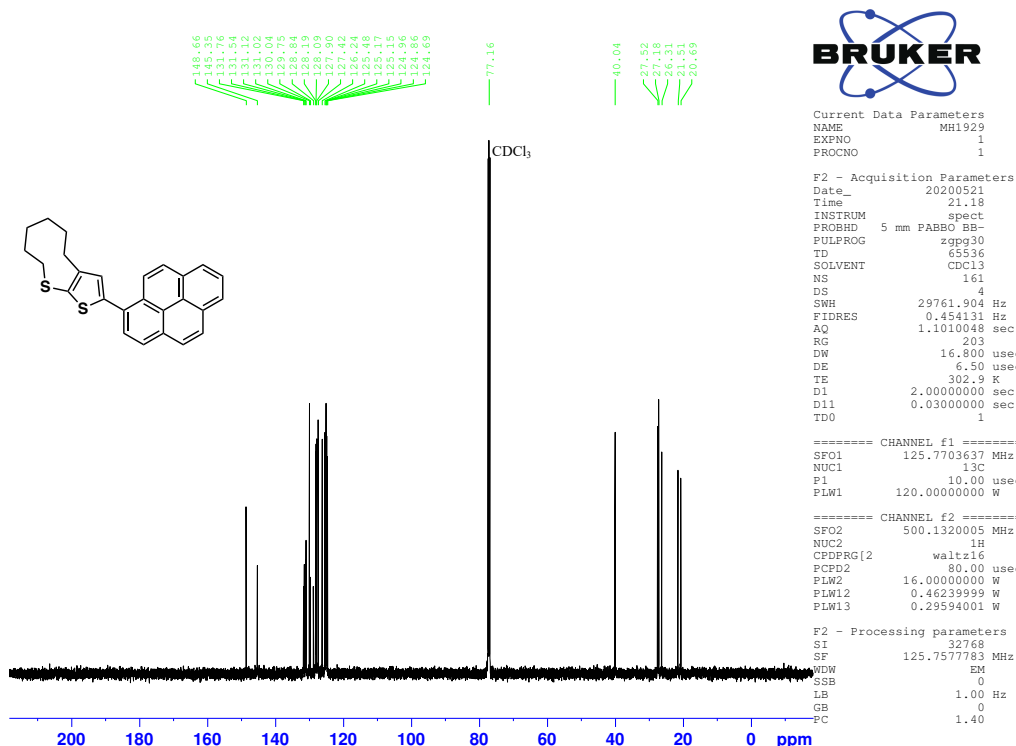


Figure S20. $^{13}\text{C}\{\text{H}\}$ NMR spectrum of **7** (125 MHz, CDCl_3).

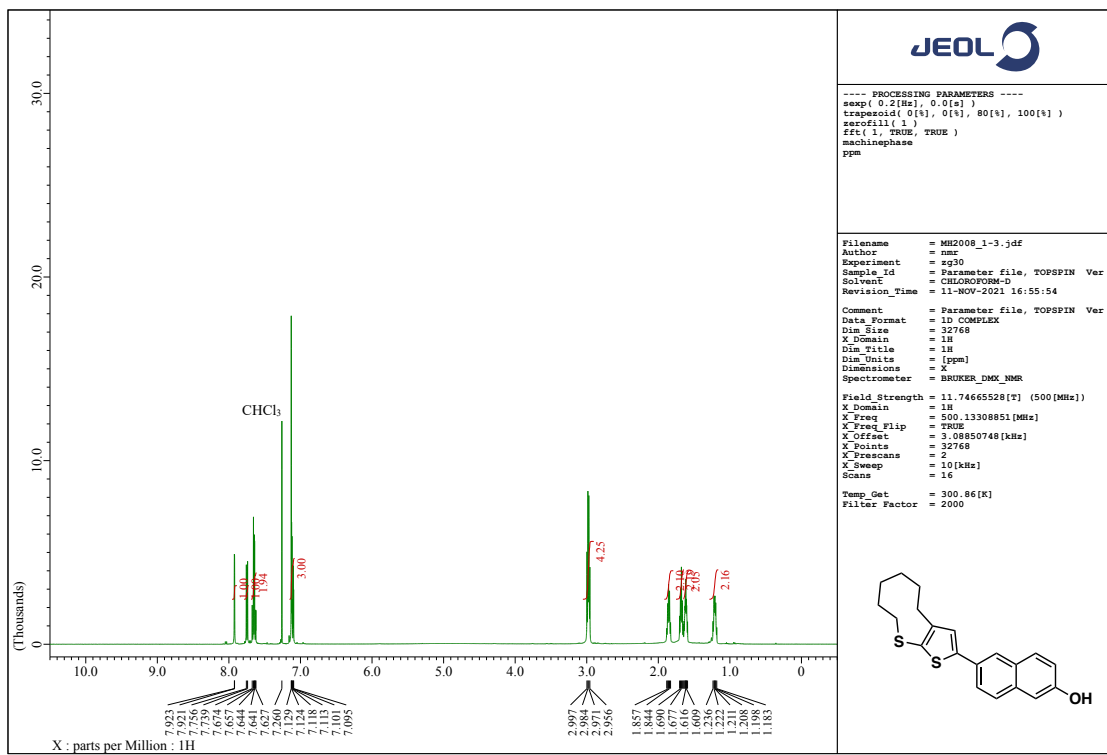


Figure S21. ^1H NMR spectrum of **16** (500 MHz, CDCl_3).

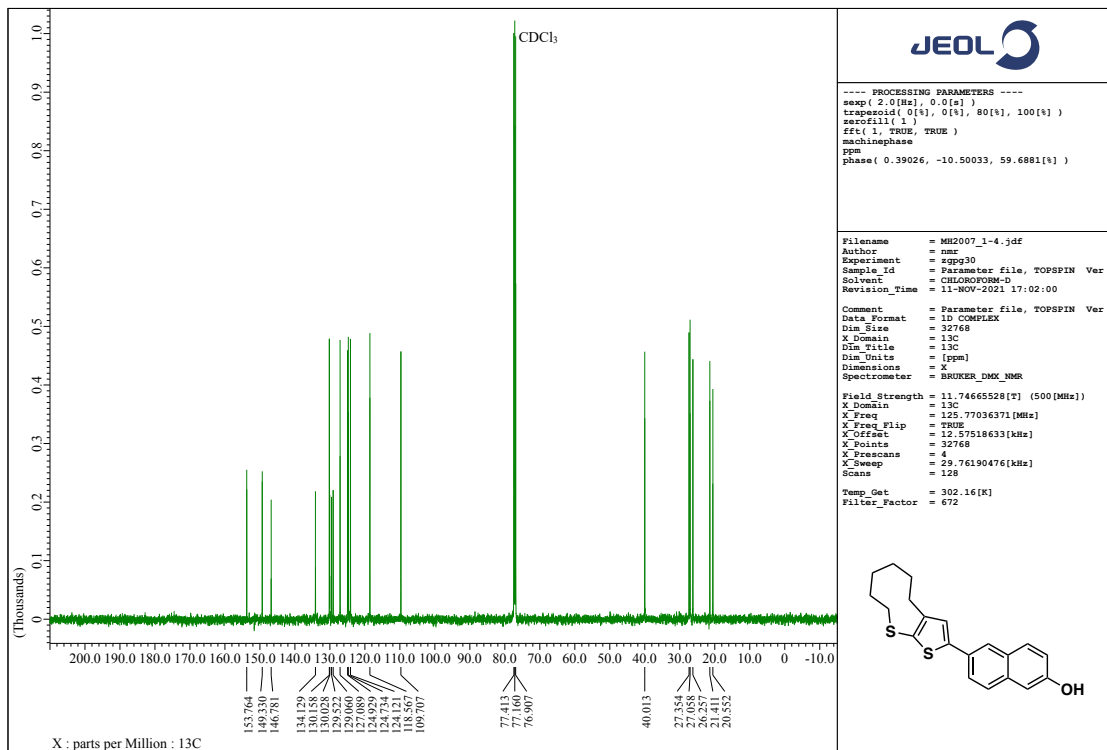


Figure S22. $^{13}\text{C}\{^1\text{H}\}$ NMR spectrum of **16** (125 MHz, CDCl_3).

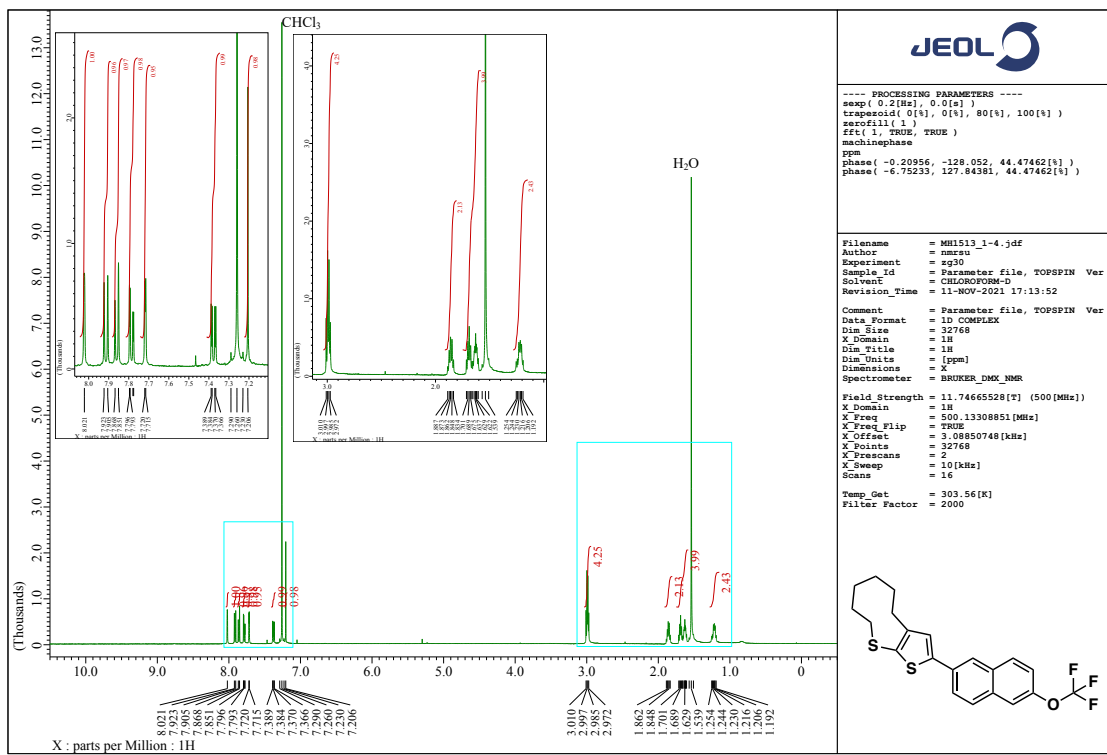


Figure S23. ^1H NMR spectrum of **17** (500 MHz, CDCl_3).

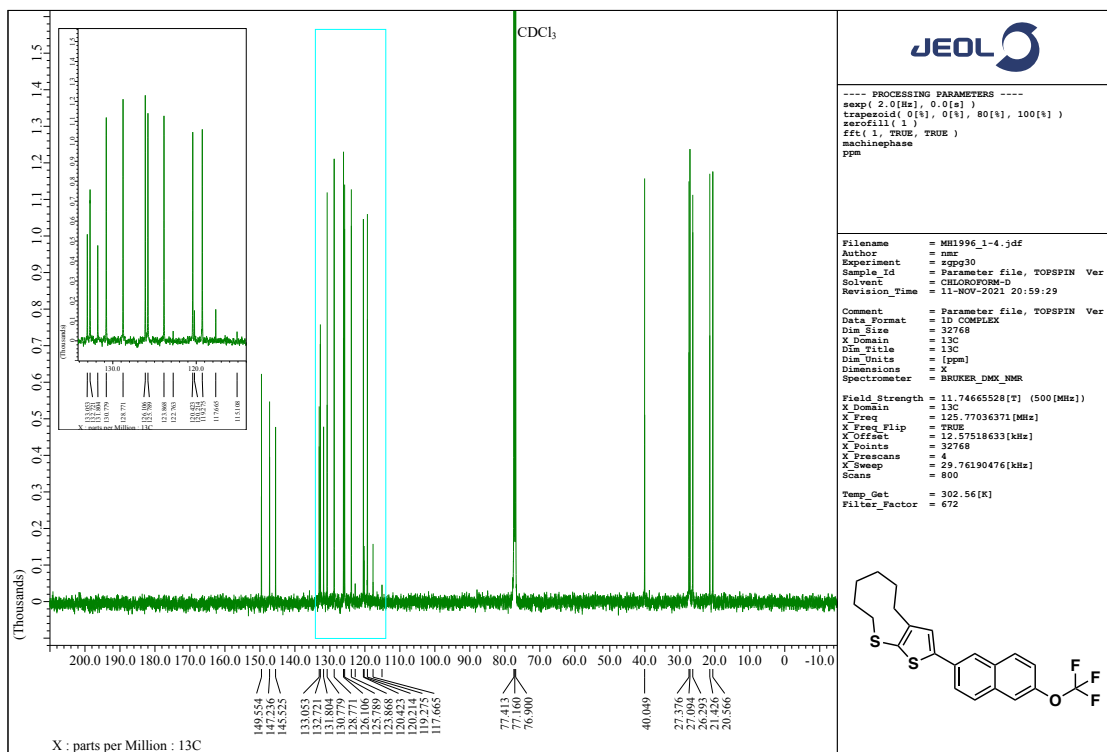


Figure S24. $^{13}\text{C}\{^1\text{H}\}$ NMR spectrum of **17** (125 MHz, CDCl_3).

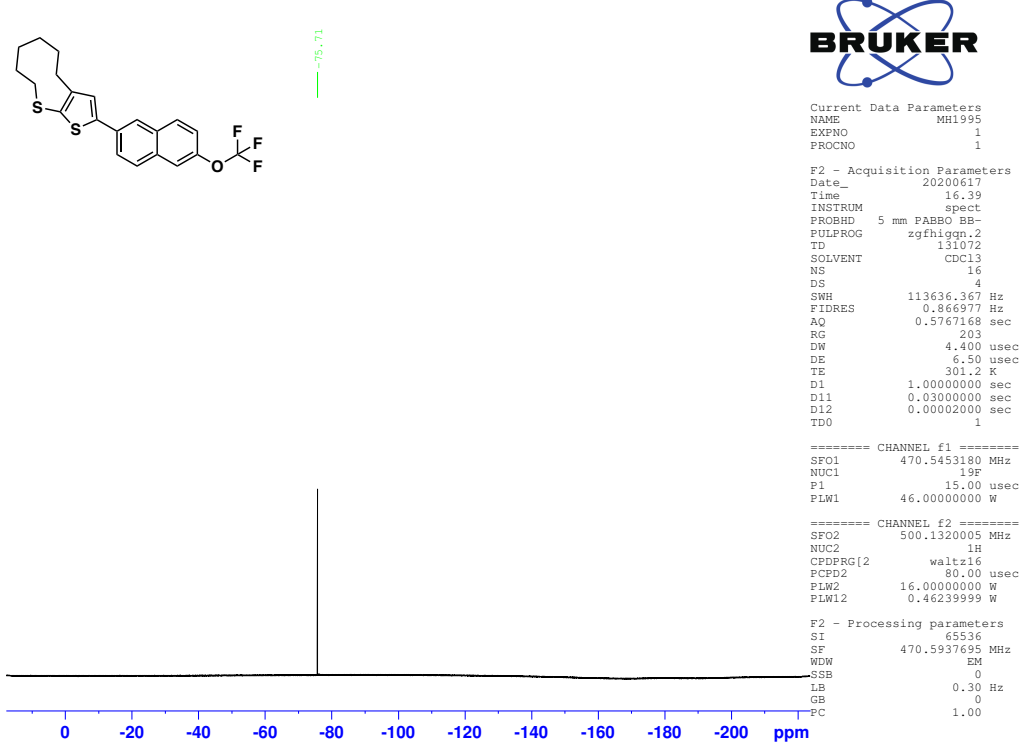


Figure S25. ^{19}F NMR spectrum of **17** (470 MHz, CDCl_3).

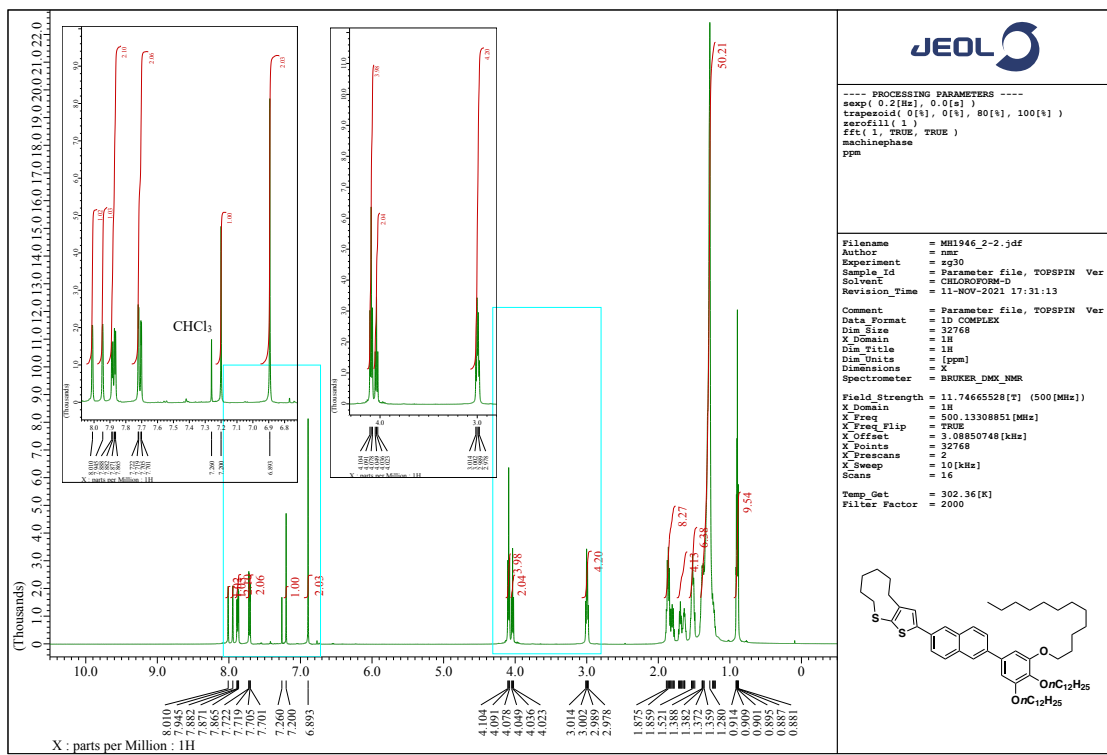


Figure S26. ^1H NMR spectrum of **8** (500 MHz, CDCl_3).

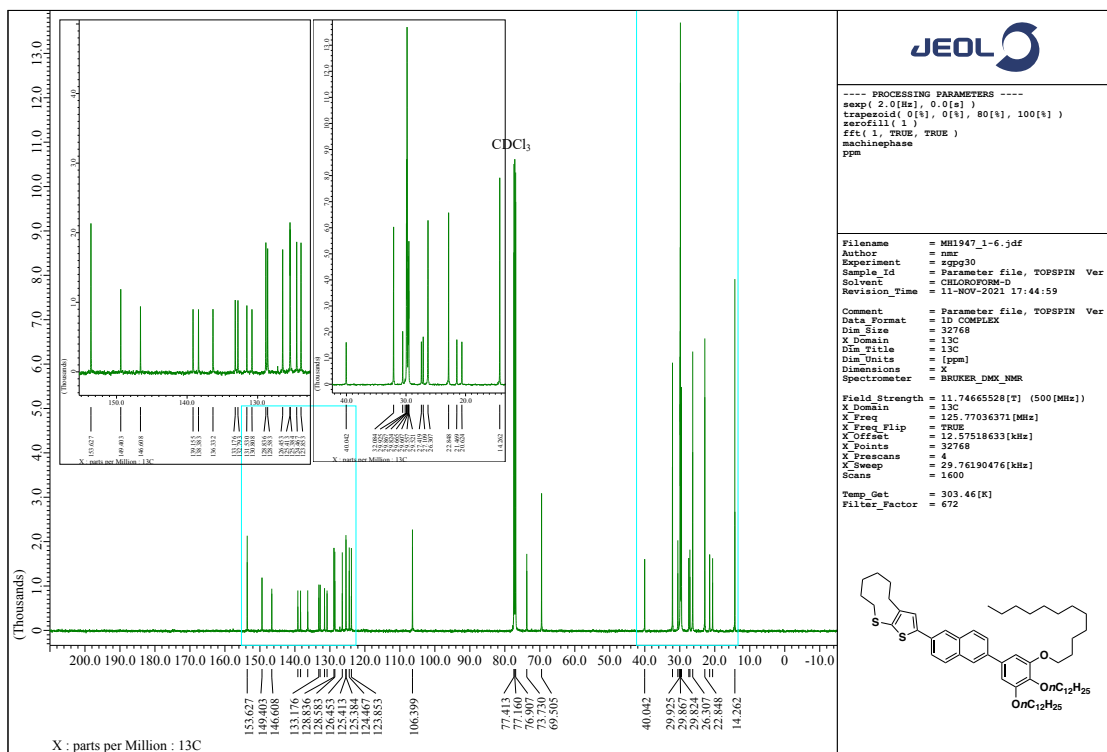


Figure S27. $^{13}\text{C}\{^1\text{H}\}$ NMR spectrum of **8** (125 MHz, CDCl_3).

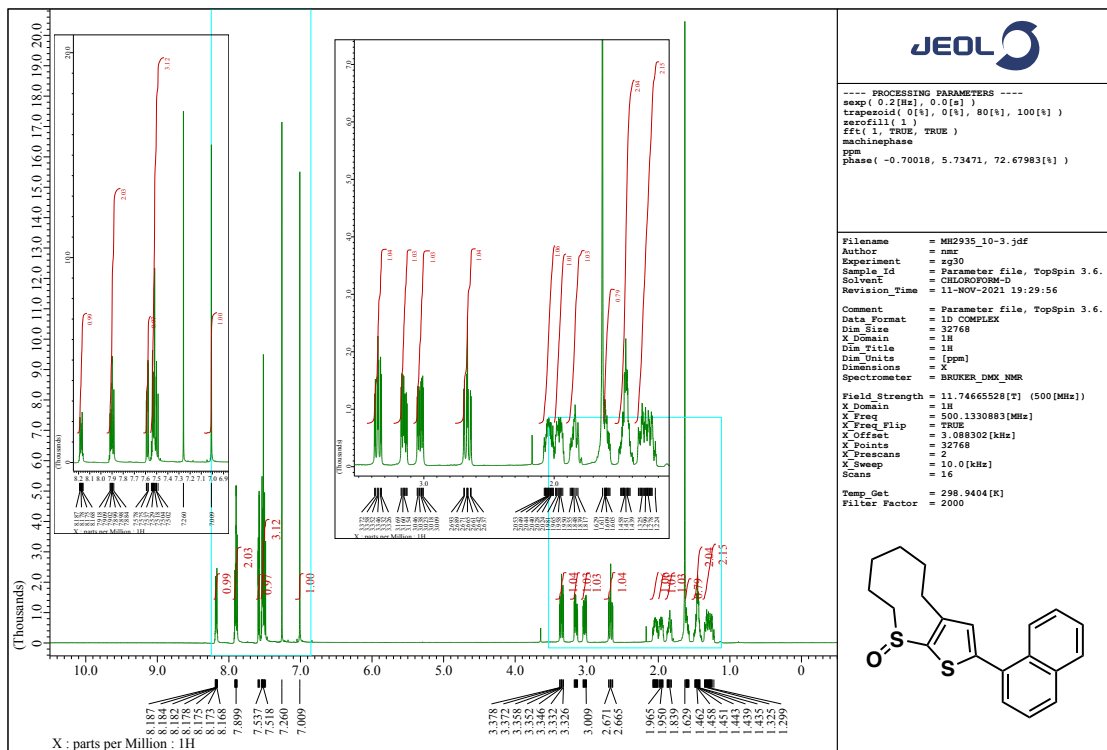


Figure S28. ^1H NMR spectrum of **9** (500 MHz, CDCl_3).

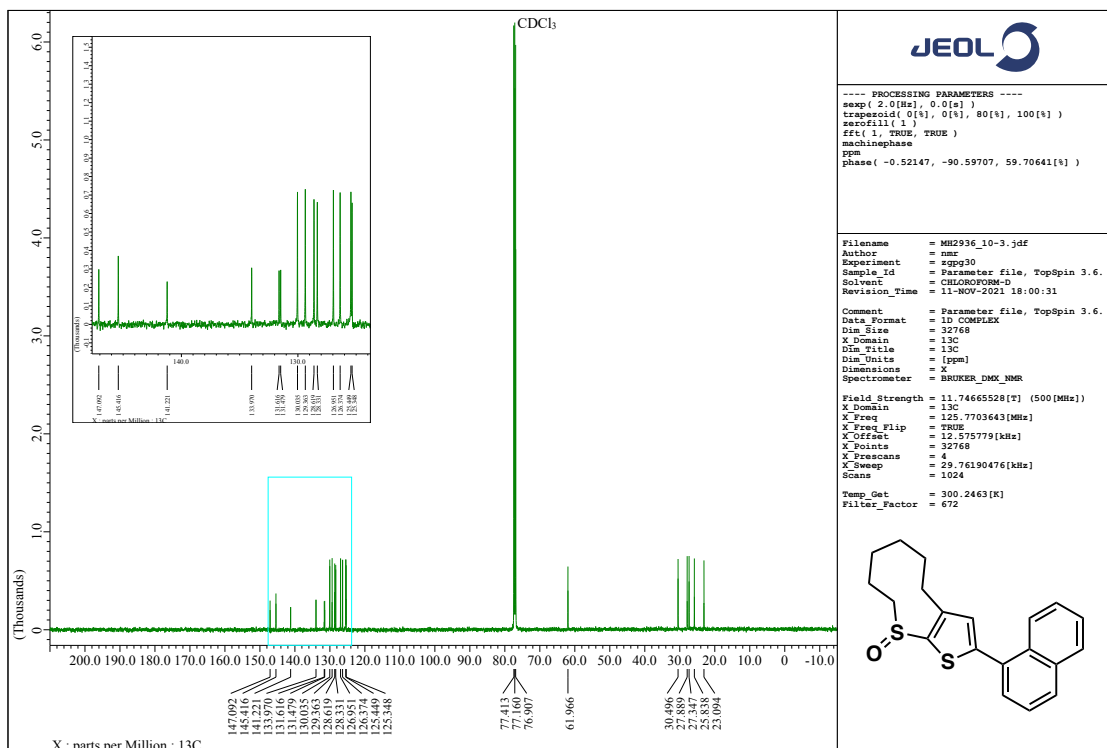


Figure S29. $^{13}\text{C}\{^1\text{H}\}$ NMR spectrum of **9** (125 MHz, CDCl_3).

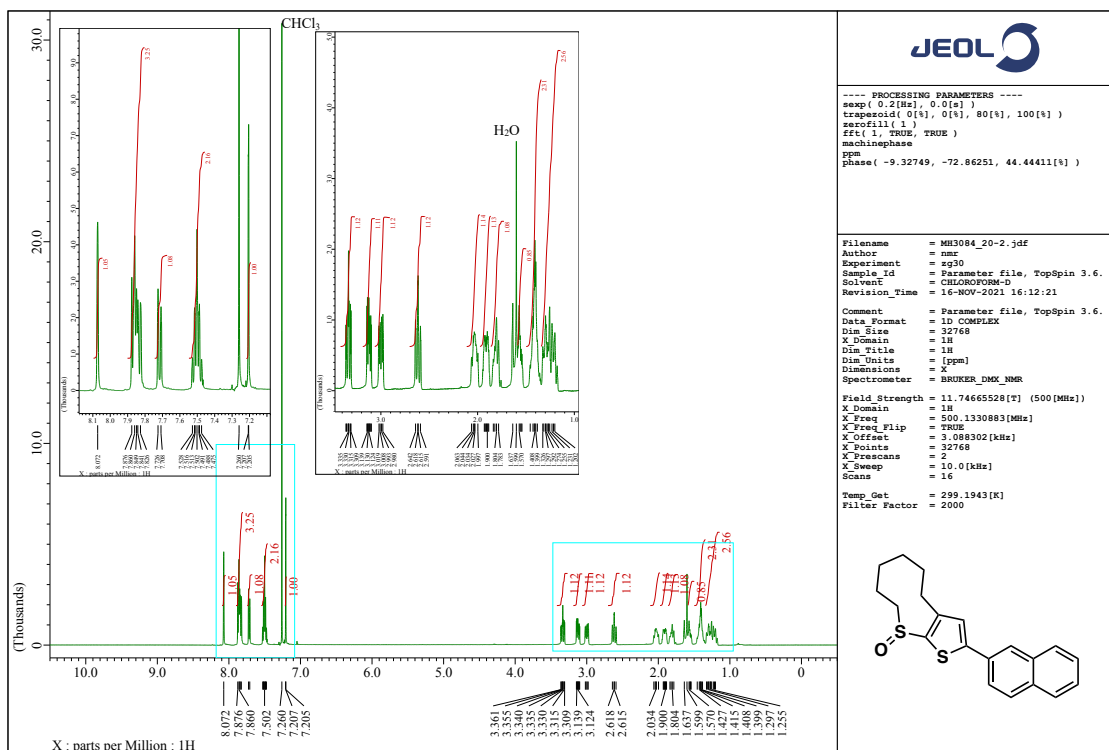


Figure S30. ^1H NMR spectrum of **10** (500 MHz, CDCl_3).

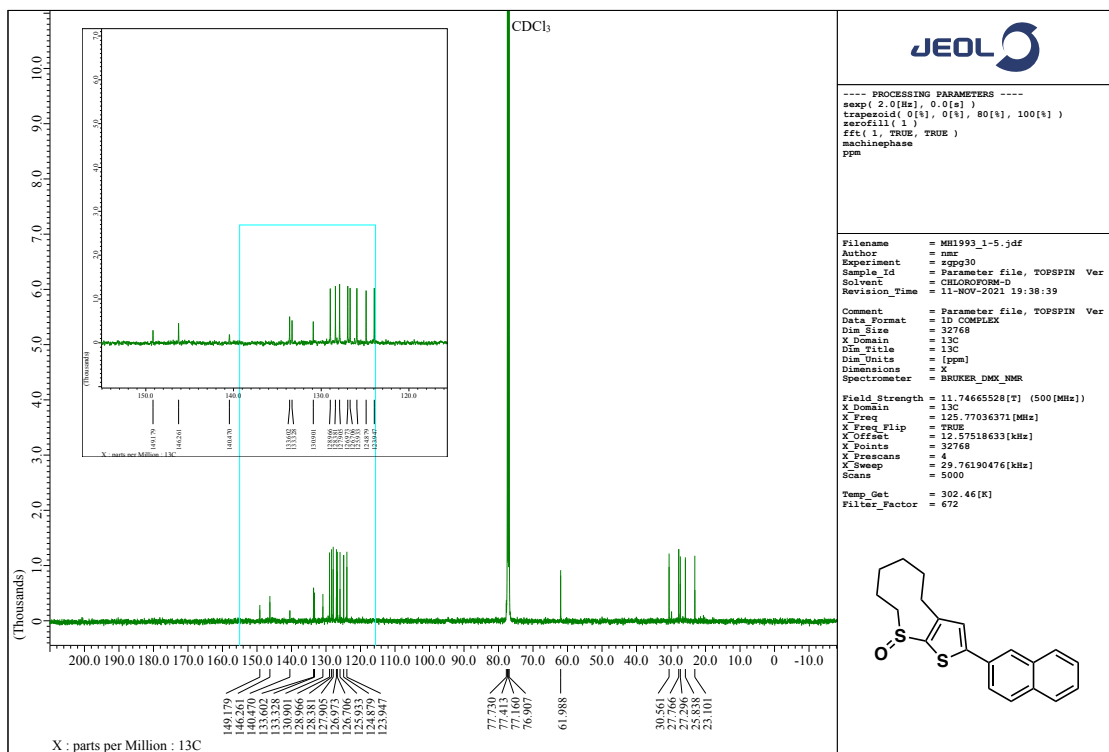


Figure S31. $^{13}\text{C}\{^1\text{H}\}$ NMR spectrum of **10** (125 MHz, CDCl_3).

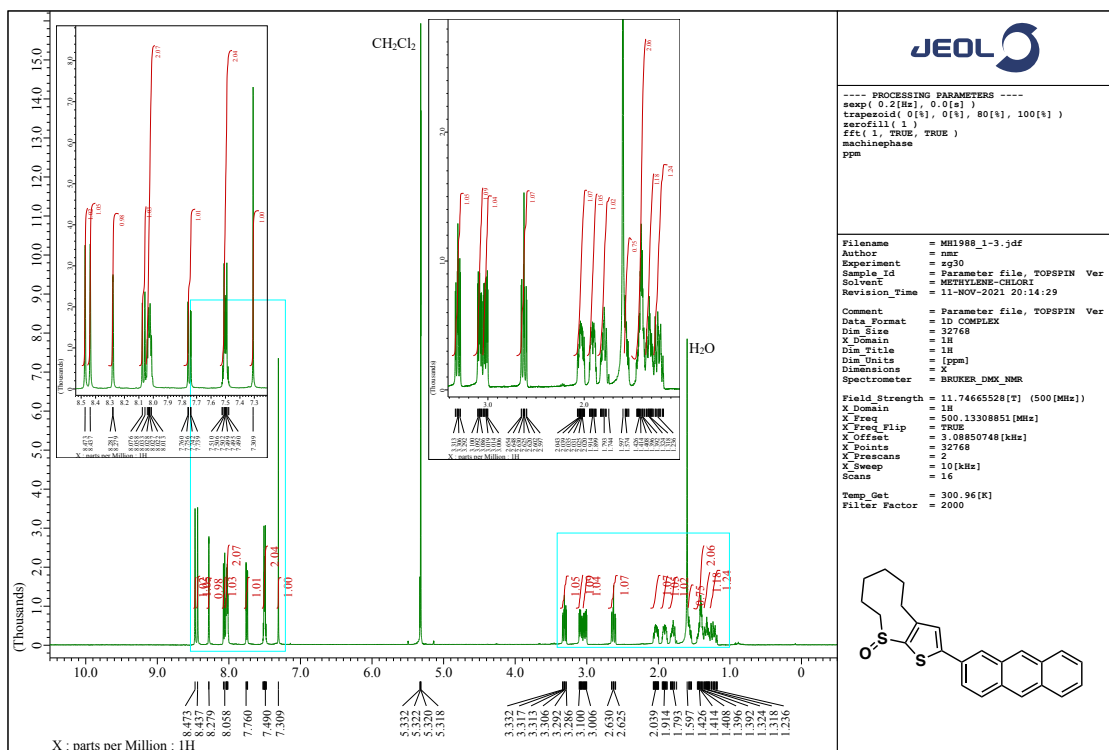


Figure S32. ^1H NMR spectrum of **11** (500 MHz, CD_2Cl_2).

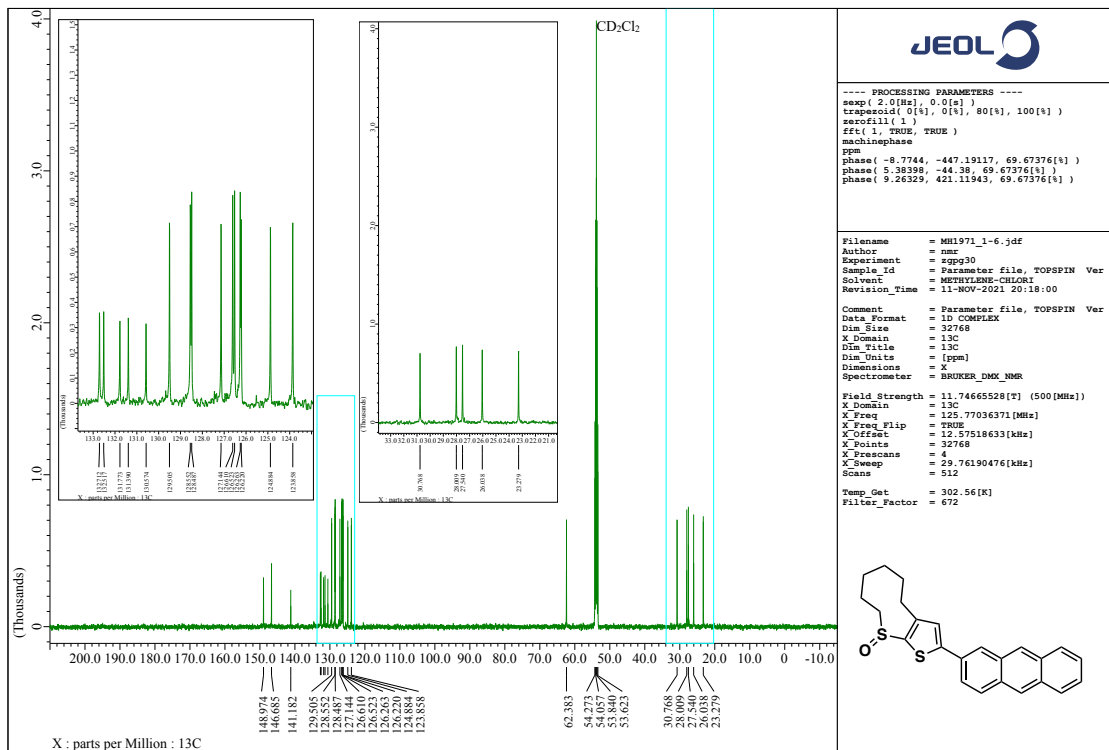


Figure S33. $^{13}\text{C}\{^1\text{H}\}$ NMR spectrum of **11** (125 MHz, CD_2Cl_2).

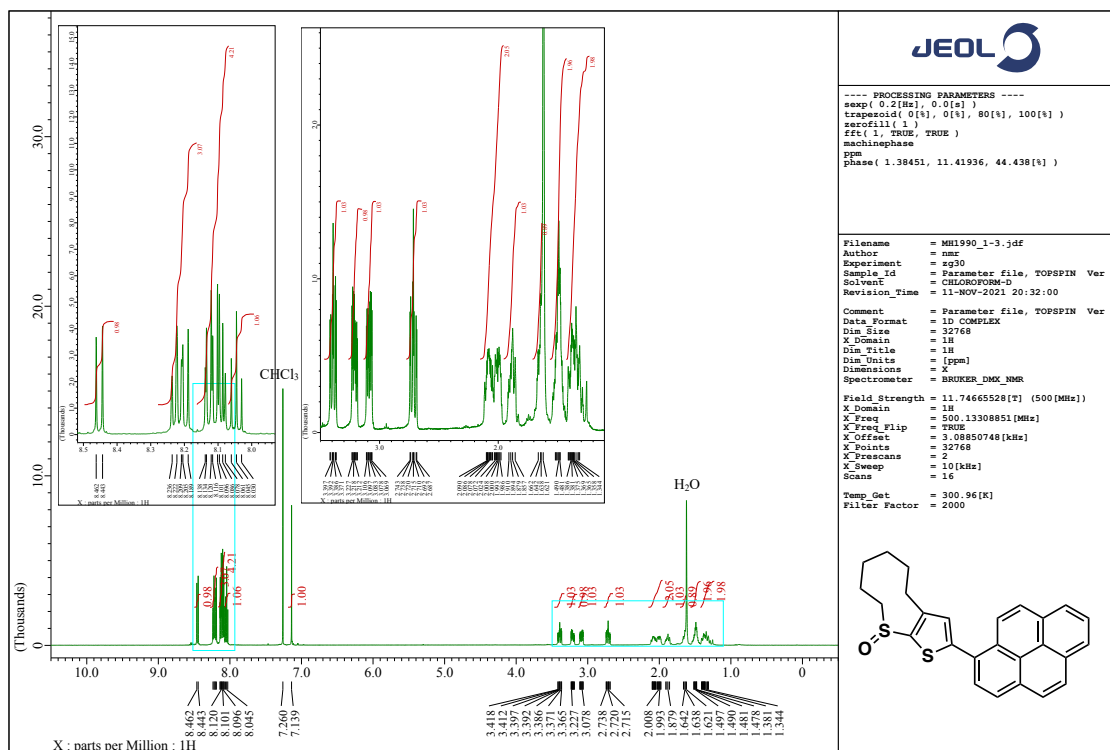


Figure S34. ^1H NMR spectrum of **12** (500 MHz, CDCl_3).

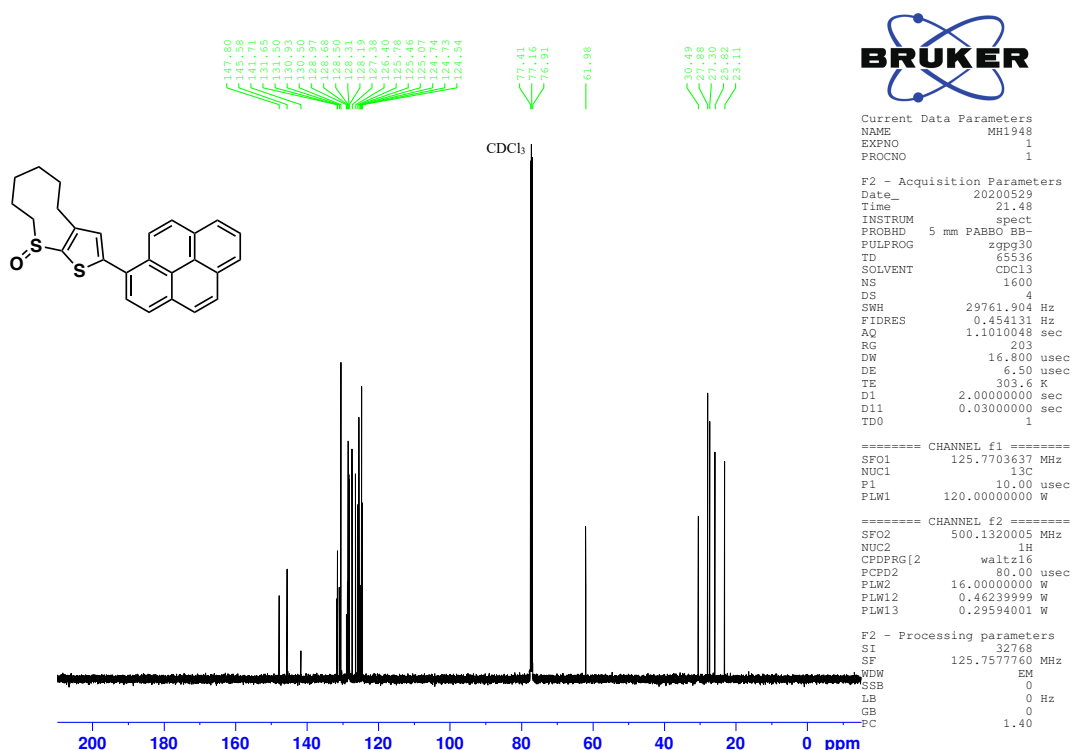
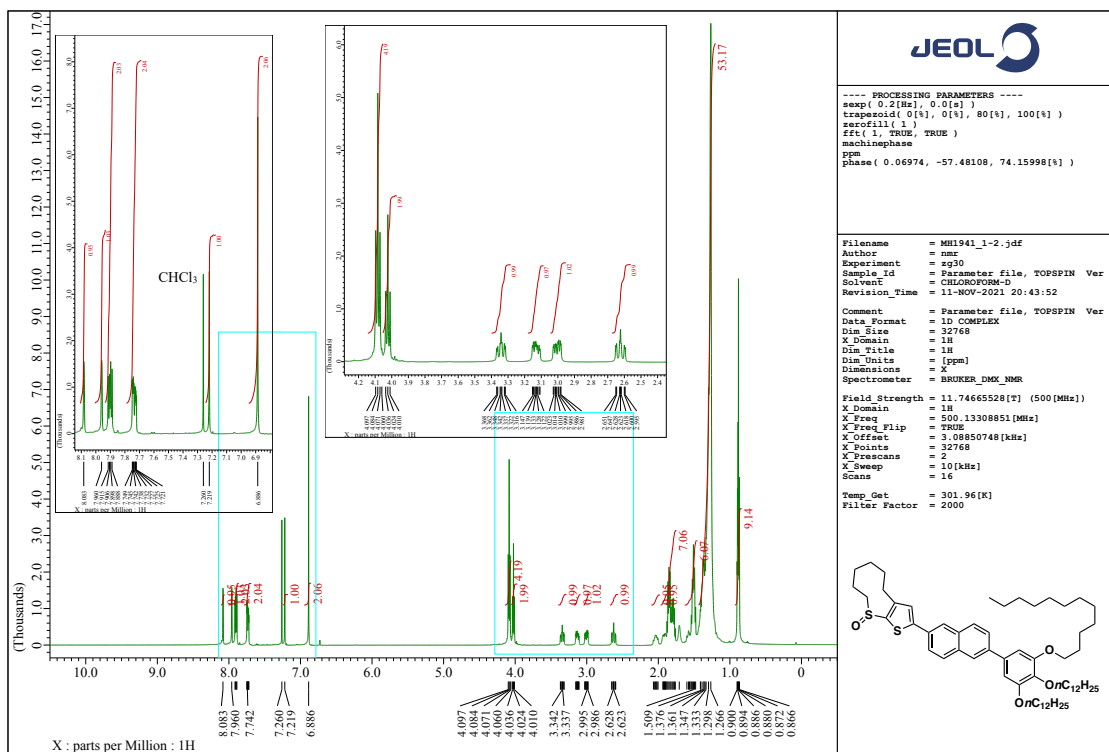


Figure S35. $^{13}\text{C}\{^1\text{H}\}$ NMR spectrum of **12** (125 MHz, CDCl_3).



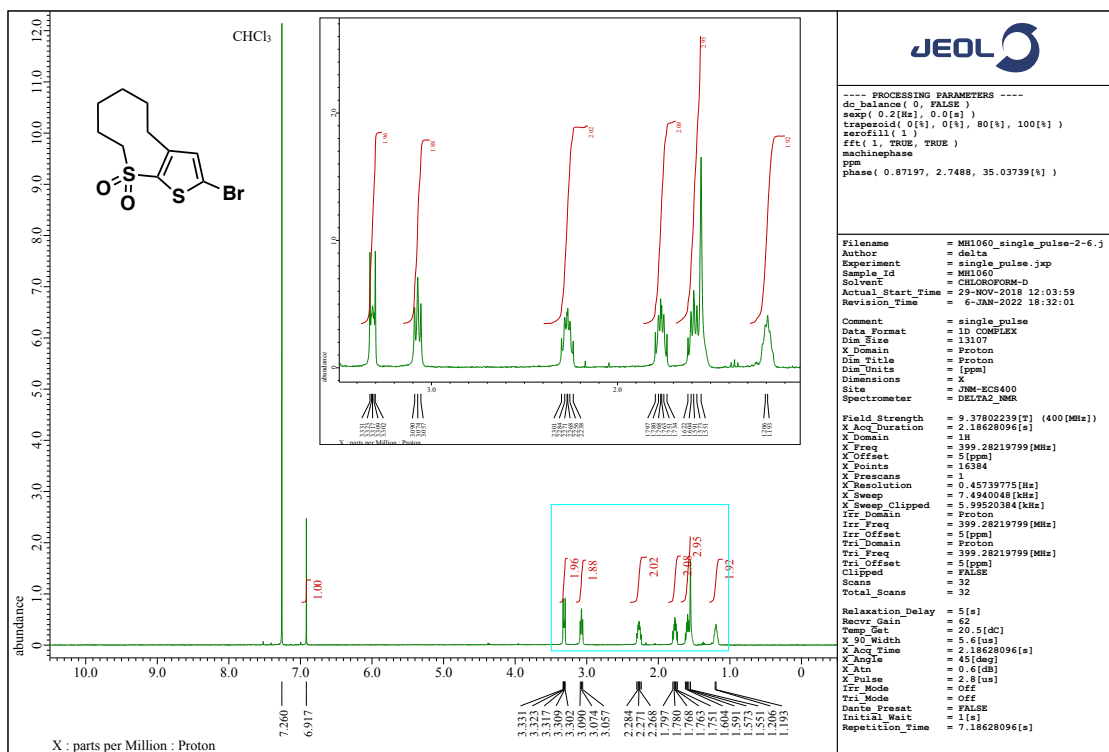


Figure S38. ^1H NMR spectrum of **18** (400 MHz, CDCl_3).

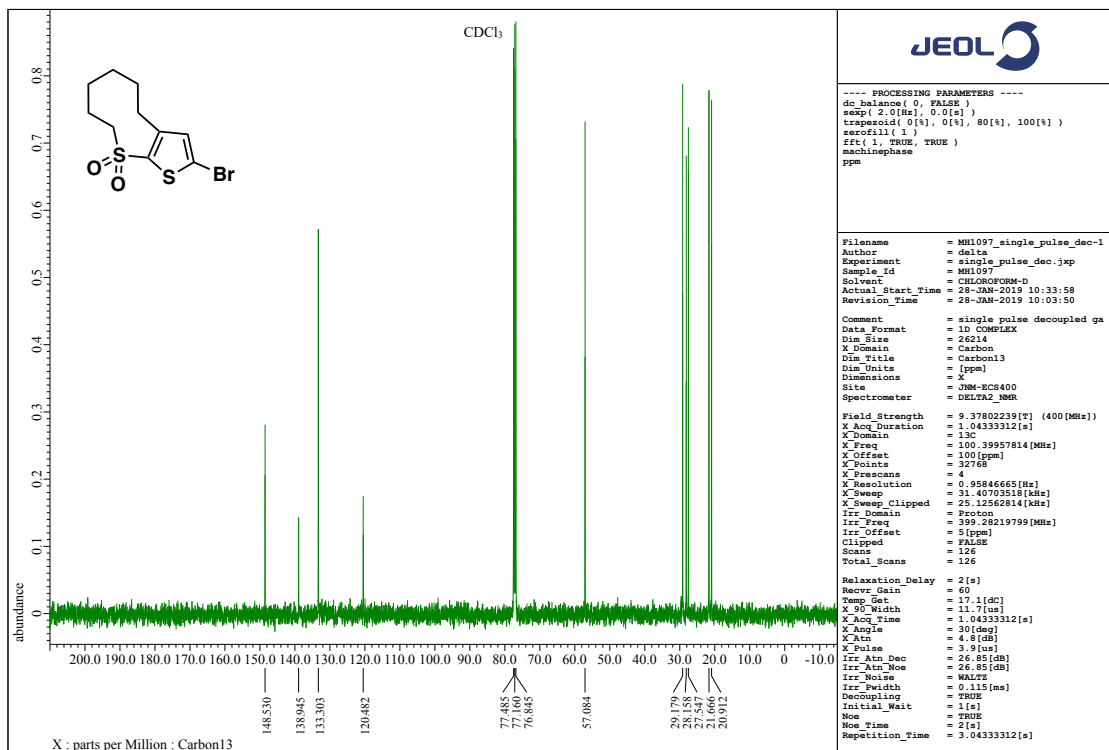


Figure S39. $^{13}\text{C}\{\text{H}\}$ NMR spectrum of **18** (100 MHz, CDCl_3).

11. Results of HPLC Analyses for Optically Active Compounds

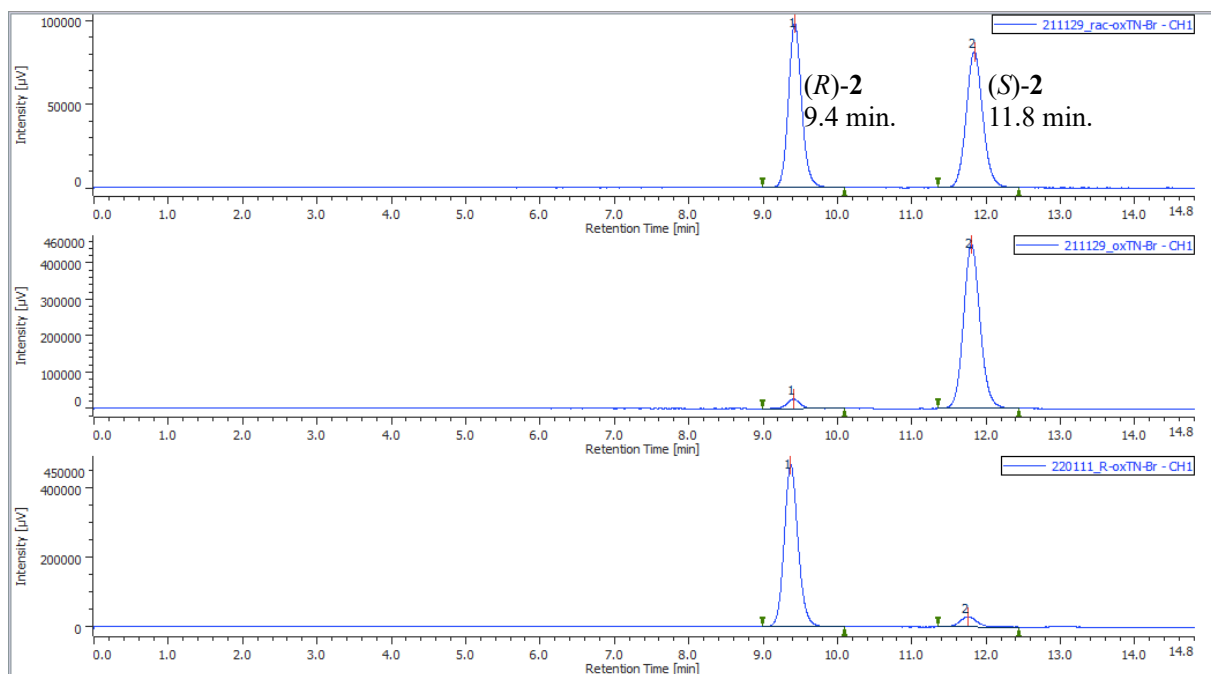


Figure S40. HPLC charts of *rac*-**2** (top), and the products of the asymmetric oxidation reactions of **1** using (*S*)-**3** (middle) and (*R*)-**3** (bottom), respectively (acetonitrile as an eluent, 1 mL/min, DAICEL Chiralpak IG).

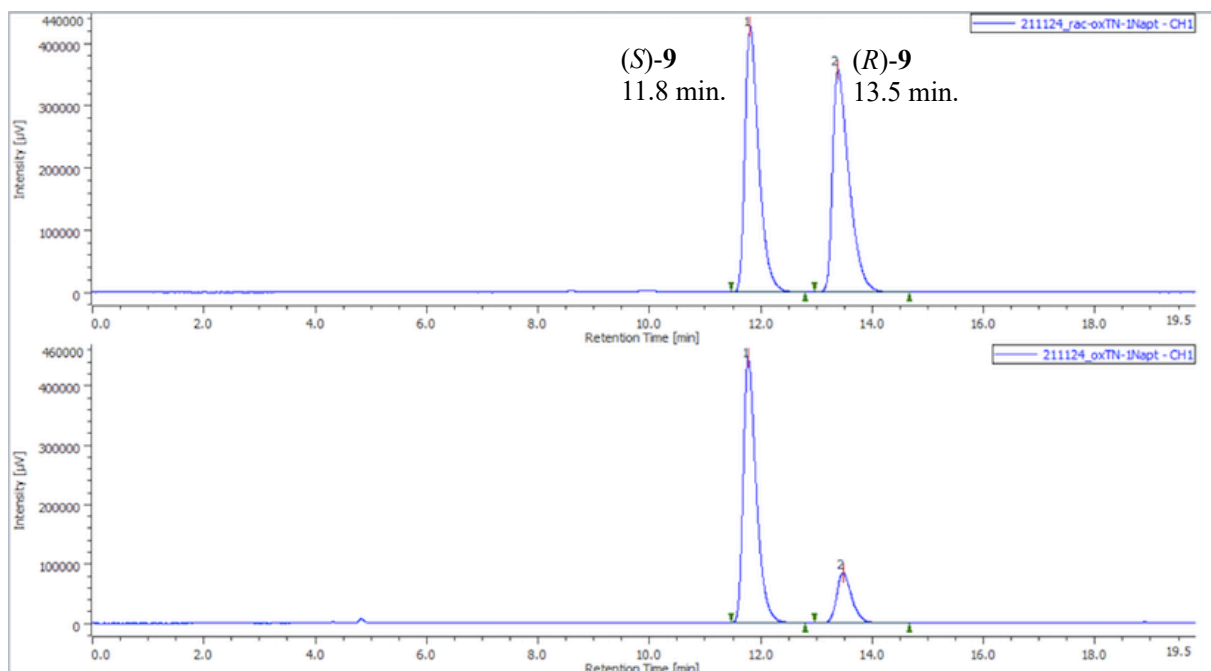


Figure S41. HPLC charts of *rac*-**9** (top) and the product of the asymmetric oxidation of **4** (acetonitrile as an eluent, 1 mL/min, DAICEL Chiralpak IG).

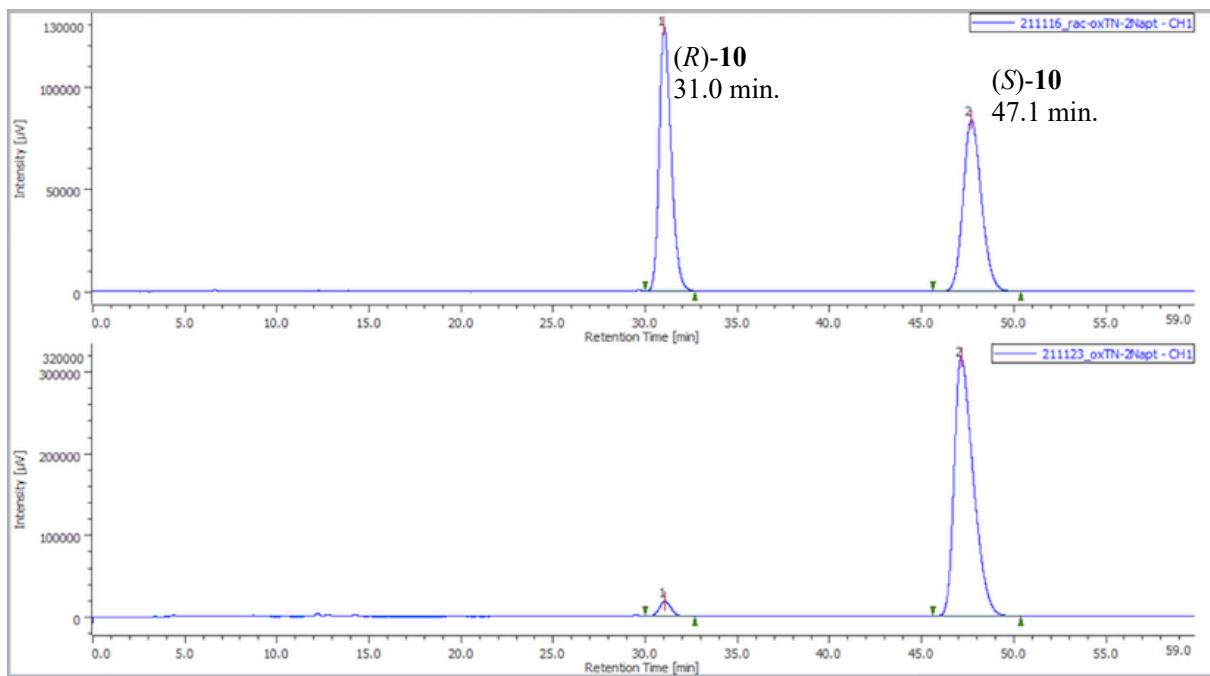


Figure S42. HPLC charts of *rac*-**10** (top) and the product of the asymmetric oxidation of **5** (acetonitrile as an eluent, 1 mL/min, DAICEL Chiralpak IG).

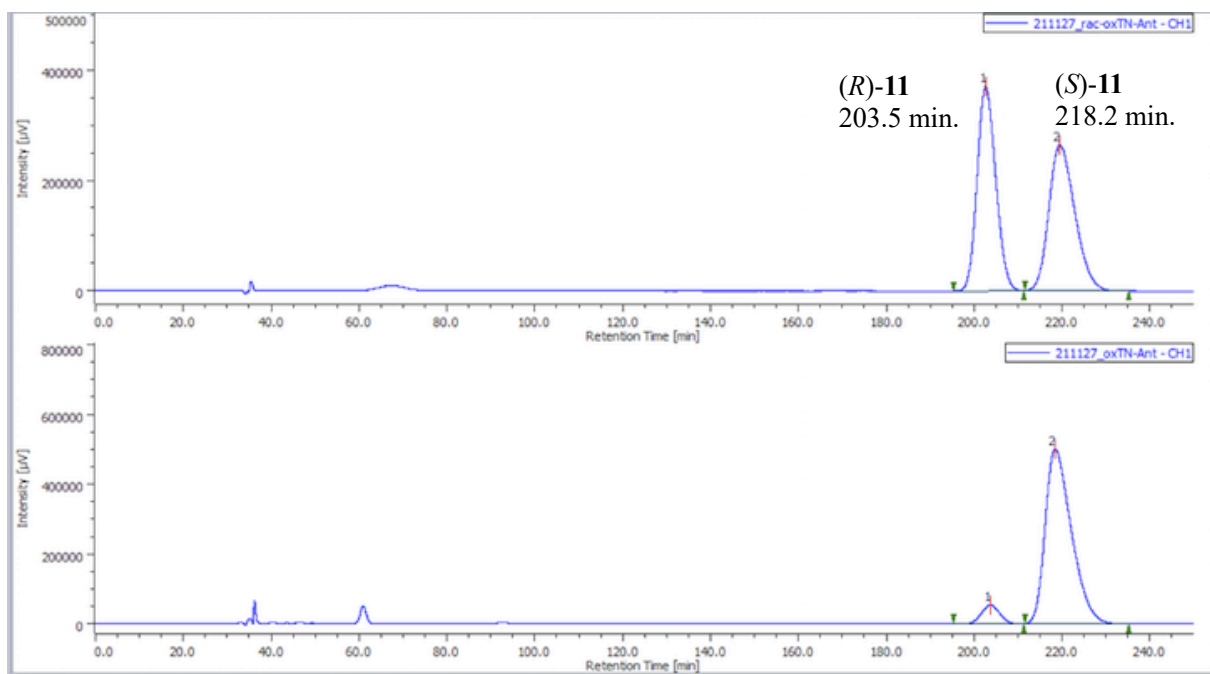


Figure S43. HPLC charts of *rac*-**11** (top) and the product of the asymmetric oxidation of **6** (acetonitrile/THF 5/1 as eluent, 0.1 mL/min, DAICEL Chiralpak IG).

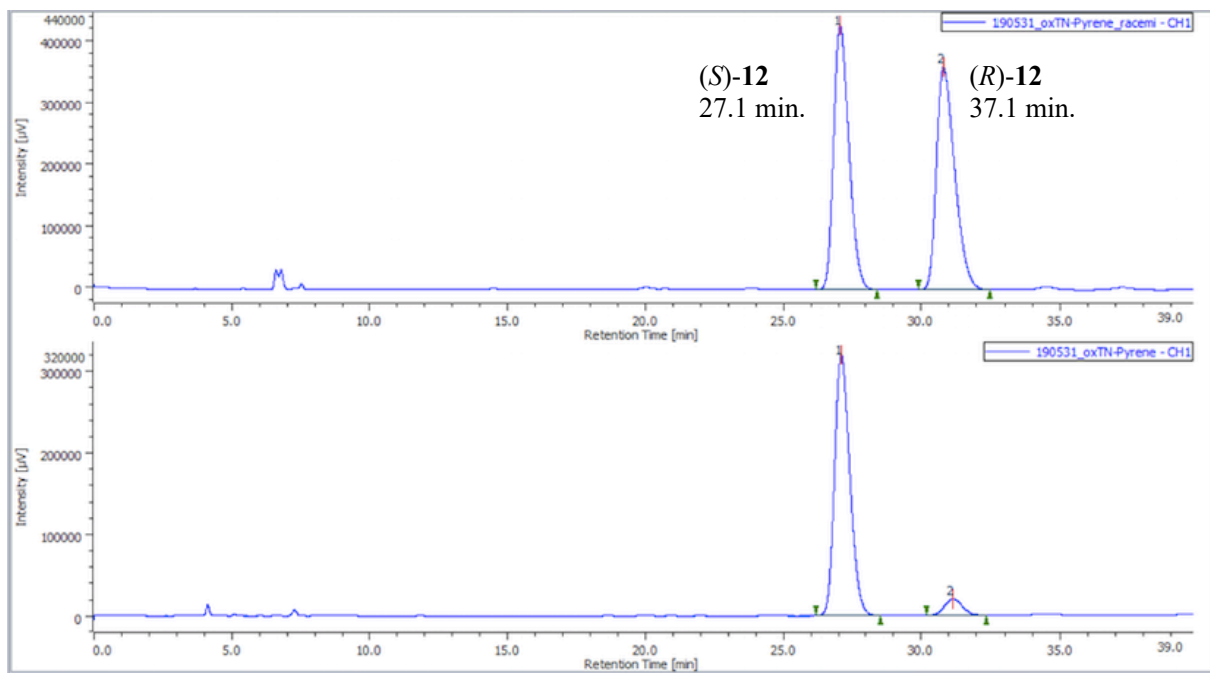


Figure S44. HPLC charts of *rac*-**12** (top) and the product of the asymmetric oxidation of **7** (acetonitrile as an eluent, 1 mL/min, DAICEL Chiralpak IG).

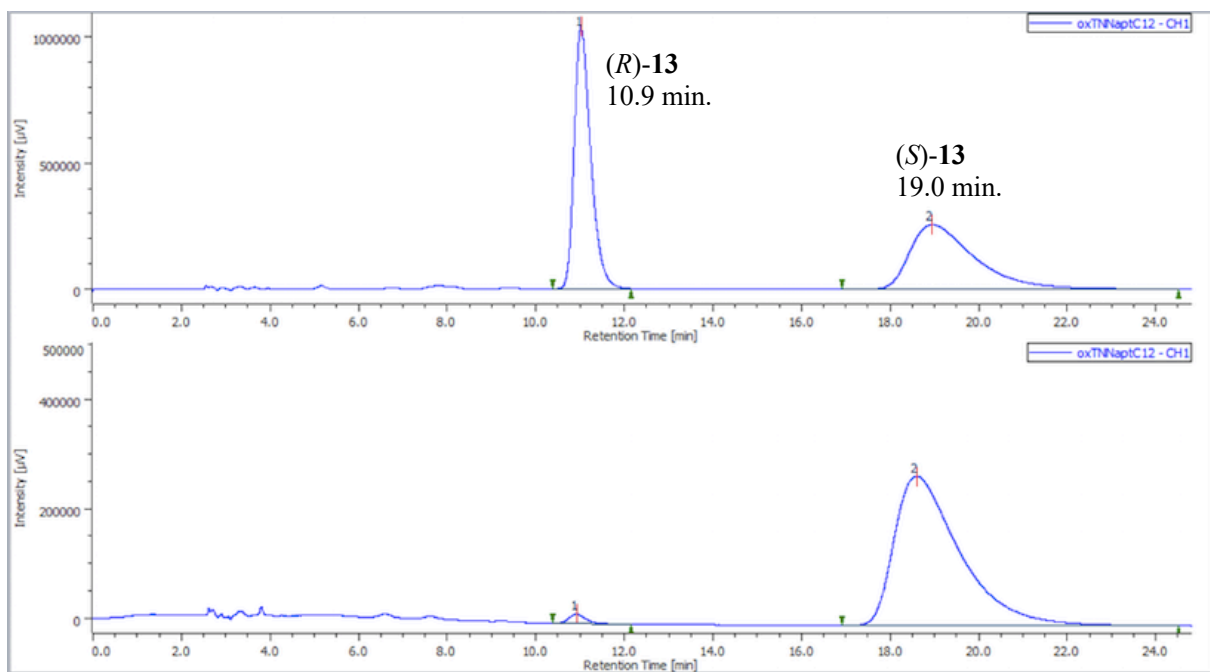


Figure S45. HPLC charts of *rac*-**13** (top) and the product of the asymmetric oxidation of **8** (hexane/EtOH 4/1 as an eluent, 1 mL/min, DAICEL Chiralpak IG).

12. Author Contributions

M.H., S.Y., and A.F. designed the project. M.H. contributed to this study by carrying out all the synthetic works and measurements of SC-XRD and photophysical properties, and DFT calculations. S.H., Y.H., and K.Y. conducted VT-PXRD measurements, DFTB-MD simulations, and measurements of optical rotation, respectively. M.H. and A.F. prepared the manuscript, and S.H., Y.H., K.Y., and S.Y. proofread it. A.F. directed all the projects.

13. References

- S1 C. Bolm and F. Bienewald, *Angew. Chem. Int. Ed. Engl.*, 1995, **34**, 2640.
- S2 (a) P. Pitchen, E. Dunach, M. N. Deshmukh and H. B. Kagan, *J. Am. Chem. Soc.*, 1984, **106**, 8188. (b) H. B. Kagan, E. Duhach, C. Nemecek, P. Pitchen, O. Samuel and S.-H. Zhao, *Pure Appl. Chem.*, 1985, **57**, 1911.
- S3 (a) K. Nakajima, M. Kojima and J. Fujita, *Chem. Lett.*, 1986, **15**, 1483. (b) K. Nakajima, K. Kojima, M. Kojima and J. Fujita, *Bull. Chem. Soc. Jpn.*, 1990, **63**, 2620.
- S4 J. Fujisaki, K. Matsumoto, K. Matsumoto and T. Katsuki, *J. Am. Chem. Soc.*, 2011, **133**, 56.
- S5 S. Liao, I. Čorić, Q. Wang and B. List, *J. Am. Chem. Soc.*, 2012, **134**, 10765.
- S6 W. Dai, J. Li, B. Chen, G. Li, Y. Lv, L. Wang and S. Gao, *Org. Lett.*, 2013, **15**, 5658.
- S7 K. P. Bryliakov, N. N. Karpyshev, S. A. Fominsky, A. G. Tolstikov and E. P. Talsi, *J. Mol. Catal. Chem.*, 2001, **171**, 73.
- S8 D. Balcells, F. Maseras and G. Ujaque, *J. Am. Chem. Soc.*, 2005, **127**, 3624.
- S9 (a) G. E. O'Mahony, A. Ford and A. R. Maguire, *J. Org. Chem.*, 2012, **77**, 3288. (b) G. E. O'Mahony, K. S. Eccles, R. E. Morrison, A. Ford, S. E. Lawrence and A. R. Maguire, *Tetrahedron*, 2013, **69**, 10168.
- S10 (a) J. Legros and C. Bolm, *Angew. Chem. Int. Ed.*, 2004, **43**, 4225. (b) J. Legros and C. Bolm, *Chem. Eur. J.*, 2005, **11**, 1086.
- S11 (a) B. Pelotier, M. Anson, I. B. Campbell, S. J. F. Macdonald, G. Priem and R. F. W. Jackson, *Synlett*, 2002, **7**, 1055. (b) C. Drago, L. Caggiano and, R. F. W. Jackson, *Angew. Chem. Int. Ed.*, 2005, **44**, 7221.
- S12 A. Fukazawa, Y. Toda, M. Hayakawa, A. Sekioka, H. Ishii, T. Okamoto, J. Takeya, Y. Hijikata and S. Yamaguchi, *Chem. Eur. J.*, 2018, **24**, 11503.
- S13 H. Maeda, K. Chigusa, T. Sakurai, K. Ohta, S. Uemura and S. Seki, *Chem. Eur. J.*, 2013, **19**, 9224.
- S14 Gaussian 16, Revision B.01, M. J. Frisch, G. W. Trucks, H. B. Schlegel, G. E. Scuseria, M. A. Robb, J. R. Cheeseman, G. Scalmani, V. Barone, G. A. Petersson, H. Nakatsuji, X. Li, M. Caricato, A. V. Marenich, J. Bloino, B. G. Janesko, R. Gomperts, B. Mennucci, H. P. Hratchian, J. V. Ortiz, A. F. Izmaylov, J. L. Sonnenberg, D. Williams-Young, F. Ding, F. Lipparini, F. Egidi, J. Goings, B. Peng, A. Petrone, T. Henderson, D. Ranasinghe, V. G. Zakrzewski, J. Gao, N. Rega, G. Zheng, W. Liang, M. Hada, M. Ehara, K. Toyota, R. Fukuda, J. Hasegawa, M. Ishida, T. Nakajima, Y. Honda, O. Kitao, H. Nakai, T. Vreven, K. Throssell, J. A. Montgomery, Jr., J. E. Peralta, F. Ogliaro, M. J. Bearpark, J. J. Heyd, E. N. Brothers, K. N. Kudin, V. N. Staroverov, T. A. Keith, R. Kobayashi, J. Normand, K. Raghavachari, A. P. Rendell, J. C. Burant, S. S. Iyengar, J. Tomasi, M. Cossi, J. M. Millam, M. Klene, C. Adamo, R. Cammi, J. W. Ochterski, R. L. Martin, K. Morokuma, O. Farkas, J. B. Foresman and D. J. Fox, Gaussian, Inc.,

Wallingford CT, 2016.

- S15 F. A. L. Anet and A. J. R. Bourn, *J. Am. Chem. Soc.*, 1967, **89**, 760.
- S16 G. M. Sheldrick, *Acta Cryst.*, 2015, **A71**, 3.
- S17 G. M. Sheldrick, *Acta Cryst.*, 2015, **C71**, 3.
- S18 M. Elstner, D. Porezag, G. Jungnickel, J. Elsner, M. Haugk, T. Frauenheim, S. Suhai and G. Seifert, *Phys. Rev. B*, 1998, **58**, 7260.
- S19 Y. Yang, H. Yu, D. York, Q. Cui and M. Elstner, *J. Phys. Chem. A*, 2007, **111**, 10861.
- S20 M. Gaus, A. Goez and M. Elstner, *J. Chem. Theory Comput.*, 2013, **9**, 338.
- S21 M. Gaus, X. Lu, M. Elstner and Q. Cui, *J. Chem. Theory Comput.*, 2014, **10**, 1516.
- S22 B. Aradi, B. Hourahine and T. Frauenheim, *J. Phys. Chem. A*, 2007, **111**, 5678.
- S23 S. Nose, *J. Chem. Phys.*, 1984, **81**, 511.
- S24 W. G. Hoover, *Phys. Rev. A*, 1985, **31**, 1695.
- S25 A. K. Rappé, C. J. Casewit, K. S. Colwell, W. A. Goddard III and W. M. Skiff, *J. Am. Chem. Soc.*, 1992, **114**, 10024.
- S26 S. Grimme, J. Antony, S. Ehrlich and H. Krieg, *J. Chem. Phys.*, 2010, **132**, 154104.
- S27 S. Grimme, S. Ehrlich and L. Goerigk, *J. Chem. Phys.*, 2011, **32**, 1456.